



8-2010

## Pattern Recognition for Fault Detection, Classification, and Localization in Electrical Power Systems

Qais Hashim Alsafasfeh  
*Western Michigan University*

Follow this and additional works at: <https://scholarworks.wmich.edu/dissertations>

 Part of the Computer Engineering Commons, and the Electrical and Computer Engineering Commons

---

### Recommended Citation

Alsafasfeh, Qais Hashim, "Pattern Recognition for Fault Detection, Classification, and Localization in Electrical Power Systems" (2010). *Dissertations*. 494.  
<https://scholarworks.wmich.edu/dissertations/494>

This Dissertation-Open Access is brought to you for free and open access by the Graduate College at ScholarWorks at WMU. It has been accepted for inclusion in Dissertations by an authorized administrator of ScholarWorks at WMU. For more information, please contact [wmu-scholarworks@wmich.edu](mailto:wmu-scholarworks@wmich.edu).



PATTERN RECOGNITION FOR FAULT DETECTION, CLASSIFICATION, AND  
LOCALIZATION IN ELECTRICAL POWER SYSTEMS

by

Qais Hashim Alsafasfeh

A Dissertation  
Submitted to the  
Faculty of The Graduate College  
in partial fulfillment of the  
requirements for the  
Degree of Doctor of Philosophy  
Department of Electrical and Computer Engineering  
Advisor: Ikhlas Abdel-Qader, Ph.D.

Western Michigan University  
Kalamazoo, Michigan  
August 2010

# PATTERN RECOGNITION FOR FAULT DETECTION, CLASSIFICATION, AND LOCALIZATION IN ELECTRICAL POWER SYSTEMS

Qais Hashim Alsafasfeh, PhD

Western Michigan University, 2010

The longer it takes to identify and repair a fault, the more damage may result in the electrical power system, especially in periods of peak loads, which could lead to the collapse of the system, causing the power outage to extend for a longer period and larger parts of the electrical network. Reducing the outage time and immediate restoration of service can be achieved if the fault type and location are determined in a timely and precise manner.

An integrated algorithm that is based on generating unique signatures from the electric current signal to detect, classify, and localize a fault in one relay is developed. This protection framework will be general enough to be deployed at any end of a transmission line without the need for data communication between the two ends. The proposed framework and algorithm in this dissertation will use values of each phase current during a  $(\frac{1}{4})^{\text{th}}$  of a cycle and will integrate the symmetrical components technique using the fault signal to generate unique signatures of events. The Principal Component Analysis (PCA) technique is used to declare, identify, and classify a fault

using these signatures in the training data set. The fault location is also determined by combining the curve fitting polynomial technique with the unique distance indices that are generated from the signatures already determined. This framework is implemented and simulated using MATLAB and Power System Computer Aided Design (PSCAD) simulation system and tested using several network scenarios including 3- and 6-Bus Electrical Networks, and the IEEE 14 Bus. This framework, as demonstrated by the results presented in the dissertation, has the following significant contributions: 1) it can detect and classify any type of fault using novel signatures approach; 2) it can determine the fault location with a significantly high accuracy; 3) it can distinguish between a real fault and a transient event; and 4) it can detect and classify high impedance faults, making it suitable for use in both transmission and distribution systems.



UMI Number: 3424508

All rights reserved

**INFORMATION TO ALL USERS**

The quality of this reproduction is dependent upon the quality of the copy submitted.

In the unlikely event that the author did not send a complete manuscript and there are missing pages, these will be noted. Also, if material had to be removed, a note will indicate the deletion.



UMI 3424508

Copyright 2010 by ProQuest LLC.

All rights reserved. This edition of the work is protected against unauthorized copying under Title 17, United States Code.



ProQuest LLC  
789 East Eisenhower Parkway  
P.O. Box 1346  
Ann Arbor, MI 48106-1346

Copyright by  
Qais Hashim Alsafasfeh  
2010

## ACKNOWLEDGEMENTS

I would like to express the deepest appreciation to my advisor, Professor Ikhlas Abdel-Qader, for her support and guidance throughout my graduate studies at Western Michigan University. She has continually and amazingly conveyed a spirit of adventure in regard to research and teaching. Without her guidance and persistent help, this dissertation would not have been possible. I know words alone cannot express my gratitude towards her.

Also, I would like to thank my committee members, Dr. Johnson Asumadu, Dr. Azim Houshyar, and Dr. Ahmad Harb for their time and effort.

Finally, I would like to thank my family for their unconditional support and love. They inspired me and gave me the strength to finish this work.

Qais Hashim Alsafasfeh

## TABLE OF CONTENTS

ACKNOWLEDGMENTS .....	ii
LIST OF TABLES .....	vii
LIST OF FIGURES .....	ix
CHAPTER	
1. BACKGROUND AND MOTIVATION .....	1
1.1 Introduction.....	1
1.2 Research Goals.....	5
1.3 Dissertation Outline .....	6
2. PERTINENT LITERATURE .....	8
2.1 On Fault Detection and Classification .....	8
2.1.1 Artificial Intelligence Based Methods .....	8
2.1.2 Wavelet Transform Based Algorithms .....	10
2.1.3 Fuzzy Logic Based Algorithms.....	12
2.1.4 Time, Frequency, and Phasors Analysis Based Algorithms	14
2.2 On Fault Localization.....	15
2.2.1 Wavelet Transform Based Algorithms .....	15
2.2.2 Artificial Neural Network Based Algorithms .....	17
2.2.3 Combinations of the Artificial Neural Network and Wavelet Transform .....	18
2.2.4 Fundamental Frequency (Pharos Quantities) Based Algorithms .....	20

Table of Contents–Continued

CHAPTER

2.2.5 Independent Component Analysis Based Algorithms .....	20
2.2.6 Fuzzy Logic Based Algorithms .....	20
2.3 Analysis and Conclusion of Literature on Fault Detection and Classification in Electrical Power System .....	21
3. FAULT DETECTION AND CLASSIFICATION FRAMEWORK BASED ON PATTERN RECOGNITION OF FAULT CURRENT SIGNAL AND PCA ANALYSIS .....	26
3.1 Introduction .....	26
3.2 Signature Estimation of Fault Signal. ....	30
3.3 Generate Fault Signatures Using Current Values Only .....	33
3.4 Principal Component Analysis Based Fault Detection and Classification .....	35
4. SIMULATION RESULTS ON FAULT DETECTION AND CLASSIFICATION.....	40
4.1 Generate Pattern Training Set .....	41
4.2 Fault Detection and Classification Based on Principal Component Analysis .....	53
4.3 Results on Fault Detection and Classification.....	64
4.3.1 Fault Classification for All Fault Types Test .....	65
4.3.2 High Impedance Fault Test.....	75
4.3.3 Power Quality Disturbances Test .....	76

Table of Contents–Continued

CHAPTER

5. FAULT LOCALIZATION USING PATTERN RECOGNITION .....	80
5.1 Introduction .....	80
5.2 Fault Localization Based on Impedance Method.....	81
5.3 Pattern Index Estimation.....	81
5.4 Fault Localization .....	83
5.5 Pattern-Based Fault Location Method-Procedure.....	85
5.6 Preliminary Experimental Results .....	87
5.6.1 Fault Location Error .....	87
5.6.2 Pattern Training Set.....	88
5.6.3 Results on Fault Localization .....	98
6. ELECTRICAL PROTECTIVE RELAYING SYSTEM VIA PATTERN RECOGNITION .....	99
6.1 Protective Relaying System .....	99
6.2 Case Study 1: Fault Detection, Classification and Localization of 3-Bus Mesh Network.....	100
6.3 Case Study 2: Fault Detection, Classification and Localization of 6-Bus Electrical Network .....	103
6.4 Case Study 3: Fault Detection, Classification and Localization of IEEE 14-Bus .....	105
7. SUMMARY, CONTRIBUTIONS AND FUTURE WORK .....	108
7.1 Summary .....	108

Table of Contents–Continued

CHAPTER	
7.2 Contributions.....	108
7.3 Future Work .....	109
BIBLIOGRAPHY .....	111
APPENDIX .....	119

## LIST OF TABLES

4.1: Classification Test for Fault a-g .....	65
4.2: Classification Test for Fault b-g .....	66
4.3: Classification Test for Fault c-g .....	67
4.4: Classification Test for Fault ab-g .....	68
4.5: Classification Test for Fault ac-g .....	69
4.6: Classification Test for Fault bc-g .....	70
4.7: Classification Test for Fault ab.....	71
4.8: Classification Test for Fault ac.....	72
4.9: Classification Test for Fault bc.....	73
4.10: Classification Test for Fault abc.....	74
4.11: Classification Performance Using One Template for Each Fault Type in the Training Set Producing a 94.54% Average Accuracy .....	76
4.12: Classification Performance by Using Two Templates for Each Fault Type in the Training Set Producing 100% Accuracy .....	76
4.13: Classification Test for High Impedance Fault.....	78
4.14: Classification Test for Power Quality Disturbances .....	79
5.1: Pattern Indices with a Varying Fault Distance Value and $R_f = 40 \Omega$ for Fault <i>a-g</i> .....	89
5.2: The Validity of Curve Fitting in Figure 5.6 for <i>a-g</i> Fault .....	90
5.3: Pattern Index at Different Fault Resistance Values.....	90

List of Tables –Continued

5.4: Pattern Indices at Several Values of Fault Distance and $R_f = 40 \Omega$ for Fault $ab-g$ .....	92
5.5: The Validity of Curve Fitting in Figure 5.10 for $ab-g$ Fault .....	92
5.6: Pattern Index at Different Fault Resistance Values.....	93
5.7: Pattern Indices with a Varying Fault Distance Value and $R_f = 40 \Omega$ for Fault $ab$ .....	95
5.8: The Validity of Curve Fitting in Figure 5.12 for $ab$ Fault.....	95
5.9: Pattern Index at Different Fault Resistance Values.....	96
5.10: Results of Fast Fault Location.....	98
6.1: Mesh 3-Bus Fault Detection and Classification Results .....	102
6.2: Mesh 3-Bus Fault Between Bus 1 and 2 Localization Results.....	103
6.3: Fault Detection, Classification and Location Estimates for 6-Bus Network...	104
6.4: Fault Detection, Classification for IEEE 14 Bus Network .....	106
6.5: Fault Location Estimates for Different Faults on the IEEE 14-Bus Network .....	107

## LIST OF FIGURES

1.1: The percentage faults occurrences in power system .....	3
2.1: Fault classification scheme based on artificial neural network by Ghosh.....	9
2.2: General design of fault detection and classification algorithms based on wavelet transforms.....	11
2.3: Wavelets-ART2 fault classification algorithm as proposed scheme in [16] ...	11
2.4: A representation of the waveform classifier as proposed by Dash et al. [24].	13
2.5: Functional block diagram for fault location based on fundamental frequency components by Raval.....	17
2.6: Functional block diagram fault detector and locator based on feedforward neural network .....	18
2.7: Summary of recent algorithms proposed for fault detection and classification in power system in the literature .....	22
2.8: Summary of recent algorithms reported in the literature for fault localization in power systems.....	23
3.1: Symmetrical component: (a) positive sequence, (b) negative sequence, and (c) zero sequence.....	27
3.2: Graphical addition of the components to obtain three unbalanced phasors ....	29
3.3: Unbalanced system signals: (a) each phase signal and (b) difference signal of current wave for phase a under a fault condition.....	30

## List of Figures–Continued

3.4: A plot of the unique signature of phase a in a 3-phase system with a fault <i>a-g</i> only.....	33
3.5: Proposed functional diagram for generating faults' signatures using the patterns discussed in section 3.3.....	35
3.6: The functional block diagram for fault detection and classification based on principal component analysis .....	39
4.1: A 220KV single circuit transmission lines using PSCAD/EMTDC simulation .....	40
4.2: The pattern, positive and negative for each phase: (a) phase a, (b) phase b, and (c) phase c under healthy conditions.....	42
4.3: The pattern of all positive and negative sequences for each phase- (a) phase a, (b) phase b, and (c) phase c for the fault simulation of pages a to g .	43
4.4: The pattern of both the positive and negative sequences for each phase - (a) phase a, (b) phase b, and (c) phase c for faulty phase b.....	44
4.5: The pattern (positive and negative sequence for each phase) (a) phase a, (b) phase b and (c) phase c for a faulty phase c.....	45
4.6: The pattern (positive and negative sequence for each phase) (a) phase a, (b) phase b and (c) phase c of faulty , under faulty conditions of phase a and phase b .....	46
4.7: The pattern (positive and negative sequence for each phase) (a) phase a, (b) phase b and (c) phase c, under faulty conditions of phase a and phase c.....	47
4.8: The pattern positive and negative for each phase. In (a) phase a, (b) phase b, and (c) phase c under faulty conditions of phase c and phase b .....	48
4.9 The pattern of both positive and negative for each phase. (a) Phase a, (b) phase b, and in (c) phase c under faulty conditions of phase a and phase b .....	49

List of Figures–Continued

4.10: The pattern of both positive and negative sequences for each phase. In (a) phase a signature, (b) phase b signature, and in (c) phase c signature for the faulty conditions involving phase ac..... 50

4.11: The pattern of both positive and negative sequences for each phase. In (a) phase a signature, (b) phase b signature, and (c) phase c signature for the faulty conditions involving phase bc ..... 51

4.12: The pattern of the (positive and negative sequences for each phase in a three-phase fault condition. In (a) phase a signature, (b) phase b signature, and (c) phase c signature..... 52

4.13: Projection of the data of (positive and negative sequence for each phase) on each Principal component (a) phase a, (b) phase b and (c) phase c ..... 53

4.14: Projection of the data of (positive and negative sequence for each phase) on each Principal component (a) phase a, (b) phase b and (c) phase c..... 54

4.15: Projection of the data of (positive and negative sequence for each phase) on each Principal component (a) phase a, (b) phase b and (c) phase c ..... 55

4.16: Projection of the data of (positive and negative sequence for each phase) on each Principal component (a) phase a, (b) phase b and (c) phase c ..... 56

4.17: Projection of the data of (positive and negative sequence for each phase) on each Principal component (a) phase a, (b) phase b and (c) phase c ..... 57

4.18: Projection of the data of (positive and negative sequence for each phase) on each Principal component (a) phase a, (b) phase b and (c) phase c ..... 58

4.19: Projection of the data of (positive and negative sequence for each phase) on each Principal component (a) phase a, (b) phase b and (c) phase c ..... 59

List of Figures–Continued

4.20: Projection of the data of (positive and negative sequence for each phase) on each Principal component (a) phase a, (b) phase b and (c) phase c .....	60
4.21: Projection of the data of (positive and negative sequence for each phase) on each Principal component (a) phase a, (b) phase b and (c) phase c .....	61
4.22: The pattern (positive and negative sequence for each phase) (a) phase a, (b) phase b and (c) phase c of faulty , under faulty conditions of phase a and phase b .....	62
4.23: Projection of the data of (positive and negative sequence for each phase) on each Principal component (a) phase <i>a</i> , (b) phase <i>b</i> and (c) phase <i>c</i> .....	63
4.24: Examples of power quality disturbances shown above, (a) voltage Sag, (b) voltage sag with a different load from that in a, (c) voltage swells, and (d) capacitor switching .....	77
5.1: The curve fitting between positive pattern index and the fault location for phase a to ground ( <i>ab-g</i> ) .....	84
5.2: The curve fitting between negative pattern index and the fault location for phase a to ground ( <i>a-g</i> ) .....	84
5.3: The curve fitting between fault resistance and distance error .....	85
5.4: Functional block diagram for fault location based on symmetrical patterns indexes .....	86
5.5: 220KV single circuit transmission lines using PSCAD/EMTDC simulation .	87
5.6: The curve fitting between negative pattern index and the fault location for phase a to ground ( <i>a-g</i> ) .....	89
5.7: The curve fitting between fault resistance and distance error .....	91
5.8: Fault location training set for <i>a-g</i> fault.....	91
5.9: Curve fitting between positive pattern index and distance of a fault .....	93

List of Figures–Continued

5.10: The curve fitting between fault resistance and distance error .....	94
5.11: Fault location training set for <i>ab-g</i> fault.....	94
5.12: The curve fitting between fault resistance and distance error .....	96
5.13: The curve fitting between resistance and distance error .....	97
5.14: Fault location training set for <i>ab</i> fault .....	97
6.1: Proposed electrical protective relaying system .....	100
6.2: Mesh network 3-bus electrical power network .....	101
6.3: Mesh network 3-bus electrical power network using PSCAD.....	102
6.4: 6-Buse electrical power network .....	104
6.5: IEEE 14 bus electrical power system network .....	105

## CHAPTER 1

### BACKGROUND AND MOTIVATION

#### 1.1 Introduction

An important attribute of electrical power system is the continuity of service with a high level of reliability. This motivated many researchers to investigate power systems in an effort to improve reliability by focusing on fault detection, classification, and localization.

Power system fault is defined as any significant changes in the system quantities, current, voltage, or frequency. A fault is declared when a disturbance in voltage, current or frequency in the power signal that affects the consumers' equipments occur. For example, a good quality power system will ensure that the voltage level at a residential customer location is 120 V and must remain within 114 to 126 V at all times. Hence, methods to keep these quantities within normal operation range and preserve excellent power quality are needed.

A fault study is an important part of power system analysis to provide the highest reliability. Factors that impact such rating are:

- Commercial Quality: the relationship between the network company and the customer.
- Continuity of Supply: frequency of long and short interruptions of power service.
- Voltage Quality: this measure is a quantitative one and determined by disturbance from the normal and expected values of the system's frequency, voltage and its

permissible variation such as voltage dips, temporary and transient over voltages, and harmonic distortion.

While the current parameter is an important factor is not explicitly used as a quality measure since it can be deduced from the voltage values [1].

The principal abnormal shunt unbalances on a power system are commonly called faults. Faults in general can be categorized as phase-to-ground faults representing 70 to 85% of all faults, phase-to-phase ones with 8 to 15% frequency, double-phase-to-ground with 4 to 10% occurrence frequency, and three-phase with 3 to 5% occurrence frequency. Faults can also evolve from one type to another, especially when the protective equipment is slow in responding and isolating the fault. Thus a phase-to-ground fault may develop into a double-phase-to-ground fault or a three-phase fault; a phase-to-phase fault may become a double-phase-to-ground or three-phase fault [2]. A representation of a power system fault types and their occurrence frequencies is shown in Figure 1.1.

A fault can result from a lightning storm causing the high voltage to flash over the insulators or a high speed wind especially around the lower voltage areas (at the distribution system) causing tree contacts to the phases. Many other factors that can cause faults to occur such as ice build up on the transmission lines, earthquakes, fire explosions, falling trees, flying objects, physical contact by humans, animals or contamination. Moreover, Faults can result from variety of accidents such as vehicles crashing into power line poles or live equipment. The frequency of accidents causing a fault varies with time and depends on several factors such as climate, geographical location, and man-made structure in the surrounding.

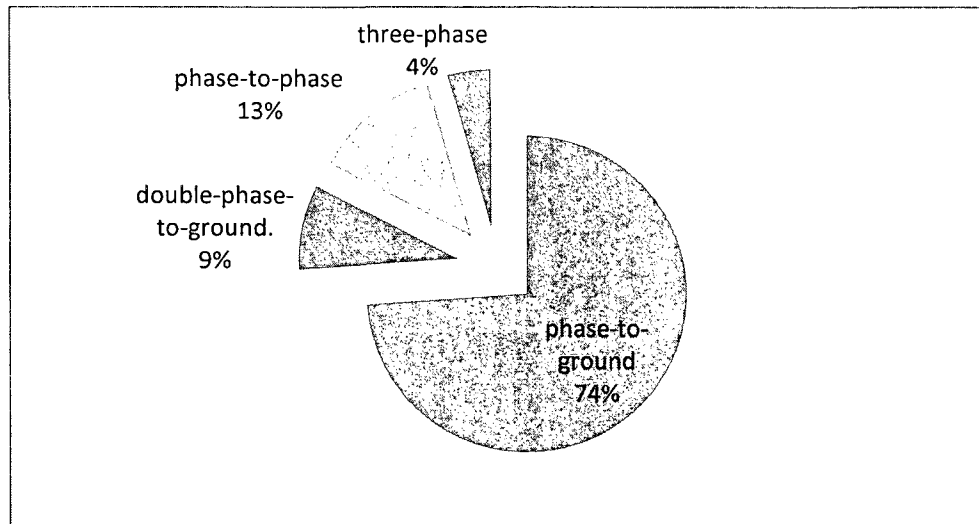


**Figure 1.1: The percentage faults occurrences in power system**

The objectives of a power system fault analysis is to provide enough information to understand the reasons that can lead to the interruption and to, as soon as possible, restore the handover of power, and perhaps minimize future occurrences if possible at all. Analysis should also provide sufficient understanding of the case of components of the system of protection so that a set of preventive measures that can be implemented to reduce the likelihood of service disruptions and equipment damage [3].

Fault detection and localization is a focal point in the research of power systems area since the establishment of electricity transmission and distribution systems. Circuit breakers and other control elements are required to help protective relays to take appropriate action [4].

Fast detection of faults will have a significant impact on the equipment safety since it will engage the circuit breakers instantaneously and before any significant damage occurs. Accuracy of fault location is not only significant for the clear reason of the timely repair and restoration of the service but also it can lead to identifying some specific

location related faults and hence a longer term goal of preventing faults can be achieved. In all, identification of faults location in a timely manner should reduce the frequency and length of power outages [5] and may result in a significant advancement in system's reliability. In recent years, with an increase in the number of power system networks within one control center, the behavior and effect of faults became more complex and as a result, fault affected area has expanded. It is increasingly necessary that the operator at the control center reacts quickly when a network fault occurs to minimize losses and damage. Hence, an accurate fully automated algorithm can help the operator in a faster and more precise reaction in recognizing and reacting to the fault type. The new algorithm should impact power system fault diagnosis in the following three stages:

- Faulty section detection
- Fault Classification
- Fault localization (network section isolation and location identification).

For nearly thirty years, electrical utilities use faulted circuit indicators (FCIs) to help them localize the power outages location within the system. These FCIs require physical inspection of the sites FCIs indicate in search for any mechanical or any other kind of significance causing the fault. Most of the methods of analysis based on the actual current or voltage phasor values measured by the current or voltage transformers in the substations or switching stations. Currently, to achieve this, at least 3 voltage transformers and 3 current transformers are required at each end of the sub-transmission or transmission lines. These transducers are expensive, especially when the system involves high voltage. Most algorithms require both current and voltage information from both ends of the transmission system [5].

Research on fault detection, classification, and localization is an ongoing activity aiming to develop new algorithms with higher accuracy and enhanced performance. Electrical power companies are still challenged with the difficulty of fault detection and localization. It is well known that the longer it takes to identify and repair a fault, a significant damage can result in the electrical system especially in periods of peak loads, which could lead to the collapse of the voltage and a power outage for a longer time and a larger part of the electrical network. In recent years, the experts in this field proposed and developed methods and various tools to detect and localize electrical faults such as utilizing principles of estimation, wavelet transforms, artificial intelligence, fuzzy logic, or a combination of tools [3-57].

## **1.2 Research Goals**

The objectives of this research are to detect and classify all types of fault at varying fault locations and fault resistance, and to determine the fault location. In this work, I am presenting a new electrical protective relaying framework to detect, classify, and localize any fault type in an electrical power system. I combined the detection, classification with recognition of fault location in the same relay. The fault detection and classification will be performed within the first  $(1/4)^{\text{th}}$  of a cycle in a highly efficient manner. Moreover, this protection framework is general so that it can be installed and operated at any end of a transmission line without the need for communication devices. Currently, most protection devices need to exchange information between both ends of a transmission line to classify a fault and hence communication devices are a necessary part of a relay. This work will use readings of the phase current

only during the first  $(\frac{1}{4})^{\text{th}}$  of a cycle and in an integrated method that combines symmetric components technique with the principal component analysis (PCA) to declare, identify, and classify a fault. Furthermore, this framework also distinguishes between a real fault and a transient event and can be used in a transmission system or a distribution system. The framework will be implemented and simulated using PSCAD simulation system and the realistic experimental results will validate it.

In order to achieve these objectives, a pattern of current signal is combined with and principal component analysis to identify a fault from normal operations and classify the fault in any of the possible ones. Localization of fault is presented in this work based on pattern index using the voltage and current symmetrical patterns. To validate this framework, I used 10 different types of faults. These are 3 single lines to ground, 3 line to line, 3 line to line to ground, and 1 three phase fault (Symmetrical Fault) and fault location at any distance from one end of transmission line. This system will have the ability to detect and classify any type of fault with variable fault resistance and at any distance from the sending moreover the framework is tested on mesh network, 6 bus network and IEEE 14 Bus system.

### **1.3 Dissertation Outline**

Chapter 2 will present the available and recent literature on fault detection, classification and localization. In addition to that, various feature extraction techniques and classification techniques using Fuzzy Logic, Neuro-fuzzy techniques, Wavelet Transform, Artificial Neural Network will be discussed.

Chapter 3 presents the research mythology part one for feature extraction framework using pattern of current along with principal component analysis while chapter 4, will present the experimental results for fault detection and classification and will detail the implementation using PSCAD and MATLAB 7.01 and the results obtained under various conditions.

In chapter 5, presents the algorithm for fault localization using the pattern of voltage and current fault signals and their pattern indexes and the corresponding polynomial curve fitting method will be presented. Chapter 6 presents the electrical protective relaying system that will encompass the complete system of fault detection, classification and fault localization in the same relay and with complex power systems structure. The system that presented in chapter 6 is a case study of a mesh network with 3 bus, 6-bus electrical power network and also IEEE 14 Bus network system.

Finally, in chapter 7 a summary and conclusions, with a presentation of insights on improvements and future work, are presented.

## CHAPTER 2

### PERTINENT LITERATURE

In recent years, researchers in applied mathematics and signal processing have developed many techniques for the detection, classification and localization of faults in electrical power system by mainly developing relaying and protection devices. Fault detection and classification techniques have been proposed for electrical systems in generation, distribution and transmission during the last few years [7]. In the following subsections I attempt to survey the major works in detection, classification and localization of faults in power system (Generation, Transmission, and Distribution).

#### **2.1 On Fault Detection and Classification**

Various signal processing tools have been proposed for electrical power system fault detection and classification. These tools include principles of estimation, wavelet transforms, artificial intelligence, fuzzy logic, and any combination of tools.

##### **2.1.1 Artificial Intelligence Based Methods**

Artificial Neural Network (ANN) is powerful pattern recognition, classification and generalization tool that motivated many ANN based algorithms for fault detection and classification in the recent years [8]. Neural networks have been used heavily in power system applications because algorithms can be trained with the data off-line. Techniques of neural networks have proven to be a good tool for fault detection and classification there was no need to use the information expressly impedance as a basis of

the information, and that learn from the examples provided to it during training. ANNs own excellent features, such as the ability to generalize, and noise immunity, and robustness' and fault tolerance. Therefore, the decision taken by the ANN-based relay is not seriously affected by differences in system parameters.

Ghosh and Lubkeman in [9] proposed the classification of electrical power system fault based artificial neural network methodology by using the capture of the disturbance waveform shown in figure2.1.

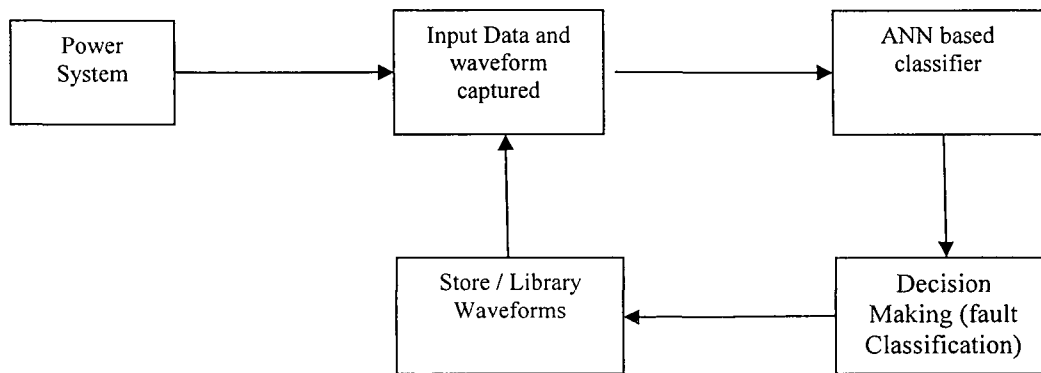


**Figure 2.1: Fault classification scheme based on artificial neural network by Ghosh**

In their work (Ghosh and Lubkeman) two different neural network schemes were proposed, feed forward network (FFNN) and a time delay network (TDNN). Their work has ability to encode temporal relationship found in input data. Also, Sanaye-Pasand and Khorashadi-Zadeh in [10] proposed to detect and classify the power system faults using artificial neural network, in their scheme various signal faults are modeled and an artificial neural network is used to recognition of these patterns.

Jain et al. in [11] proposed a new way to detect and classify the fault in double circuit transmission line using ANN, in this type of transmission line their some problem in fault

detection and calcification because mutual coupling. Mutual coupling .the design process have of the ANN based fault detector and classifier goes through the following steps:

- 1- Preparation of a suitable training data set comprising of all possible cases that the ANN needs to learn.
- 2- Selection of a suitable ANN structure for a given application.
- 3- Training the ANN.
- 4- Evaluation/validation of the trained ANN using test patterns to check its correctness in generalization.

Jain also in [12] discussed the same scheme proposed in reference [11] using feed forward neural network (FFNN) algorithm and Marquardt Levenberg algorithm. The algorithm employs the fundamental components of current and voltage. In their scheme no communication devices between the two ends are needed.

### **2.1.2 Wavelet Transform Based Algorithms**

Ramaswamy and Kashyap in [13 and 14] proposed a novel approach of Power System fault classification using Wavelets to analyze Power System transients. They have incorporated a Probabilistic Neural Network (PNN) for detecting the type of fault after decomposing the fault signal to get the details coefficients. PNN is used for distinguishing the detail coefficients for each fault then classifies the fault. Gayathri and Kumarappan in [15] suggested that an appropriate method for high-voltage transmission line fault detection and classification can be designed using wavelet transforms integrated with an artificial neural network. This method does not depend on the amplitude of the

voltage transient but on the frequency found in the transients. Their proposed algorithm is shown in figure 2.2.

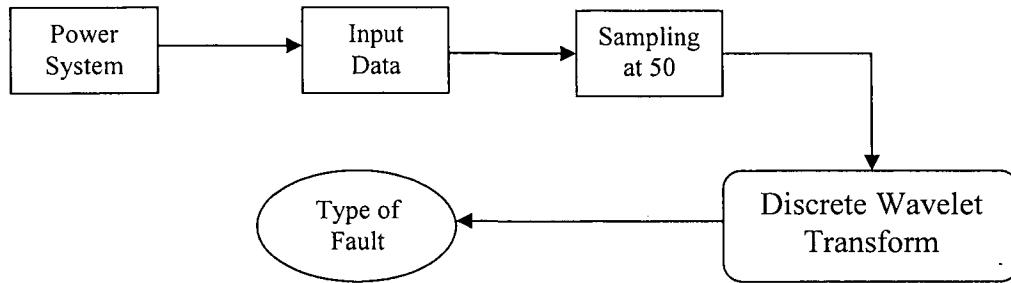


**Figure 2.2: General design of fault detection and classification algorithms based on wavelet transforms**

Upendar [16] proposed the use of discrete wavelet transform and adaptive resonance theory (ART2) to extract the fault feature to classify the fault type respectively. An illustration of this algorithm is presented in figure 2.3.

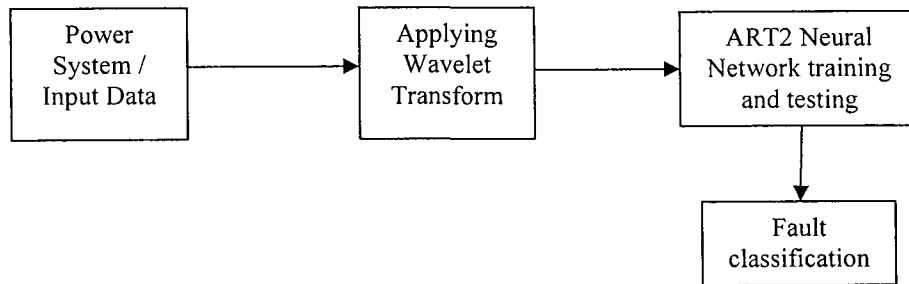


**Figure 2.3: Wavelets-ART2 fault classification algorithm as proposed scheme in [16]**

Swarup [17] proposed a new algorithm for the protection of parallel transmission lines using wavelet transform and adaptive Neural Fuzzy Inference system (ANFIS). ANFIS is a product of adding the fuzzy inference system with a neural network). The scheme can be separated into two stages, namely, the time frequency analysis by the wavelet

transform component and ANFIS for the pattern recognition component to identify the type of fault.

Zheng-You [18,19] decomposed a current waveform during a fault into approximation and detail sub-signals. Using wavelet entropy principle, they were able to achieve acceptable performance in power system fault detection.

Malathi [20] proposed a paradigm to classify the fault in power systems using wavelet and multi-class support vector machine (SVM). SVM is a learning method in which a nonlinearly input vector can be mapped into a high dimensional feature space, followed by a multi-class support vector machine for classification of various faults that may occur in a power system. Upendar [21] proposed a new approach for the classification of power system fault using discrete wavelet transform and genetic algorithms. He used discrete wavelet transform to decompose the current signal and followed it by a genetic based process to classify faults.

### **2.1.3 Fuzzy Logic Based Algorithms**

Fuzzy logic has also its share in this research area as it has been proposed by several researchers to detect and classify the type of fault in an electrical power system. For example, Biswarup and REDDY [22] presented a fault detection and classification algorithm based on a combination of Discrete Fourier Transform (DFT) and fuzzy logic using a full cycle and a separate sequence of the symmetrical components of the fundamental frequency. The angular differences between the sequence components during a fault current in each phase and their magnitudes are fed into the fuzzy classifier.

K. Razi, M. Hagh and G, Ahrabian [23] proposed an improved fuzzy logic based fault classification scheme using membership function to solve problem in overlap.

Dash et al. [24] proposed a new scheme using Fourier linear combiner and fuzzy expert system. Their algorithm uses Fourier linear combiner to estimate the normalized peak amplitude of the voltage signal and its rate of change which become the input signal into the fuzzy expert system as shown in figure 2.4. They used their scheme in many types of disturbance signals such as normal sag and swell but they did not use it for faults classification.

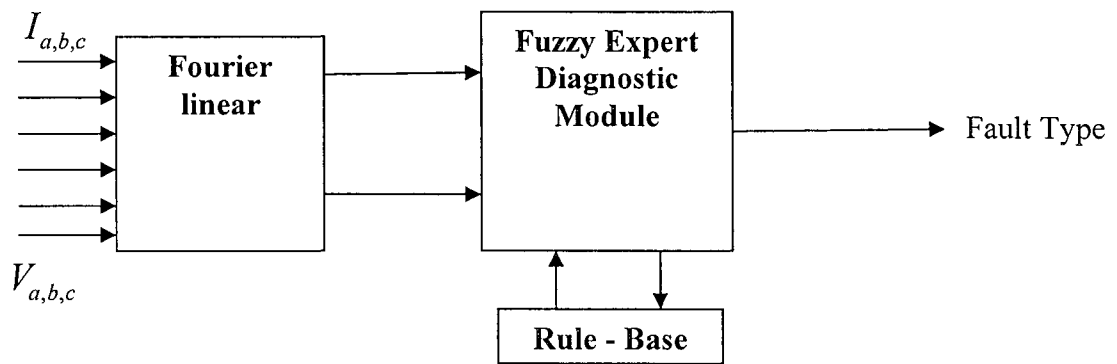


**Figure 2.4: A representation of the waveform classifier as proposed by Dash et al. [24]**

Vaslilc [25] proposed a new way for fault classification based on fuzzy logic and neural network. His algorithm used an adaptive resonance theory (ART), a special type of self organized competitive neural network, to introduce several enhancements on previous work of his. Also, Zhang [26] used the same algorithm used in [25] but based his work on Fuzzy K-NN decision rule while the fuzzy ART neural network was focused on detection of faults associated with the transmission lines. They reported improvements in algorithm

performance and reported to have produced an algorithm of practical detection and classification capabilities.

Pradhan [27] attempted to classify the fault for compensated transmission line (adding series capacitor in transmission line) using a discrete wavelet transform algorithm integrated with fuzzy logic. Using Discrete Wavelet transform on current fault signal, the fault feature is extracted using a fuzzy logic system.

#### **2.1.4 Time, Frequency, and Phasors Combination Based Algorithms**

F. Crusca and M. Aldeen [7] presented a new approach to fault detection and classification problem based on the principles of estimation. The faults signal are modeled as unknown inputs and then estimated systematically through the use of unknown input observer theory. This approach is applied to a power system including a synchronous generator, an exciter and a network of lines and loads.

Samantaray et al. [28] presented an algorithm that is based on time domain analysis. Their work is dependent on short Fourier transform for generating frequency contours, using these contours to distinguish the fault condition from no-fault condition. The fault current is processed through the short Fourier transform, in fault condition the contours are concentric at higher frequency and no-fault conditions the contours are concentric at lower frequency.

Adu [29] proposed an algorithm that is based on the measurement of phase angles between the positive and negative sequence components of the current phasors. This algorithm also measured the relative magnitudes of the zero and negative sequence

quantities present in the current waveforms to differentiate between grounded and ungrounded faults.

Styvaktakis et al [30] proposed a method to characterize changes in the power system using rms voltage measurements to consider in this category, discrete measurements of rms voltage will be considering where the time interval between two consecutive rms values in one cycle then used the rms of signatures and features for classification.

## **2.2 On Fault Localization**

The conventional tool of fault localization in power systems is impedance based, in which the voltage and current data measured at many point along the transmission line using the impedance per unit length is accurate because this method is subject to errors caused by high resistance ground fault, circuits topology, and interconnection to multiple sources [31]. Most tools are based on wavelet transform, artificial intelligence, or a combination. Other methods use independent component analysis, time frequency analysis, and sinusoidal steady state analysis.

### **2.2.1 Wavelet Transform Based Algorithms**

Many researchers used wavelets to localize faults in power systems using traveling wave and support vector machine. Hizam et al. [32] and Magnago et al. [33] used wavelet transform using traveling wave theory of a transmission line. They also reported that the algorithm of wavelet transform can be used not only for transmission line but also for disruption systems. Borghetti et al. [34] reported an algorithm that

utilizes continuous wavelet transform to find the fault location. They [35] also in proposed to extend his previous algorithm to improve performance and to overcome some limitations on the use of continuous wavelet transforms. They proposed to improve the method by which he constructs the mother wavelet directly from the recorded fault originated voltage transient signal. Also, Yerekar [36] presented a new algorithm for finding a fault location based on impedance traveling wave, which combines measurement impedance method with traveling wave method.

Chen et al. [37] used the traveling wave principle to find the fault location in High voltage DC transmission lines .This method can support the new dual-ended, principles, and single ended in a traveling wave at the same time. Implementation of the algorithm consisted by three main parts: a travelling wave data acquisition, processing system and communication network, and a computer.

Gilany et al. [38] he used the wavelet transform for underground cable fault based on the current and voltage traveling wave, after extract the high frequency components initiated due to faults from the stored voltage signal.

A.ABUR [39] described alternative techniques. The main point in these techniques is to monitor the waves travel initiated by the fault until to receive end of transmission line and use of information from the network to infer the location of the fault. This is done by identifying the arrival times of waves traveling at end of transmission line through the application of the discrete wavelet transform to the modal components of the fault signals.

Malathi and Marimuthu [40] presented a wavelet transform to localization fault in power system based on support vector machine. The data extracted from discrete wavelet transform are used for training and testing support vector machine.

**2.2.2 Artificial Neural Network Based Algorithms**

There are many researchers used artificial neural network in fault location. P. Raval [41] used the artificial neural network by using fundamental frequency components of the voltage and current at pre fault and post fault measured in the end of transmission line and the proposed neural fault locator was trained using various sets of data. Figure 2.5shpws functional block diagram, this block diagram is a part of relaying scheme and current and voltage transformer is feed to the relay and the fault classifier and location have tensing for hidden layer and linear for output layer .

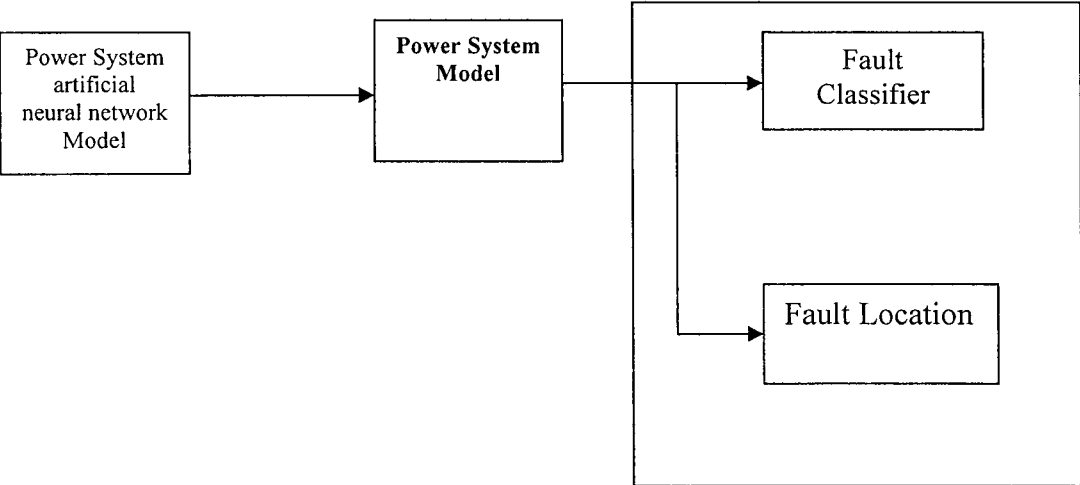


**Figure 2.5: Functional block diagram for fault location based on fundamental frequency components by Raval**

In this scheme the fault locator methodology based on the traveling wave theory and based on assessing electrical magnitudes at fundamental frequencies are presented. J.

Gracia et al. [42] tried to select best artificial neural network structures as a tool developed specifically for this aim, called SARENEUR. This tool allows to select the ANN that fulfills certain conditions or to verify the operation of a specific network. Gracia et al. [43] proposed new algorithm to localize faults using artificial neural network based on the variation of fault resistor not dependant on fault inspection angle, this algorithm is proposed for decreasing of training time and dimensions of ANN.

Hagh et al. [44] used artificial neural network to detect and located fault in power system and the fault located is activated when the fault is detected by the fault detector in figure 2.6 show the block diagram, in this work, fault detection from one end and fault locators are proposed for on-line applications using ANNs. A feedforward neural network based on the supervised back propagation learning algorithm was used to implement the fault detector and locators.

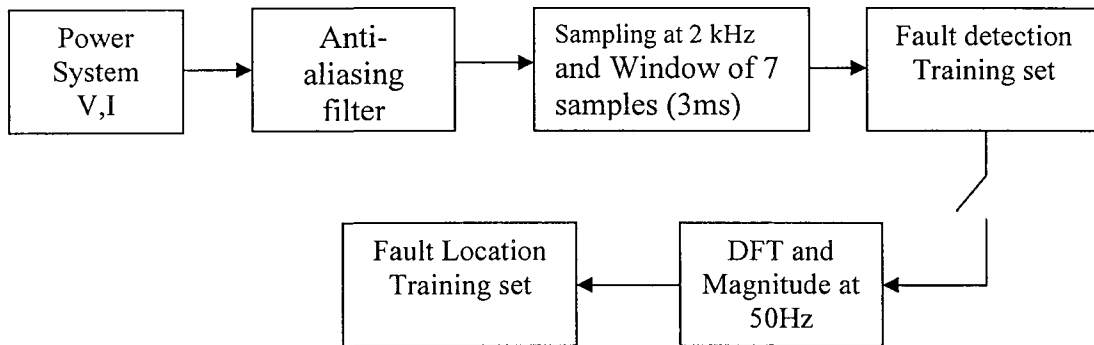


**Figure 2.6: Functional block diagram fault detector and locator based on feed forward neural network**

### 2.2.3 Combinations of the Artificial Neural Network and Wavelet Transform

Ekici and Yildirim [45] proposed a new tool to estimation fault location in power system based on wavelet transform and artificial neural network. This algorithm is

develop as one end frequency based technique and used both voltage and current effect resulting from remote end of transmission line. Ngaopitakkul and Pothisarn [46] proposed a technique using discrete wavelet transform (DWT) and back-propagation neural network (BPNN) for locating of fault location on single circuit transmission lines. There algorithm depends on the fault current waveforms, this wave obtained from the simulation, after that discrete wavelet transform (DWT) will apply to extract the feature for fault location. The decision algorithm, therefore, are constructed based on the back-propagation neural network.

Ekici [47] proposed, using discrete wavelet transform and Elman recurrent neural networks, an algorithm consists of two main stages. The first stage is to obtain distinctive features about the fault signal, using the DWT method is ideal, which provides useful information by analyzing the signals in the time-scale range. The second phase, the location of the fault expected by using Elman recurrent networks. Then measure the performance of Elman recurrent networks output.

Reddy and Mohanta [48] and Sadeh and Afradi [49] proposed Fuzzy inference system (FIS) for the integration of expert assessment in order to extract important features from wavelet multi-resolution analysis (MRA) coefficients to obtain consistent results on the fault location. The basic structure of kind of fuzzy inference system (FIS) is a model that maps input characteristics to the membership functions of inputs and input membership function to rules, rules for a set of output characteristics, and characteristics of production and output membership functions, production and post production of the membership of the single-valued or a decision associated with production.

#### **2.2.4 Fundamental Frequency (Pharos Quantities) Based Algorithms**

The fault location in power systems based on fundamental pharos quantity of voltage and current and power frequency. F. Han [50] discussed the fault location in power systems using sinusoidal steady state analysis, where the current and voltage are measured at sending end, and by solving the nonlinear parameter equation of transmission line. But this method is limited, it just apply for one type of fault, single phase to ground fault.

Carvalho and Carneiro [51] used Coupling Capacitor Voltage Transformer (CCVT). After applying the secondary voltages to conventional protection schemes, high frequency tap of the CCVT, normally used for PLC application to transfer the steep characteristics of the traveling waves, induced by fault transients, to its neutral side. By using this method the necessary information can be provided for a traveling wave fault locator scheme.

#### **2.2.5 Independent Component Analysis Based Algorithms**

There many feature extraction methods used for fault localization in power system, one of them is Independent Component Analysis. M. B. de Sousa and Allan K. Barros [52] proposed a new algorithm for localization fault in power systems based on efficient coding technique through Independent component analysis.

#### **2.2.6 Fuzzy Logic Based Algorithms**

Many researchers and engineers start to use fuzzy logic in fault location. Qais: put the name [53] proposed new technique in fault location using advance signal processing

tools by combined wavelet transform and fuzzy logic. After using wavelet transform some features will be extracted from fault signal, then applied fuzzy logic to decide the fault location.

Sadeh and Afradi [49] proposed a new algorithm for locating a fault in combined power system such as over head transmission lines and underground cables using Adaptive network based fuzzy inference system. They used 10 methods of Adaptive network based fuzzy inference system divided into three stages, namely, fault type, fault section detection, and fault location.

### **2.3 Analysis and Conclusion of Literature on Fault Detection, Classification and Localization in Electrical Power System**

A summary of most algorithms on fault detection and classification in power systems is given in figure 2.7, while in figure 2.8 a block diagram that summarizes most of techniques used in fault localization. In general, all researchers attempted to detect and classify all types of faults in electrical power systems such as phase to ground, two phases to ground, two phases and three phases to ground, but many of approaches did not cover all type of faults. However, Wavelet Transform based algorithms have many advantages over other algorithms such as:

- It has been reported that wavelet transform based methods for fault detection are computationally fast and provide effective analysis methods during the current power system disturbances and defects. Scaling, for instance, gives the Discrete Wavelets Transform logarithmic frequency coverage when compared with the uniform frequency coverage resulted from Fourier transform based methods [54].

- Wavelet transform has the advantage of capturing abrupt signals changes which is very useful since a signal recorded in a transmission network during a fault should have an abrupt change [55]

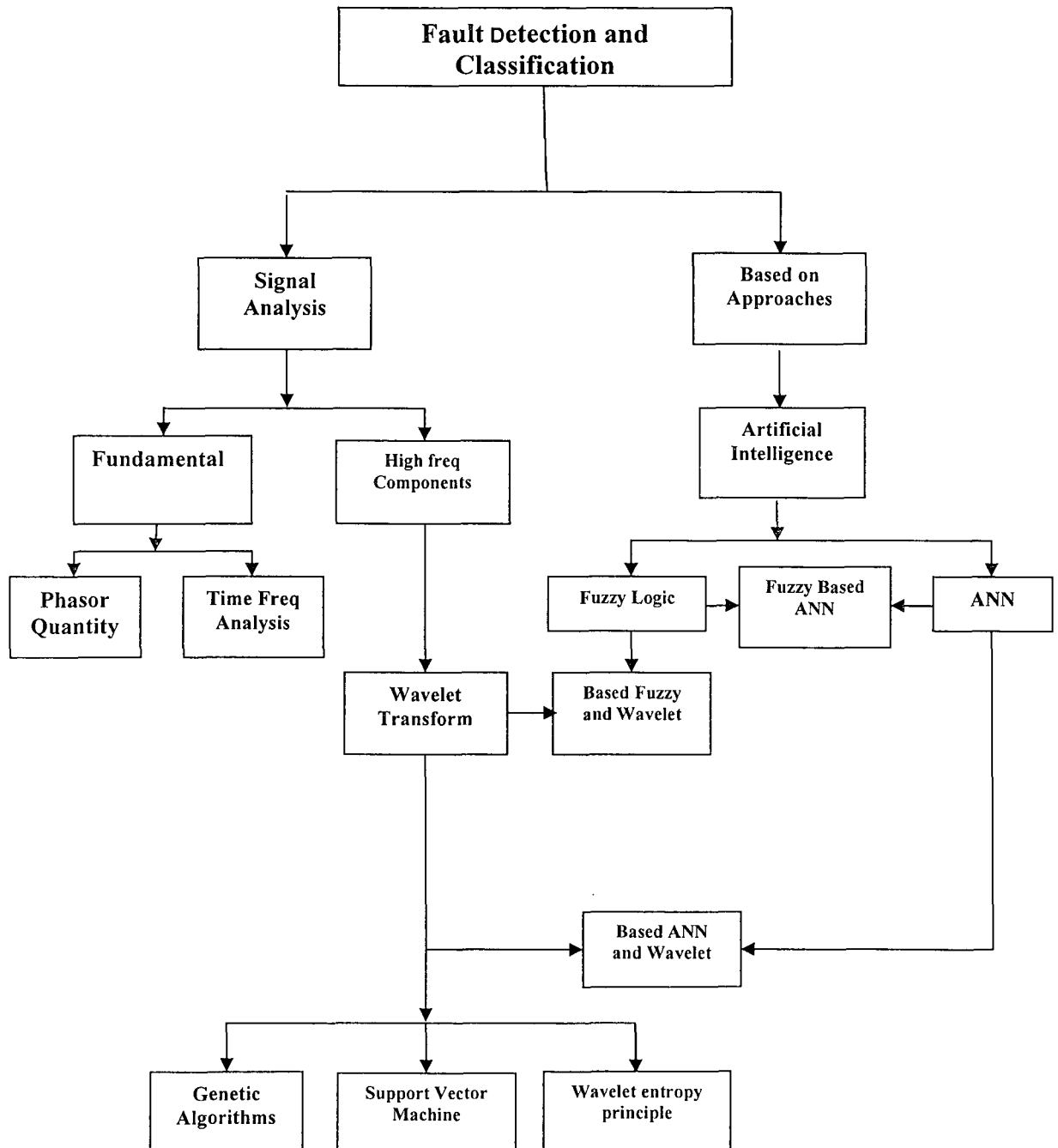


**Figure 2.7: Summary of recent algorithms proposed for fault detection and classification in power system in the literature**

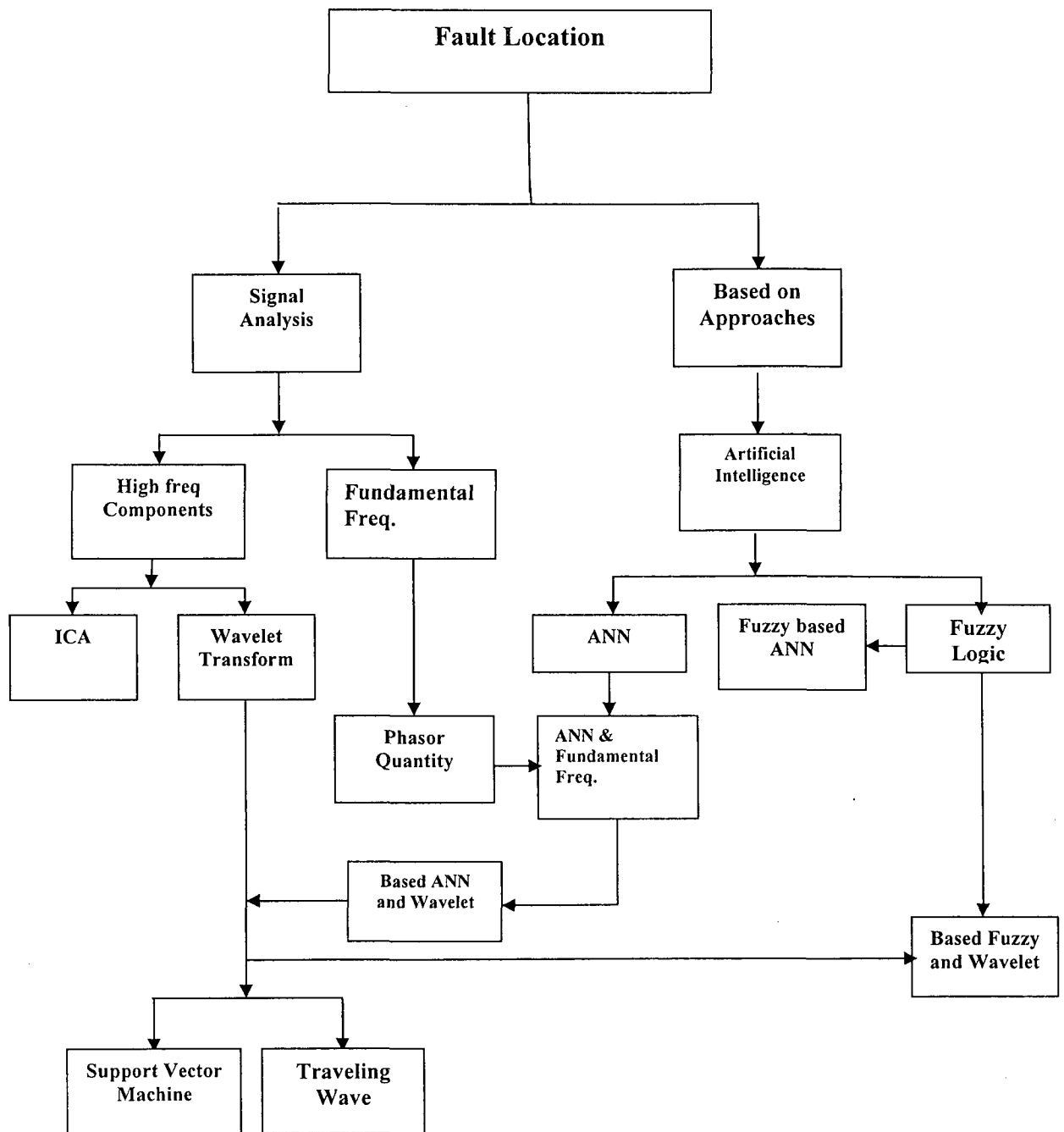


**Figure 2.8: Summary of recent algorithms reported in the literature for fault localization in power systems**

- The property of multi-resolution in time and frequency allows for automated window selection allowing to algorithms to be very effective but they are all threshold dependent. These algorithms are independent of fault location, fault inception angle, or fault impedance [56].

A second group of research used Artificial Neural Network (ANN) to detect and classify a fault in the last 20 years. These algorithms can be described and/or credited for the following:

- ANN based algorithms depend on indentifying the different patterns of associated information using impedance information and learning from previous events during training stages.
- The neural network architectures suffer from large number of training cycles and a huge computational burden.
- One of the significant drawbacks for using ANN is that the resolution is not efficient since it can be a very sparse network with the need for large size training data which will even increase the burden of its computational complexity [9].

Recently, many researchers proposed fuzzy logic in power system fault detection, classification, and localization. We would like to note many of the advantages and drawbacks of these methods as follows:

- A drawback of ANN, its implicit knowledge representation that gives an important key benefit to fuzzy logic. Its knowledge representation is an explicit using simple (if, then) relation.
- While neural networks have the shortcoming of being implicit, Fuzzy logic systems are subjective and heuristic.

- In General, Fuzzy logic techniques are simpler than the ones based on wavelet transform or neural network.
- The fuzzy logic based fault detection, classification, and localization approaches involve some linguistic rules such as Principles of Estimation and Independent Component Analysis [23 and 57].

Unfortunately, most of the current available tools for fault detection, classification and localization are not efficient nor they can be utilized in real time [11]. The need for new algorithms that have high efficiency and applicable in real time is pressing now more than at any other time before.

## CHAPTER 3

### FAULT DETECTION AND CLASSIFICATION FRAMEWORK BASED ON PATTERN RECOGNITION OF FAULT CURRENT SIGNAL AND PCA ANALYSIS

#### 3.1 Introduction

One of the most powerful tools associated with multi-phase unbalanced circuit is the symmetrical component method that was introduced by Fortes cue [58]. He showed that a system of unbalanced load with  $n$  phasors can be remodeled by using the symmetrical components approach. The  $n$  phasors from each of the elements are equal in terms of length and angles between any adjacent phasor of the group. Although the method is applicable to any unbalanced multiphase system, its use in three phase system is presented in this section.

Under normal operation, a three phase system is usually balanced, however, when a fault occurs, the system becomes unbalanced with unbalanced currents and voltages in each phase. When the voltage and current applied to a fixed load (constant impedances), then the system is said to be linear and the principle of superposition applies. This allows for the voltage response of the linear system of unbalanced currents to be determined by considering the separate responses of the individual elements to the symmetrical components of the currents [58]. The method of symmetrical components is a mathematical technique that allows us to solve unbalanced systems by still utilizing systematic analysis and design tools of balanced three phase systems. Decomposing three phase network into three simpler sequence networks reveals complicated phenomena in

more simplistic terms. Sequence network results can then be superimposed to obtain three phase results.

In three phase system, the phase sequence is defined as the order in which they pass through a positive maximum. Consider the phasor representation of three phase voltage under normal, no fault, conditions as follows:

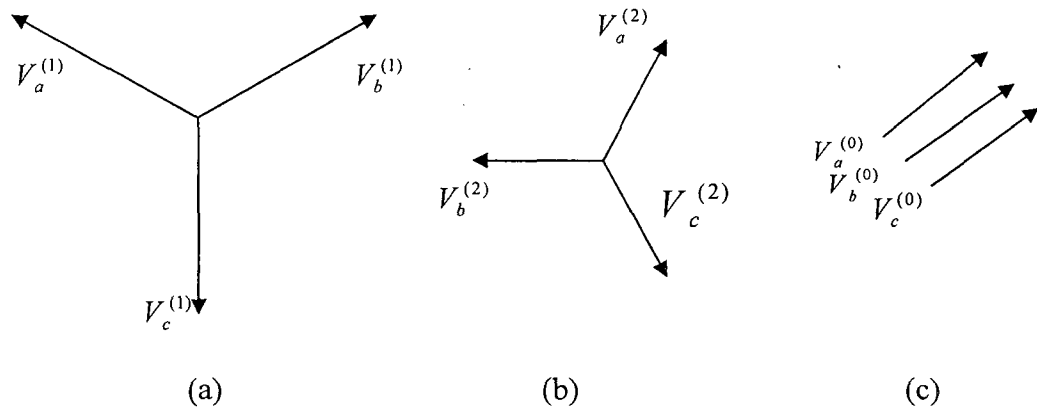


**Figure 3.1: Symmetrical component: (a) positive sequence, (b) negative sequence, and (c) zero sequence**

From figure 3.1-a

$$\left. \begin{aligned} V_a^{(1)} &= V_a^{(1)} \angle 0^\circ = V_a^{(1)} \\ V_b^{(1)} &= V_a^{(1)} \angle 240^\circ = a^2 V_a^{(1)} \\ V_c^{(1)} &= V_a^{(1)} \angle 120^\circ = a V_a^{(1)} \end{aligned} \right\} \quad (3.1)$$

From figure 3.1-b

$$\left. \begin{aligned} V_a^{(2)} &= V_a^{(2)} \angle 0^\circ = V_a^{(2)} \\ V_b^{(2)} &= V_a^{(2)} \angle 120^\circ = a V_a^{(2)} \\ V_c^{(2)} &= V_a^{(2)} \angle 240^\circ = a^2 V_a^{(2)} \end{aligned} \right\} \quad (3.2)$$

From figure 3.1-c

$$V_a^{(0)} = V_b^{(0)} = V_c^{(0)} \quad (3.3)$$

Where  $a = 1 \angle 120^\circ$ .

Any three phase unbalanced system can be resolved into balanced systems of phasor as follows:

- 1- Positive-sequence components consisting of three phasors equal in magnitude, displaced from each other by  $120^\circ$  in phase, and having the same phase sequence as the original phasors,
- 2- Negative-sequence components consisting of three phasors equal in magnitude, displaced from each other by  $120^\circ$  in phase, and having the phase sequence opposite to that of the original phasors, and
- 3- Zero-sequence components consisting of three phasors equal in magnitude and with zero phase displacement from each other [59].

From the 3.1-3.3 and definition of symmetrical components, one can rewrite the symmetrical components in terms of phase a components

$$\begin{bmatrix} V_a \\ V_b \\ V_c \end{bmatrix} = \begin{bmatrix} 1 & 1 & 1 \\ 1 & a^2 & a \\ 1 & a & a^2 \end{bmatrix} \begin{bmatrix} V_a^0 \\ V_a^+ \\ V_a^- \end{bmatrix} \Rightarrow A = \begin{bmatrix} 1 & 1 & 1 \\ 1 & a^2 & a \\ 1 & a & a^2 \end{bmatrix}$$

$$\text{Where } \underline{a = 1\angle 120^\circ}, A = \begin{bmatrix} 1 & 1 & 1 \\ 1 & a^2 & a \\ 1 & a & a^2 \end{bmatrix}$$

$$\begin{bmatrix} V_a \\ V_b \\ V_c \end{bmatrix} = A \begin{bmatrix} V_a^0 \\ V_a^+ \\ V_a^- \end{bmatrix}$$

$$\begin{bmatrix} V_a^0 \\ V_a^+ \\ V_a^- \end{bmatrix} = A^{-1} \begin{bmatrix} V_a \\ V_b \\ V_c \end{bmatrix} \Rightarrow \begin{bmatrix} V_a^0 \\ V_a^+ \\ V_a^- \end{bmatrix} = \frac{1}{3} \begin{bmatrix} 1 & 1 & 1 \\ 1 & a & a^2 \\ 1 & a^2 & a \end{bmatrix} \begin{bmatrix} V_a \\ V_b \\ V_c \end{bmatrix} \Rightarrow$$

$$\begin{aligned}
V_a^0 &= \frac{1}{3}(V_a + V_b + V_c) \\
V_a^+ &= \frac{1}{3}(V_a + aV_b + a^2V_c) \\
V_a^- &= \frac{1}{3}(V_a + a^2V_b + aV_c)
\end{aligned}
\tag{3.4}$$

Where:

$V_a^0$ : Zero sequence	$V_a$ : Voltage of phase a
$V_a^+$ : Positive sequence	$V_b$ : Voltage of phase b
$V_a^-$ : Negative sequence	$V_c$ : Voltage of phase c

Equation 3.4 represent the symmetrical components for phase a figure 3.2, is showing a graphical addition of the components to obtain the three unbalanced phasors.

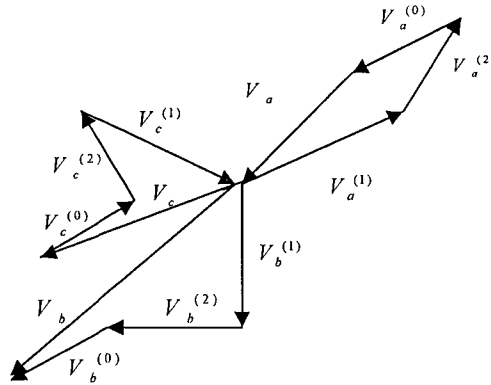


**Figure 3.2: Graphical addition of the components to obtain three unbalanced phasors**

In this Dissertation, we use symmetrical components to demonstrate that the response of unbalanced system has a unique pattern of its own and will integrate such an attribute to create a signature of each fault, regardless of its type, can be identified and classified in a fully automated framework.

### 3.2 Signature Estimation of Fault Signal

Figure 3.3 represents a 3-phase system signals in the time domain extracted from a power system. In Part a, the three current signals from each phase are shown while part b is showing the diagram of the difference signal,  $\Delta S$ , from an unbalanced three-phase system.

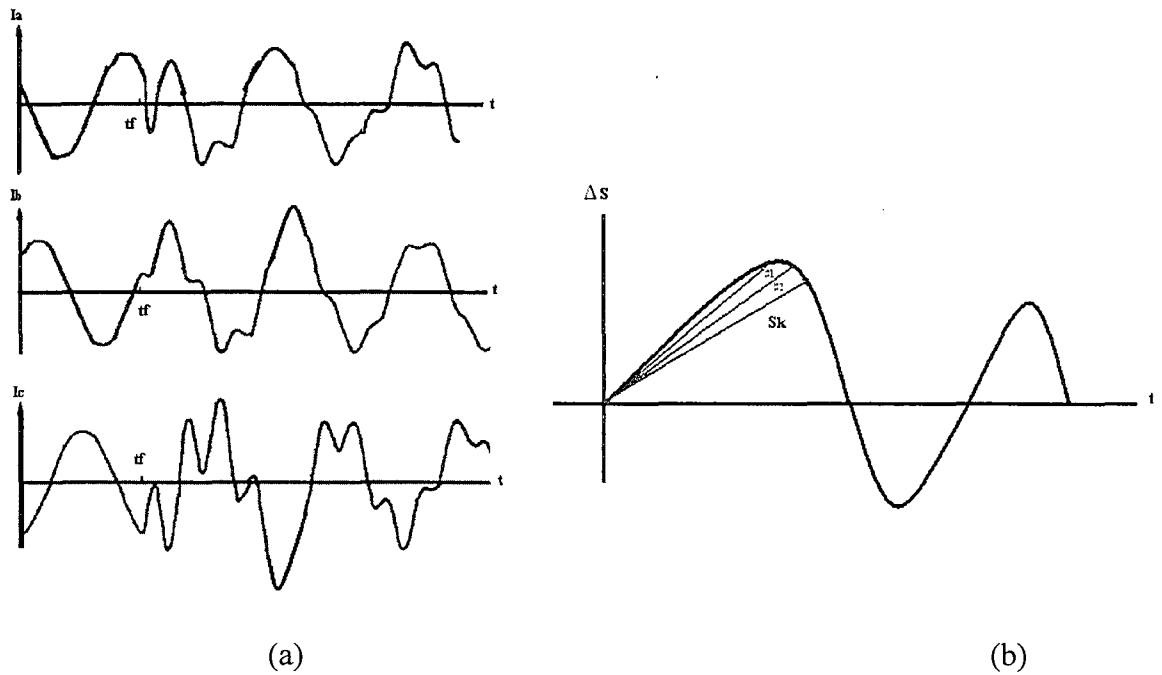


**Figure 3.3: Unbalanced system signals: (a) each phase signal and (b) difference signal of current wave for phase a under a fault condition**

The difference signal  $\Delta S$  between current signal and its previous reading at each  $(1/4)^{\text{th}}$  of a cycle is generated at the sending end of the transmission line. The difference signal, shown in figure 3.2.b, at each instant of time is assumed to model a line equation of the form:

$$A\Delta S + Bt + C = 0 \tag{3.5}$$

where A, B and C are constant derived from line specific intersect points. Once  $\Delta S$  is modeled using the line equation given in Eq.3.5, it is used to transform the data into a phasor domain by transforming each value of the difference signal as a magnitude and phase of its line representation using Eq.3.6 and producing the vectors in the  $\rho$ - $\lambda$  space as

$$\rho = \begin{bmatrix} B \\ -A \end{bmatrix} \lambda + \begin{bmatrix} 0 \\ -\frac{C}{B} \end{bmatrix} \quad (3.6)$$

The magnitude and phase values for this new vector representation are computed using equations 3.7 and 3.8 as follows:

$$|r| = \sqrt{B^2 + \left(-A + \frac{C}{B}\right)^2} \quad (3.7)$$

$$\alpha = \tan^{-1} \frac{\left(-A + \frac{C}{B}\right)}{B} \quad (3.8)$$

where  $|r|$  and  $\alpha_k$  are the mathematical magnitude and phase at each value of the  $\Delta S$  signal, respectively. Considering three variables for the three phases  $a$ ,  $b$ , and  $c$ , we will produce the following 3-phase set of equations:

$$\begin{aligned} r_{1-ia} &= |r_{1-ia}| \angle \alpha_1 \\ r_{1-ib} &= |r_{1-ib}| \angle \gamma_1 \\ r_{1-ic} &= |r_{1-ic}| \angle \beta_1 \end{aligned} \quad (3.9)$$

where  $|r_{1-ia}|$ ,  $|r_{1-ib}|$ , and  $|r_{1-ic}|$  are the mathematical magnitude values at one instant of  $\Delta S$  signal for phase a, b, and c, respectively and  $\alpha_1$ ,  $\gamma_1$ , and  $\beta_1$  are the mathematical phase values at one instant of the of  $\Delta S$  signal for phase a, b and c, respectively. Our data transformation is followed by a transformation into symmetrical components via the symmetrical components technique [17], which allows for systematic analysis and design of three phase systems as shown in Eq.3.10. In the left hand side of Eq.3.10 are the

sought symmetric quantities while the right hand side is the system phasor quantities. In Eq.3.11 we replace the phasor quantities of Eq.3.10 by our transformed data of the difference signal  $\Delta S$ ,

$$\begin{bmatrix} I_a^0 \\ I_a^+ \\ I_a^- \end{bmatrix} = \frac{1}{3} \begin{bmatrix} 1 & 1 & 1 \\ 1 & a & a^2 \\ 1 & a^2 & a \end{bmatrix} \begin{bmatrix} I_a \\ I_b \\ I_c \end{bmatrix} \quad (3.10)$$

$$\begin{bmatrix} P_{1-ia}^+ \\ P_{1-ia}^- \\ P_{1-ia}^0 \end{bmatrix} = \frac{1}{3} \begin{bmatrix} 1 & a^2 & a \\ 1 & a & a^2 \\ 1 & 1 & 1 \end{bmatrix} \begin{bmatrix} r_{1-ia} \\ r_{1-ib} \\ r_{1-ic} \end{bmatrix} \quad (3.11)$$

This allows us to capture the symmetric components of  $\Delta S$  by generating positive and negative patterns of each instant. Hence for total  $k$  samples, the symmetrical components will be:

$$\left. \begin{aligned} P_{1-ia}^+ &= \frac{1}{3}(r_{1-a} + a^2 r_{1-b} + a r_{1-c}) & P_{k-ia}^+ &= \frac{1}{3}(r_{k-a} + a^2 r_{k-b} + a r_{k-c}) \\ P_{1-ia}^- &= \frac{1}{3}(r_{1-a} + a r_{1-b} + a^2 r_{1-c}), \dots, & P_{k-ia}^- &= \frac{1}{3}(r_{k-a} + a r_{k-b} + a^2 r_{k-c}) \\ P_{1-ia}^0 &= \frac{1}{3}(r_{1-a} + r_{1-b} + r_{1-c}) & P_{k-ia}^0 &= \frac{1}{3}(r_{k-a} + r_{k-b} + r_{k-c}) \end{aligned} \right\} \quad (3.12)$$

Leading to

$$\begin{bmatrix} P_{k-ia}^+ \\ P_{k-ia}^- \\ P_{k-ia}^0 \end{bmatrix} = \frac{1}{3} \begin{bmatrix} 1 & a^2 & a \\ 1 & a & a^2 \\ 1 & 1 & 1 \end{bmatrix} \begin{bmatrix} |r_{k-a}| \angle \alpha_k \\ |r_{k-b}| \angle \gamma_k \\ |r_{k-c}| \angle \beta_k \end{bmatrix}$$

by computing  $P_{k-ia}^+$  and  $P_{k-ia}^-$  over a time series all within  $(1/4)^{\text{th}}$  of a cycle, we generate, shown in Eq.3.13 the positive and negative signatures which is a model for any

unbalanced and nondeterministic time three-phase system which was allowed by symmetrical components method utilization.

$$P_{ia}^+ = [P_{1-ia}^+, P_{2-ia}^+, P_{3-ia}^+, \dots, P_{k-ia}^+] \quad (3.13a)$$

$$P_{ia}^- = [P_{1-ia}^-, P_{2-ia}^-, P_{3-ia}^-, \dots, P_{k-ia}^-] \quad (3.13b)$$

Figure 3.4 shows a plot of the unique signature of phase a in a 3-phase system with a fault *a-g* only generated by plotting  $P_{ia}^+$  versus  $P_{ia}^-$ . Other signature samples are presented in the experimental work in chapter 4.

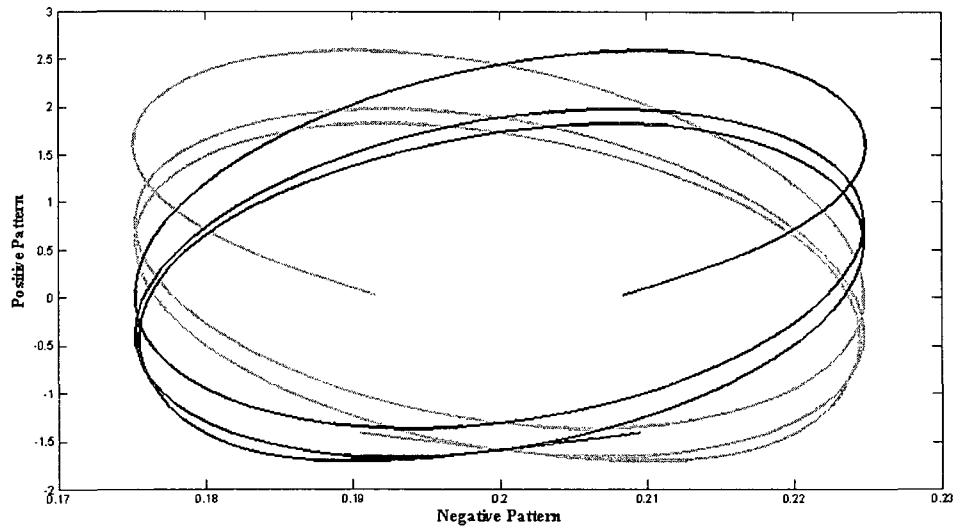


**Figure 3.4:** A plot of the unique signature of phase a in a 3-phase system with a fault *a-g* only

### 3.3 Generate Fault Signatures Using Current Values Only

Most methods of fault detection and classification depend on measurements of electrical quantities provided by current and voltage transformers from the two ends of the system. Such data collection can be expensive and requires physical contact with the

monitored high voltage equipments and several communication devices between the two ends of transmission line.

This section presents a method for pattern calculation in power system relaying signals. The presented method is computationally inexpensive. Simulation results clearly indicate that the method is capable of responding with a fault alert and type instantaneously once a disturbance occur. Moreover, this algorithm requires the knowledge of the voltage or current fault signal from one end of the system. By represent the (3.13a) and (3.13b) in the same plan the fault signatures will be generated. The output of this process will then be supplied into the classification process to detect the fault and obtain a classification for the event. This proposed work is implemented and simulated using several PSCAD simulations. In figure 3.5 a functional block diagram for the framework steps is shown.

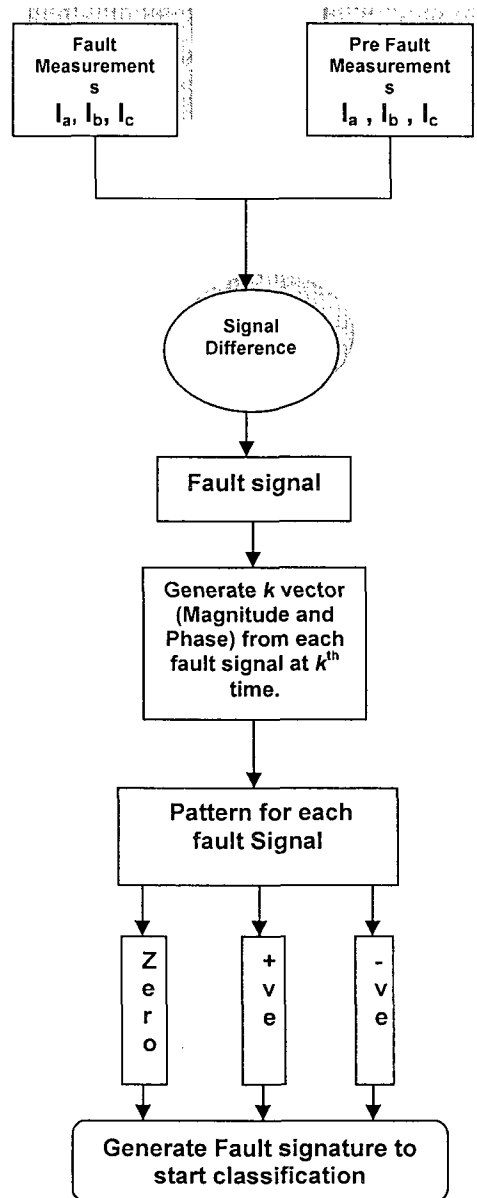


**Figure 3.5: Functional diagram for generating faults' signatures using the symmetrical patterns discussed in section 3.3**

### **3.4 Principal Component Analysis Based Fault Detection and Classification**

PCA has proven to achieve excellent results in feature extraction and data reduction in large datasets [61-63]. Typically PCA is utilized to reduce the dimensionality of a dataset in which there are a large number of interrelated variables

while the current variation in the dataset is maintained as much as possible. This reduction is accomplished by transforming the original set of variables to a new set of variables that are uncorrelated and ordered by their significance so that the first few variables retain most of the variation present in all of the original data. PCA has many applications in signal understanding and pattern recognition that includes pattern matching [64 and 65], neural networks [62, 66], speech analysis [67], visual learning [68, 69], and active vision [70]. In feature recognition, PCA has been extensively used to identify face features [71].

The principal components (PCs) are calculated using the covariance matrix after a simple normalization procedure. Then the covariance matrix is calculated for these images simply as

$$\text{cov}(P_{ia}^+, P_{ia}^-) = \frac{\sum [(P_{ia}^+ - \overline{P_{ia}^+})(P_{ia}^- - \overline{P_{ia}^-})]}{(k-1)} \quad (3.14)$$

Where  $P_{ia}^+$  the symmetrical positive pattern and  $P_{ia}^-$  the symmetrical negative pattern generated by Eq. (3.13). For an  $n \times n$  covariance matrix,  $n$  PCs and consequently  $n$  eigenvalues can be found using Eq. (3.15).

$$C\alpha_n = \lambda_n\alpha_n \quad (3.15)$$

where  $C$  is the covariance matrix;  $\alpha_n$  is the principal component in the  $n^{\text{th}}$  dimension and  $\lambda_n$  is its corresponding eigenvalue. The PCs are then sorted in the order of their significance. Eigenvectors (principal components) related to eigenvalues with higher value carry major information of the given data and thus eigenvectors related to small eigenvalues can be discarded. Feature matrix is constructed from principal eigenvectors

$p$ ; the  $n \times p$  matrix constructed from the principal components is also ordered by their significance.

In this work, once all data, reading of Eq. (3.10), are projected onto the principal eigenvectors, a search for pertained data is initiated. Once similar components are found they are determined to be of similar nature also in the original data space. It is common to use distance measures as similarity measures. These may include Chebyshev, Euclidean, Manhattan, City Block, Canberra, and Minkowski, [72]. In this project and based on experimental results the Euclidean distance measure is adapted. This process is summarized in figure 3.5 showing the general framework.

The design of the classifier is based on the projection of the data on the subspaces spanned by the principal components corresponding to the different classes. Pattern templates are preserved into the training set to be used in the classification process that will follow. PCA consists of two phases. The first phase finds  $I$  uncorrelated and orthogonal vectors and the second phase projects the test data into a subspace spanned by these  $v$  vectors, this can be explained in the steps;

1. Construct training matrix,  $A$ , with dimensions of  $N \times M$ , generate its transpose and a normalized matrix  $P_{M \times N}$ .

2. Covariance matrix is found per the following

$$C_{N \times N} = P'_{N \times M} \cdot P_{M \times N} \quad (3.16)$$

3. Let  $\lambda_i$  and  $E_i$ ,  $i = 1, 2 \dots N$  be its Eigen values and Eigenvectors respectively and should satisfy the equation  $[C] [E_i] = \lambda_i [E_i]$  where:  $\lambda_1 \geq \lambda_2 \geq \dots \geq \lambda_n \geq 0$ . Discard all components of values less than a predetermined threshold  $T$ , and retain the rest, these

are the principal components. The second phase projects the given testing data  $A$  into a space spanned by the reduced training matrix  $A_R$  using

$$W_{V \times N} = A'_{R \ V \times M} A_{test \ M \times N} \quad (3.17)$$

4. PCA algorithm in pattern recognition needs to be followed with some other tools to define the similarities. Optimal method to find similarities between two patterns is to find the difference. Minimum distance means maximum similarity. Different types of distance measurements are being used, however Euclidean is the one usually follows PCA algorithm. In this study, Euclidean is employed. This type of distance is the standard metric, which is shortest distance between two points and can be formulated as equation 3.18 for 2D:

$$\left. \begin{aligned} d_x &= \sqrt{\sum (PC_{1-tested-i} - PC_{1-stored-i})^2} \\ d_y &= \sqrt{\sum (PC_{2-tested-i} - PC_{2-stored-i})^2} \end{aligned} \right\} \quad (3.18)$$

The classification process of a fault is divided into two stages; the first is the training procedure using all signatures generated prior to testing, to enforce their projections onto the principal components space. The second stage is the testing process, in which steps in figure 3.4 are followed to project the test pattern onto PCA space followed by measuring for similarity of the PCs using the minimum distance between the stored projections and test one. This minimum distance will identify a match of a pattern to a fault or no fault at all. In figure 3.6 we display the general framework for fault classification.

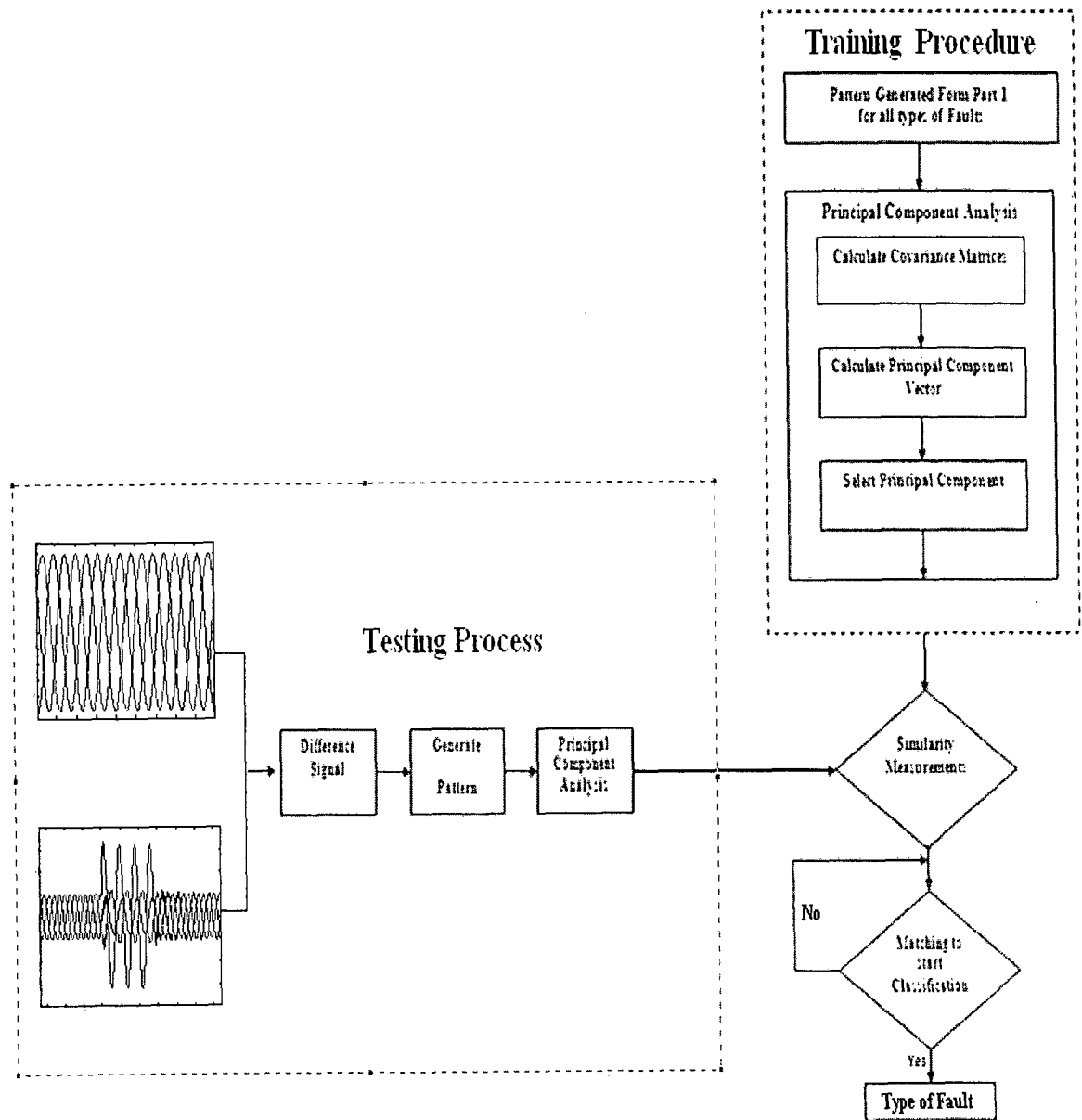


**Figure 3.6: The functional block diagram for fault detection and classification based on principal component analysis**

## CHAPTER 4

### SIMULATION RESULTS ON FAULT DETECTION AND CLASSIFICATION

As a case study, simulation is modeled on a 220KV single circuit transmission lines, 69 km in length, connected to a source at each end as shown in figure 4.1. This system will be simulated with PSCAD/EMTDC. PSCAD was first conceptualized in 1988 and began its long evolution as a tool to generate data files for the EMTDC simulation program. PSCAD Version 4 represents the latest developments in power system simulation software. With much of the simulation engine being fully mature for many years. This software is powerful and easy to use. Version 4 retains the strong simulation models of its predecessors while bringing to the table an updated and fresh new look and feel to its windowing and plotting new single-line representations and new compiler enhancements improve both the accuracy and reliability of the simulation. New editors and easier navigation mean that finding your way and maintaining larger systems is far easier to do [60].

Using PSCAD simulation we generate fault signals for various faults. The power system specifications of figure 4.1 are:

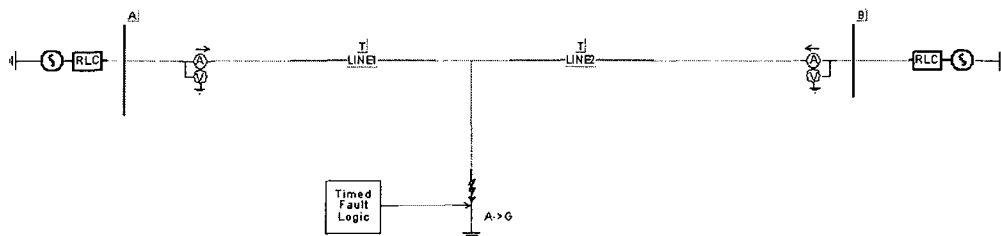


**Figure 4.1: A 220KV single circuit transmission lines using PSCAD/EMTDC simulation**

- Line length = 69 km;
- Source voltages:  $220 \angle \delta$  kV, where  $\delta$  is the load angle;
- Source impedance (both sources):
- Positive sequence impedance =  $1.31 + j15.0 \Omega$ ; zero sequence impedance =  $2.33 + j26.6 \Omega$
- Frequency = 60 Hz;
- Transmission line impedance:
  - Positive sequence impedance =  $8.25 + j94.5 \Omega$ ;
  - Zero sequence impedance =  $82.5 + j308 \Omega$ ;
  - Positive sequence capacitance = 13 nF/km;

#### 4.1 Generate Pattern Training Set

After filtering the signal and generating the zero, positive and negative sequence patterns by utilizing magnitude and angle for the phase current at each instant of time in the current-time space, the fault pattern can then be generated by generating positive and negative patterns or signatures for all phases. The following are the signatures of the all 9 faults simulated.

- **Healthy Conditions**

No fault is the healthy conditions of power system results for the signatures of the phase currents are shown in figure 4.2. We note that pattern (positive and negative sequence for each phase) is pure ellipse shape and this pattern is unique for the no fault conditions.

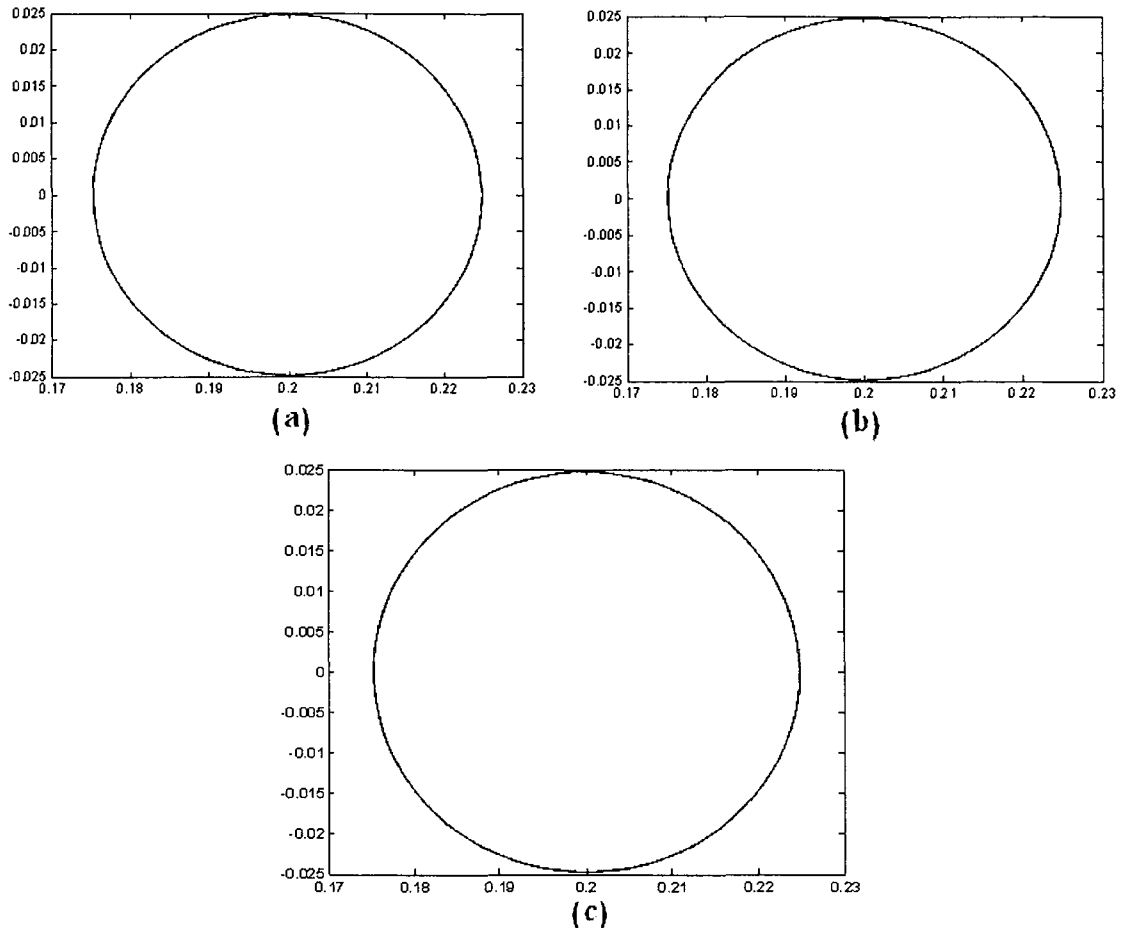


**Figure 4.2: The pattern, positive and negative for each phase: (a) phase a, (b) phase b, and (c) phase c; under healthy conditions**

- **Single Phase to Ground-Fault Phase  $a$  to  $g$**

In this simulation, a fault in phase a-to-ground is modeled. In figure 4.3, we display the Pattern of both the positive and negative sequences. For phase a, the signature is completely different from phase b and c. It is clear that the signature of the faulty line is standing out.

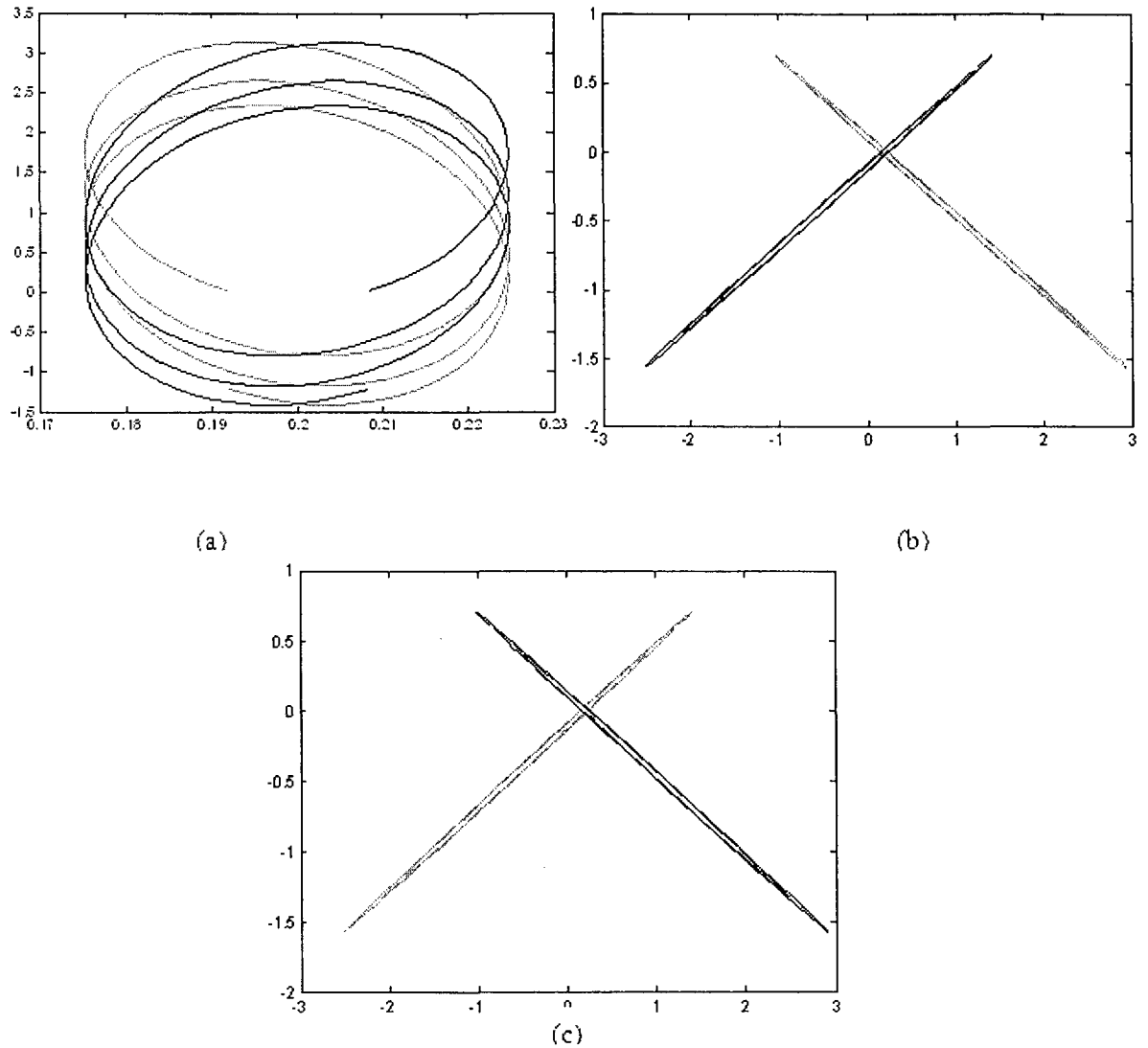


**Figure 4.3: The Pattern of all positive and negative sequences for each phase- (a) phase a, (b) phase b, and (c) phase c for the fault simulation of pages  $a$  to  $g$**

- **Single Phase to Ground-Fault Phase  $bg$**

Figure 4.4 demonstrates the uniqueness of the faulty phase signatures by comparing figure 4.4a to figure 4.4b and c. Clearly, the faulty phase,  $b$ , has more curvature and torsion than the Pattern in phase  $a$  and  $c$ .

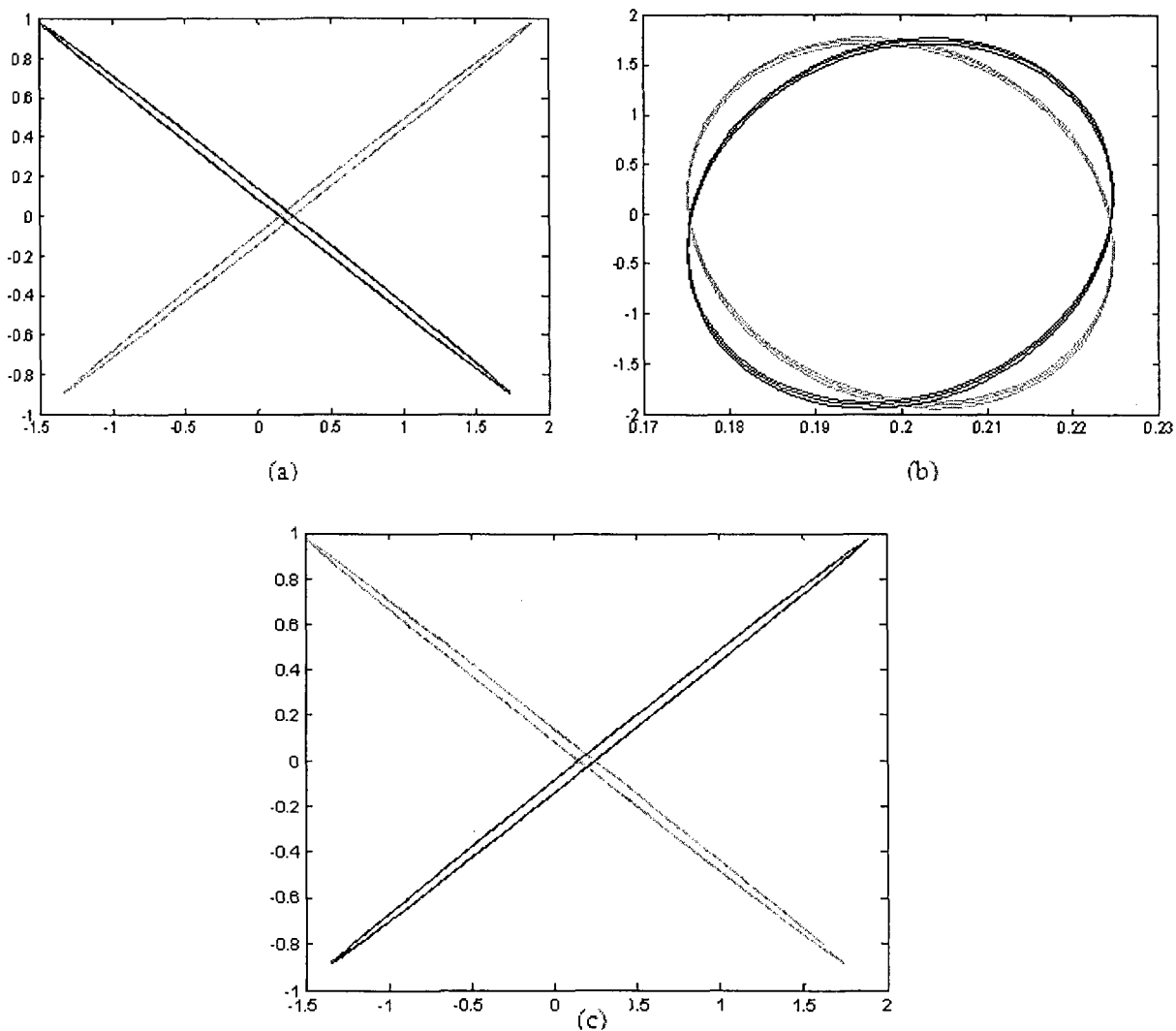


**Figure 4.4: The pattern of both the positive and negative sequences for each phase- (a) phase  $a$ , (b) phase  $b$ , and (c) phase  $c$  for faulty phase  $b$ .**

- **Single Phase to Ground-Fault Phase  $c$  to  $g$**

In the case of a Fault in phase  $c$  to ground, we observe a pattern shown in figure 4.5, we note the Pattern positive and negative sequence for phase  $c$  has more curvature and torsion than the Pattern (positive and negative sequence) in phase  $a$  and  $b$ .

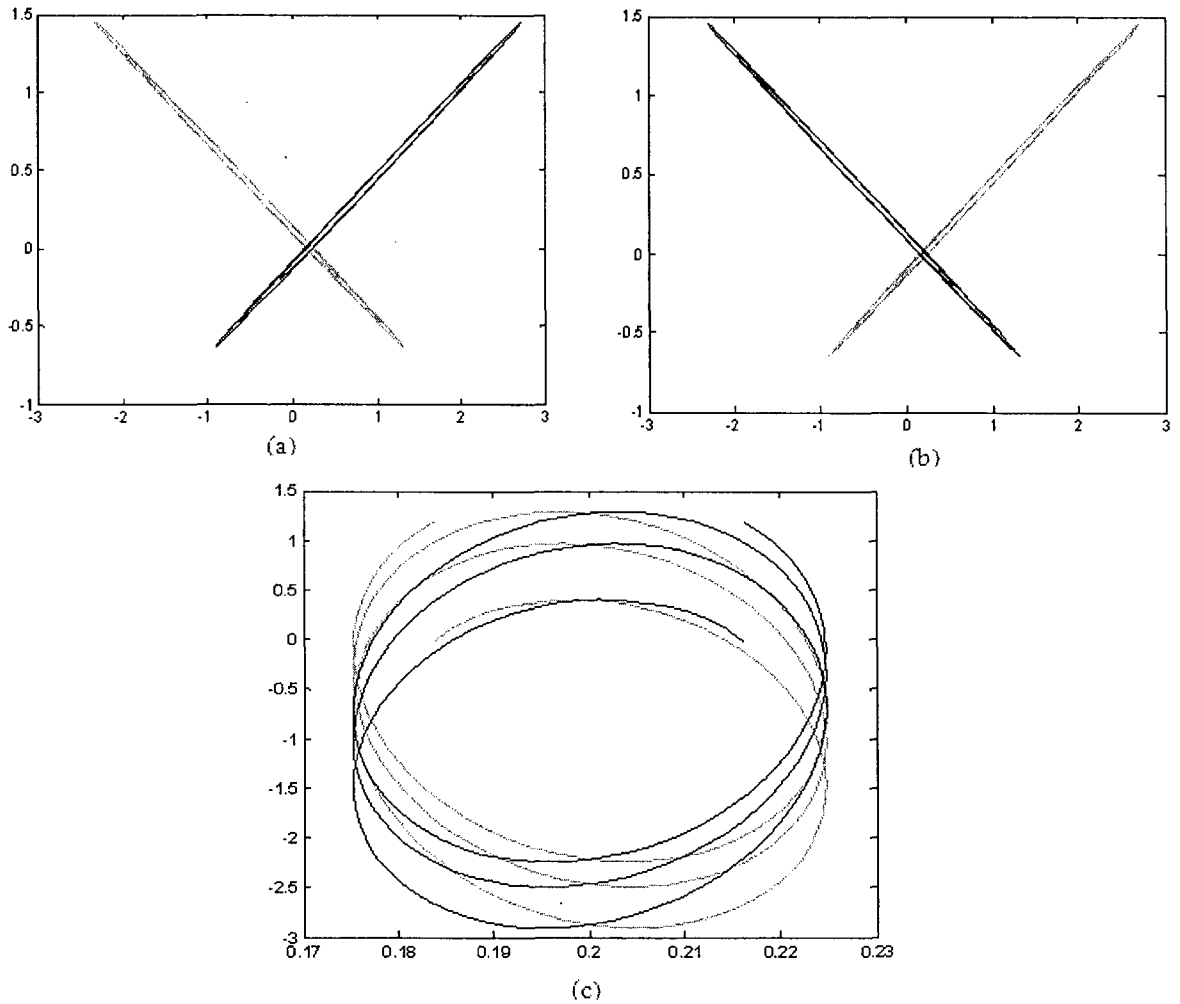


**Figure 4.5: The pattern (positive and negative sequence for each phase) (a) phase  $a$ , (b) phase  $b$  and (c) phase  $c$  for a faulty phase  $c$**

- **Double Phase to Ground-Fault in Phase  $ab$  to  $g$**

The Fault in phase  $a$ - $b$  to ground produced a pattern shown in figure 4.6. Note that the positive and negative sequences for phase  $a$  and phase  $b$  have approximately the same shape (a butterfly shape) which make them easily distinguishable.

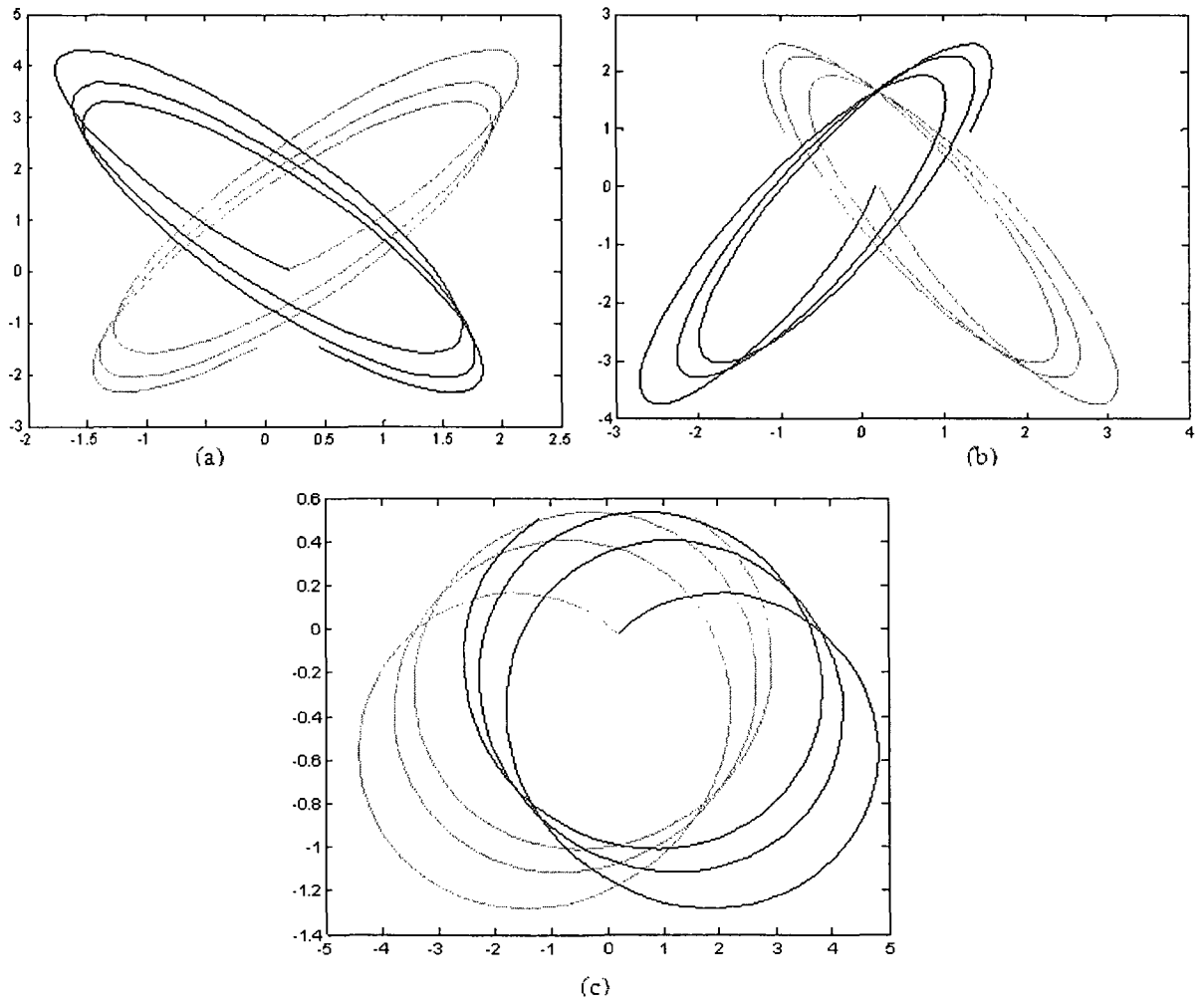


**Figure 4.6: The pattern (positive and negative sequence for each phase) (a) phase  $a$ , (b) phase  $b$  and (c) phase  $c$  of faulty, under faulty conditions of phase  $a$  and phase  $b$**

- **Double Phase to Ground-Fault in Phase  $ac$  to  $g$**

For Fault in phase  $a$ - $c$  to ground is shown in figure 4.7. Note that positive and negative sequences for phase  $a$  and phase  $c$  have approximately the same pattern (a butterfly shape). One can easily distinguish that the faulty lines are different than the healthy one.

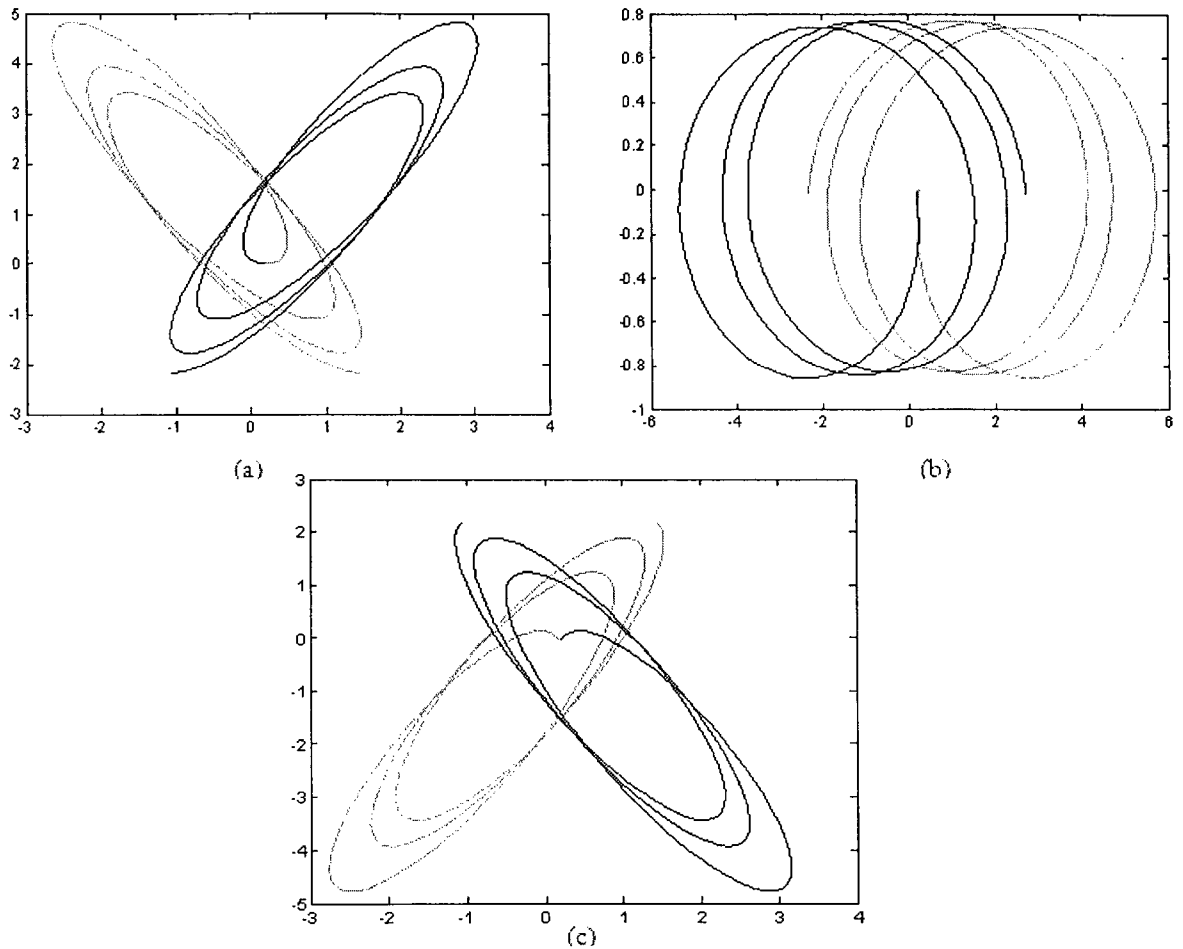


**Figure 4.7: The pattern (positive and negative sequence for each phase) (a) phase  $a$ , (b) phase  $b$  and (c) phase  $c$ , under faulty conditions of phase  $a$  and phase  $c$**

- **Double Phase to Ground-Fault in Phase  $bc$  to  $g$**

For Fault in phase  $b$  and  $c$  to ground we see the result in figure 4.8 , we note the Pattern positive and negative sequence for phase  $b$  and phase  $c$  have both the butterfly shape in contrast to the non-faulty line.

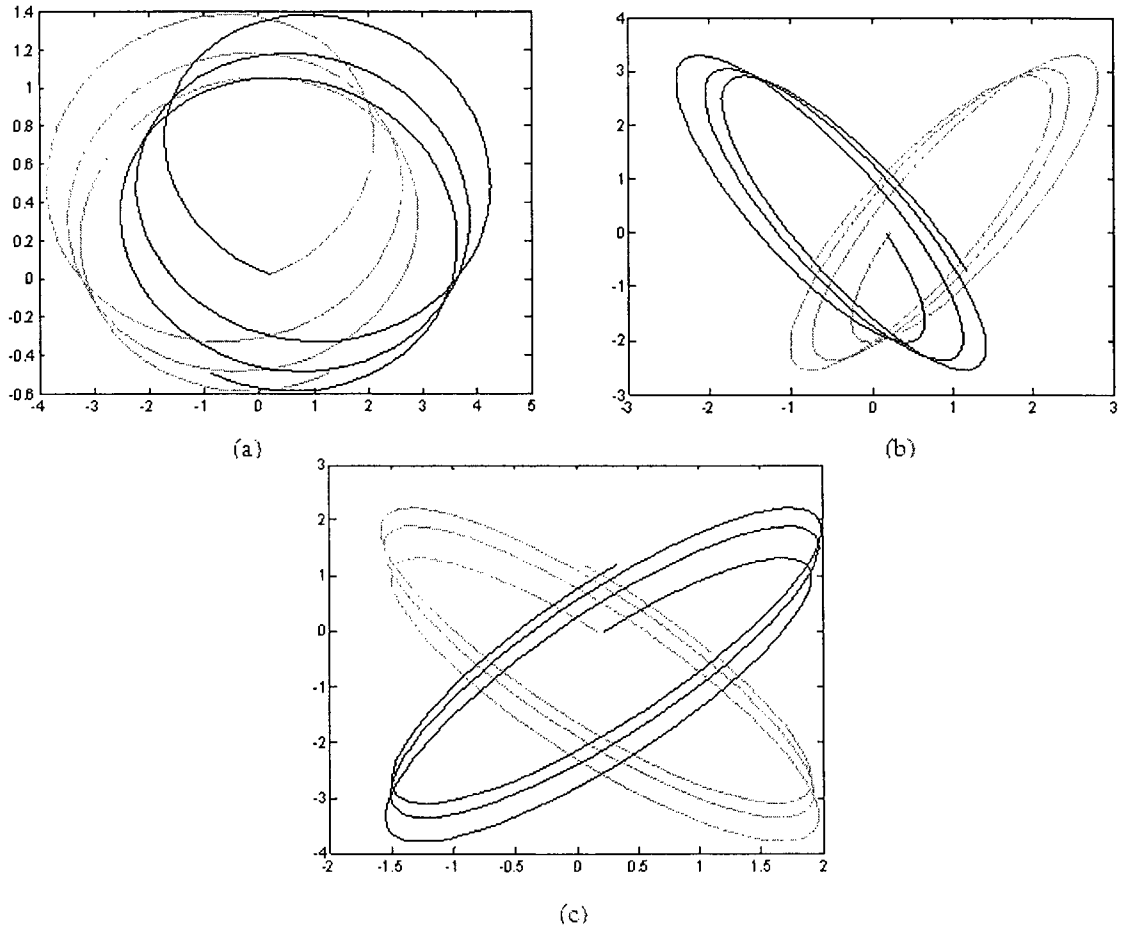


**Figure 4.8: The pattern positive and negative sequences for each phase. In (a) phase  $a$ , (b) phase  $b$ , and (c) phase  $c$  under faulty conditions of phase  $c$  and phase  $b$**

- **Line to Line Fault-Fault Phase  $ab$**

For Fault in phase  $a$  and  $b$  we see the result in figure 4.9, we note the Pattern positive and negative sequence for phase  $a$  and phase  $b$  have approximately the same pattern we can easily distinguishes where the fault is occurring as the pattern for the line that is not involved in the fault is different from the other two.

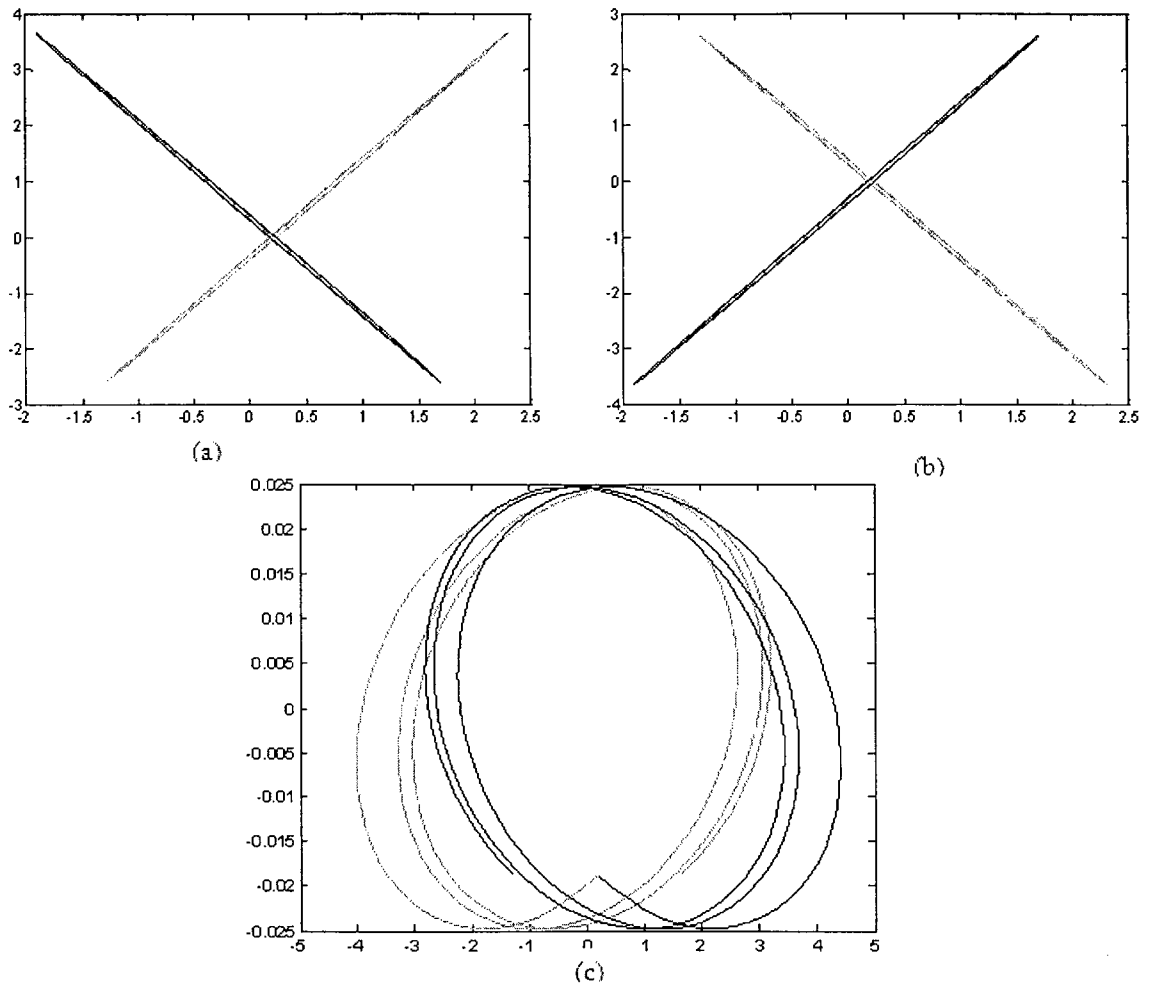


**Figure 4.9:** The pattern of both positive and negative sequences for each phase. (a) phase  $a$ , (b) phase  $b$ , and in (c) phase  $c$  under faulty conditions of phase  $a$  and phase  $b$

- **Line to Line Fault-Fault in Phase  $ac$**

For Fault in phase  $a$  and  $c$  signatures are shown are shown figure 4.10. Symmetrical positive pattern and negative pattern for phase  $a$  and phase  $c$  have approximately the same pattern while phase signatures of  $b$  is distinguished from the faulty signatures.

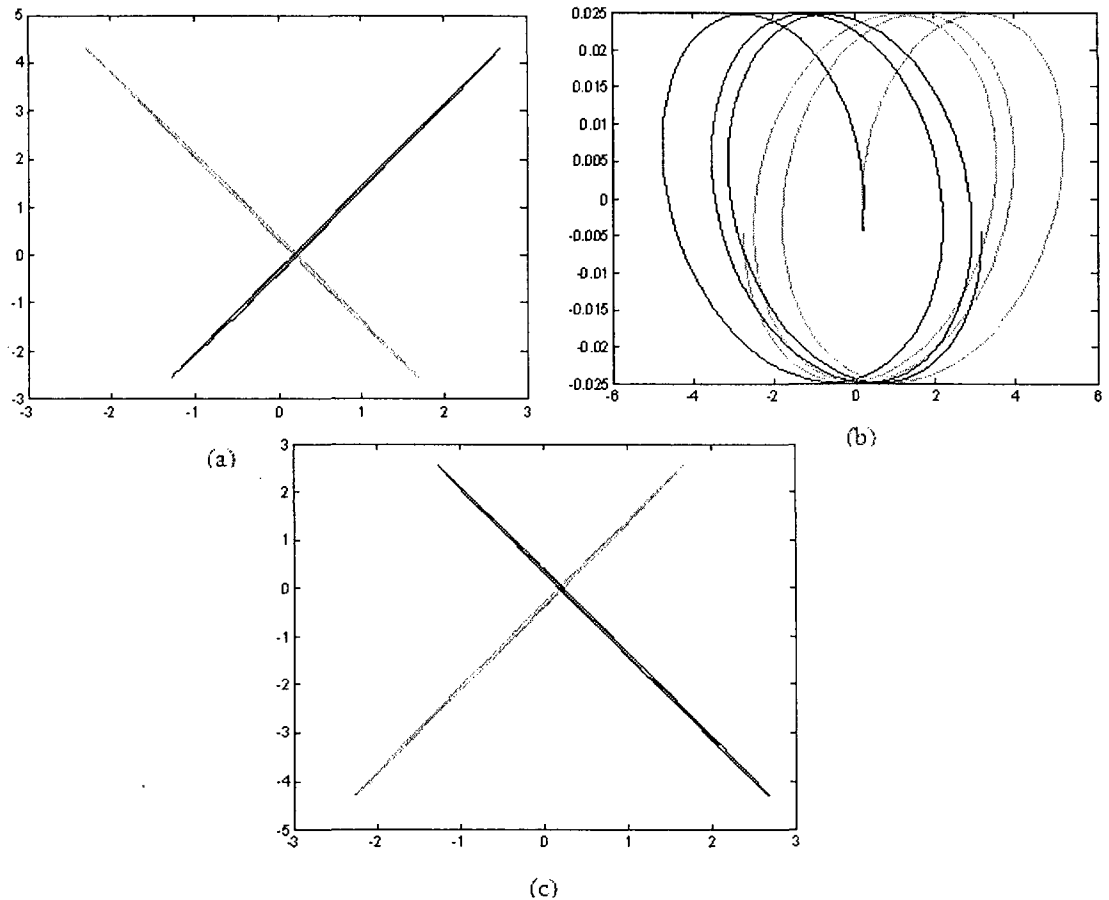


**Figure 4.10: The pattern of both positive and negative sequences for each phase. In (a) phase  $a$  signature, (b) phase  $b$  signature, and in (c) phase  $c$  signature for the faulty conditions involving phase  $ac$**

- **Line to Line Fault-Faulty Phase  $bc$**

For Fault in phase  $b$  and  $c$  signatures are shown in figure 4.11, we note the symmetrical positive pattern and negative pattern for phase  $b$  and phase  $c$  have approximately the same pattern we can easily distinguish where the fault happen in  $ab$  or  $bc$  or  $ac$ .

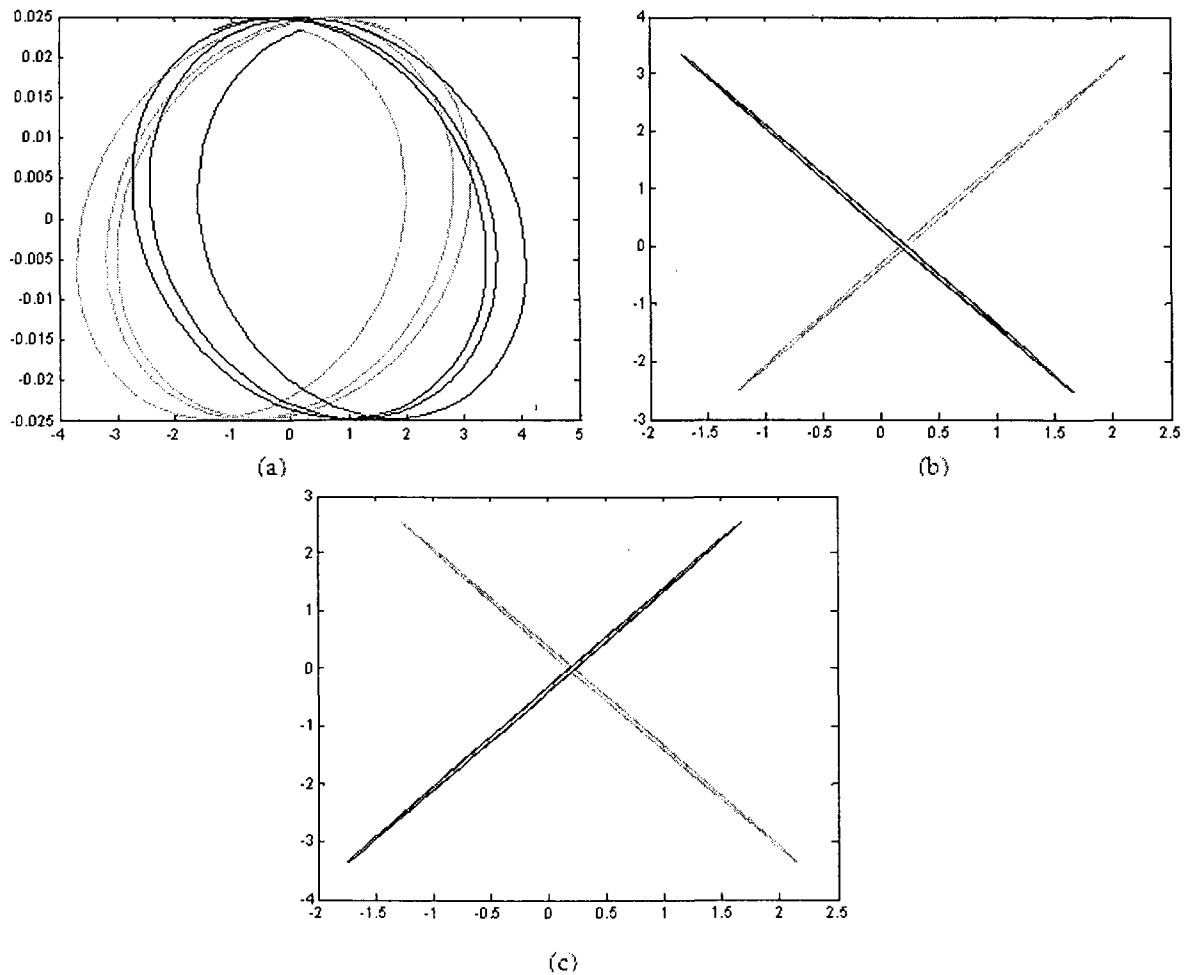


**Figure 4.11: The pattern of both positive and negative sequences for each phase. In (a) phase a signature, (b) phase  $b$  signature, and (c) phase  $c$  signature for the faulty conditions involving phase  $bc$**

- **Symmetrical Fault Three Phase Fault-Fault Phase  $abc$**

A fault in phases  $a$ ,  $b$ , and  $c$  signatures are shown in figure 4.12. We note the Pattern of both the positive and negative sequences for phase  $a$ , phase  $b$ , and phase  $c$  have curvature and torsion. It is evident that these signatures are distinguishable from the healthy conditions and any other faulty conditions.

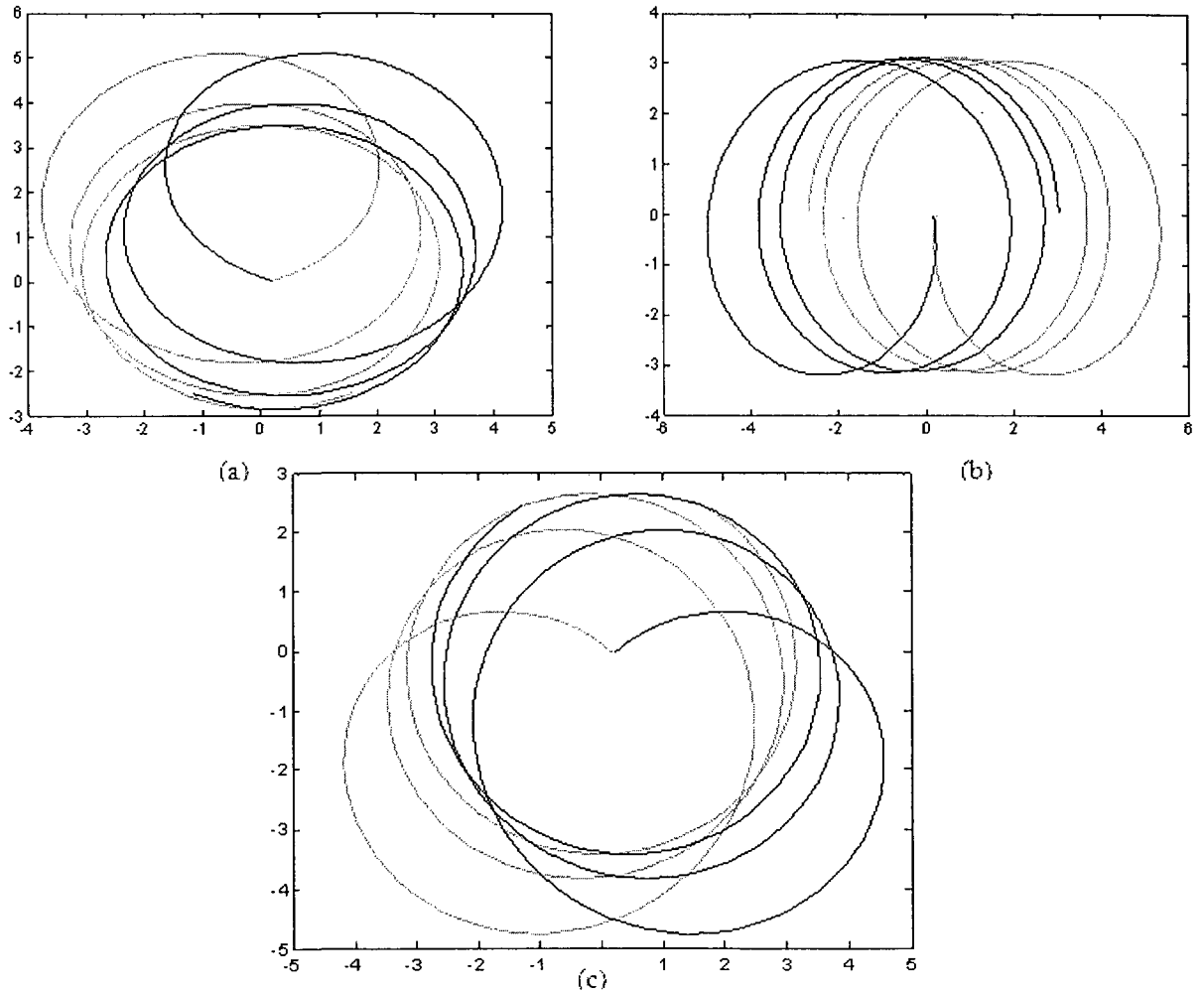


**Figure 4.12: The pattern of the (positive and negative sequences for each phase in a three-phase fault condition. In (a) phase  $a$  signature, (b) phase  $b$  signature, and (c) phase  $c$  signature**

## 4.2 Fault Detection and Classification Based on Principal Component Analysis

Based on the detection and classification method proposed in figure 3.5, this method calculated the principal component analysis of each type of fault and design the classifier according to the projection of the data on the subspaces spanned by the principal component analysis corresponding to different classes, in figure 4.13-figure 4.23 shown the projection of the data on the subspaces .

- **Healthy Conditions**

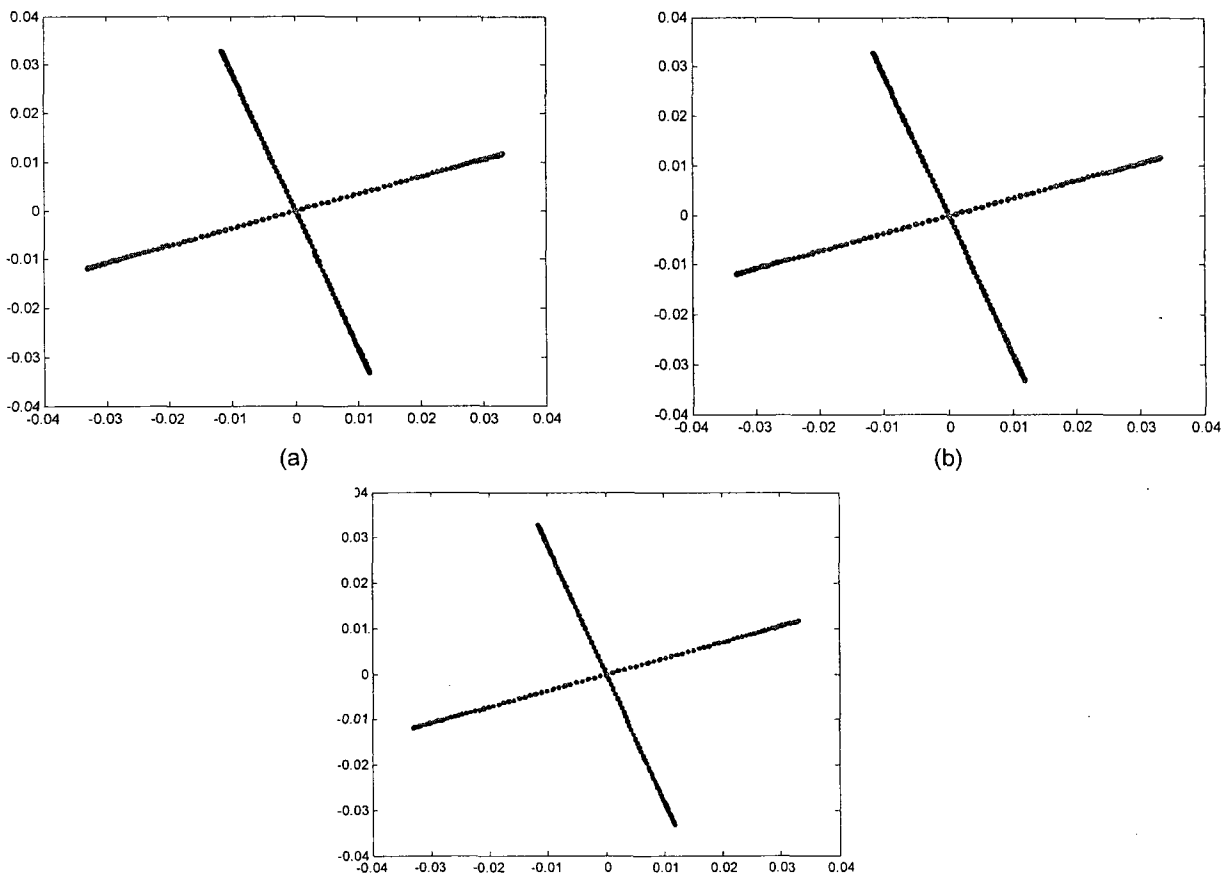


**Figure 4.13: Projection of the data of (positive and negative sequences for each phase) on each principal component. In (a) phase a, (b) phase b, and in (c) phase c**

- **Single Phase to Ground-Fault Phase  $a$  to  $g$**

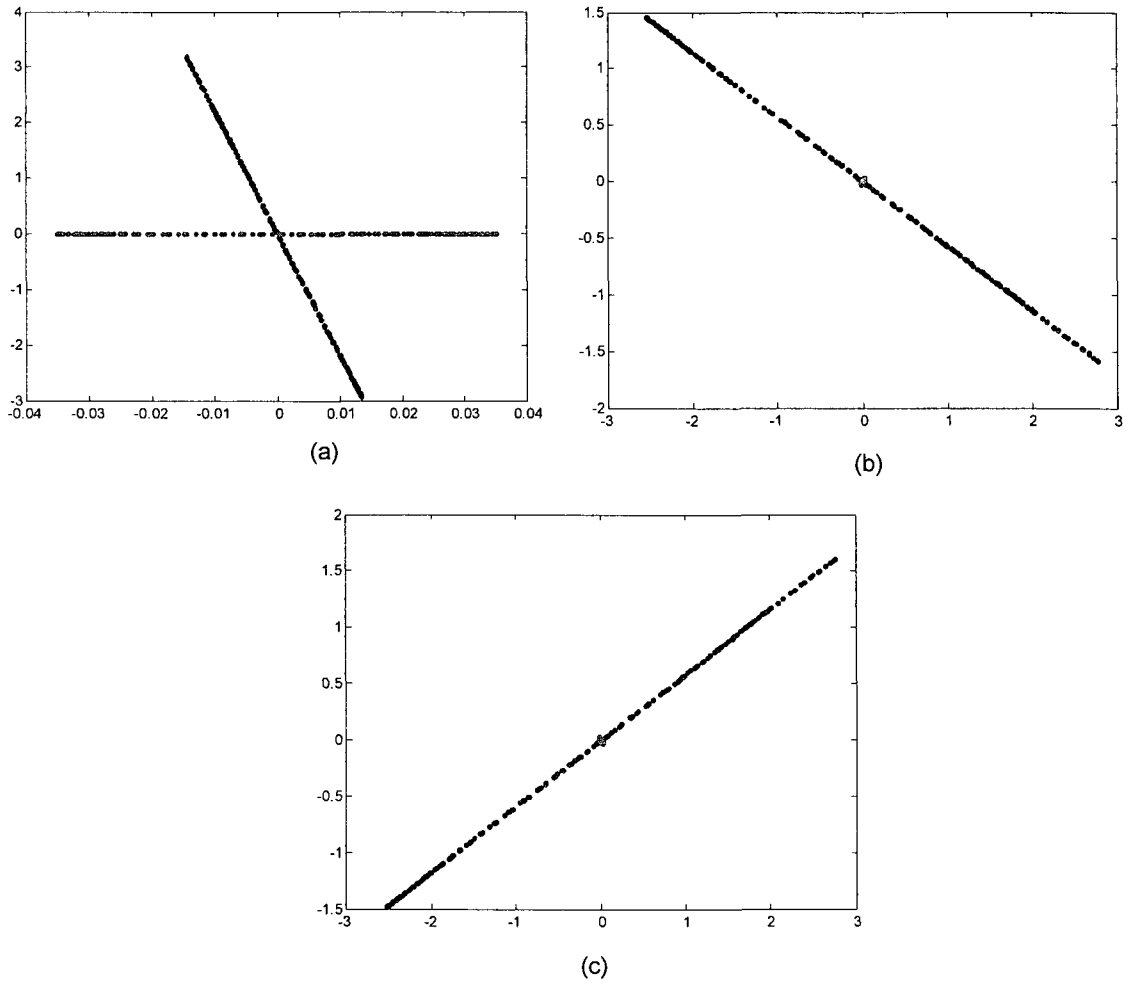


**Figure 4.14: Projection of the data of (positive and negative sequence for each phase) on each principal component (a) phase a, (b) phase b and (c) phase c**

- Single Phase to Ground- Fault Phase  $b$  to  $g$

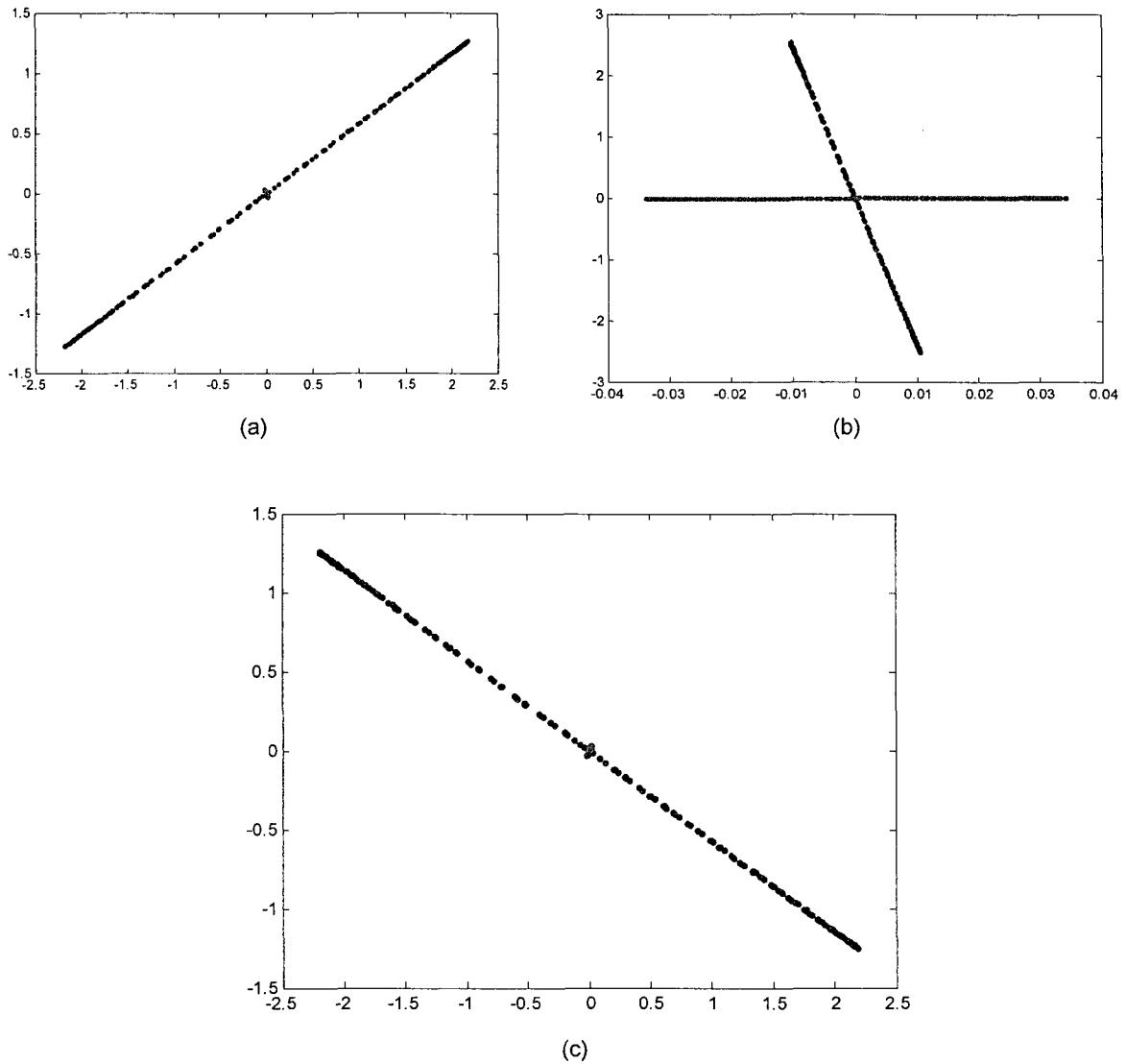
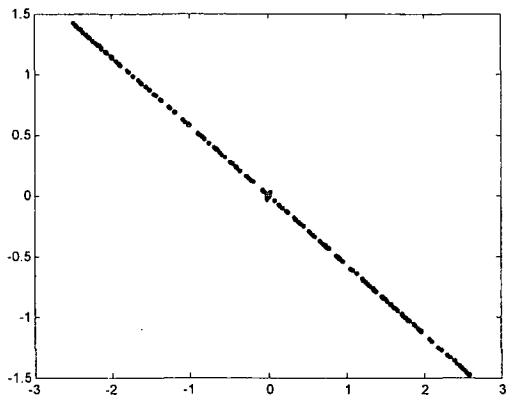
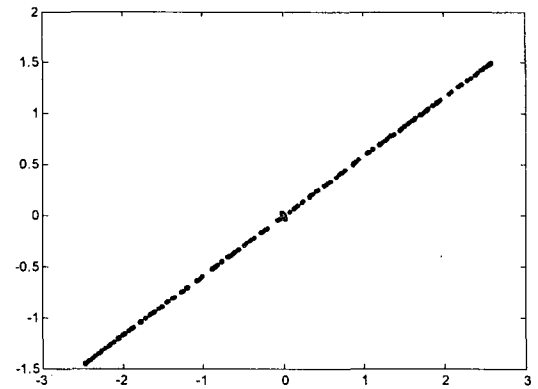


**Figure 4.15: Projection of the data of (positive and negative sequence for each phase) on each principal component. In (a) phase a, (b) phase b, and in (c) phase c**

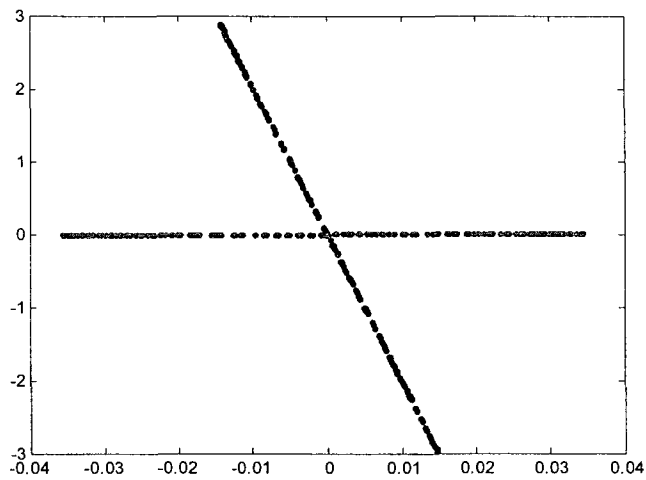
- Single Phase to Ground-Fault Phase  $c$  to  $g$



(a)



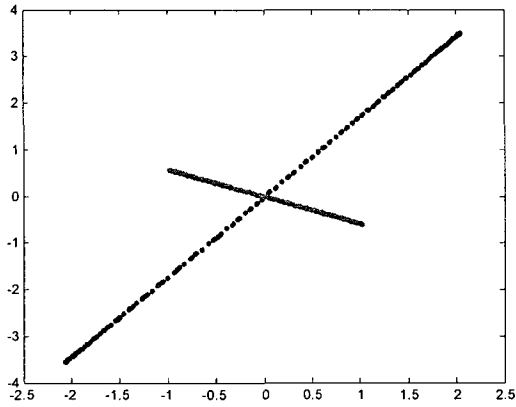
(b)



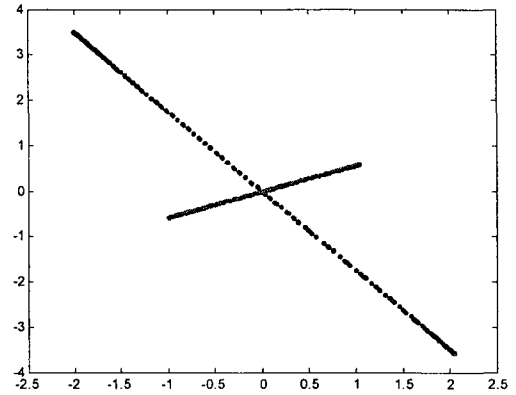
(c)

**Figure 4.16: Projection of the data of (positive and negative sequence for each phase) on each principal component. In (a) phase a, (b) phase b, and in (c) phase c**

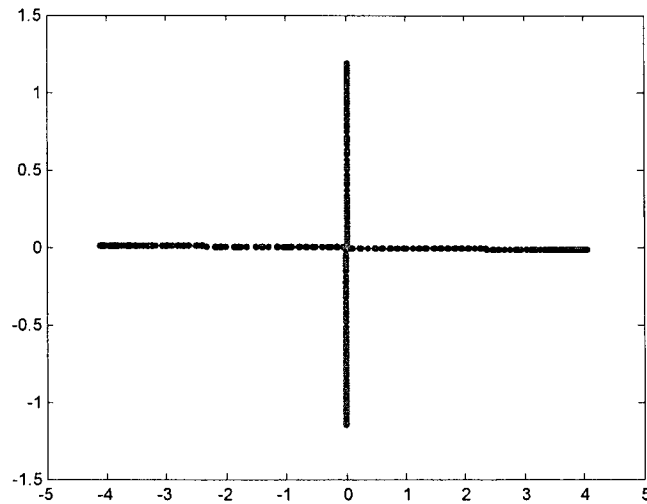
- Double Phase to Ground-Fault Phase  $ab$  to  $g$



(a)



(b)



(c)

Figure 4.17: Projection of the data of (positive and negative sequence for each phase) on each principal component (a) phase a, (b) phase b and (c) phase c

- Double Phase to Ground-Fault Phase  $ac$  to  $g$

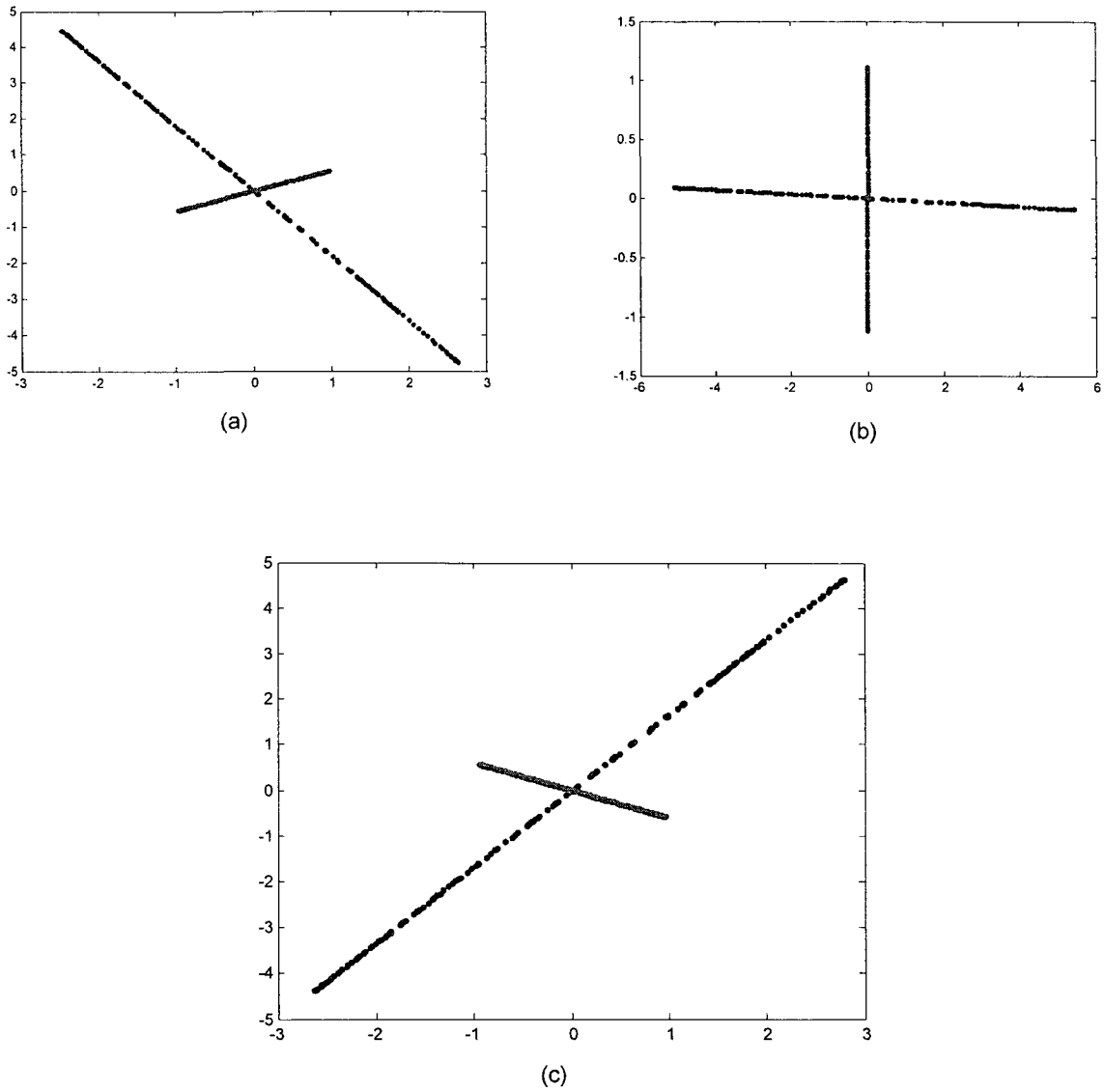
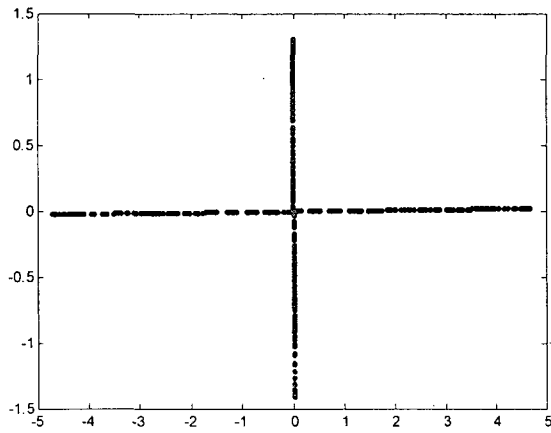
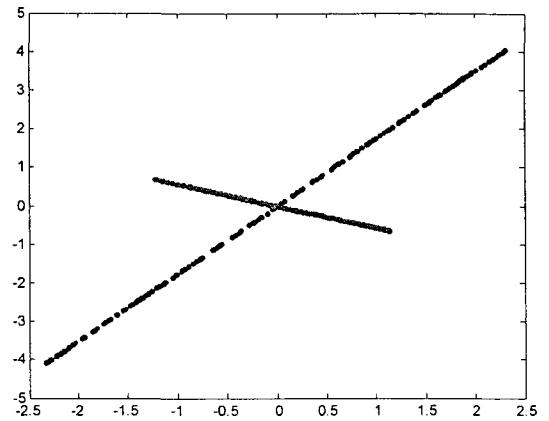


**Figure 4.18: Projection of the data of (positive and negative sequence for each phase) on each principal component (a) phase a, (b) phase b and (c) phase c**

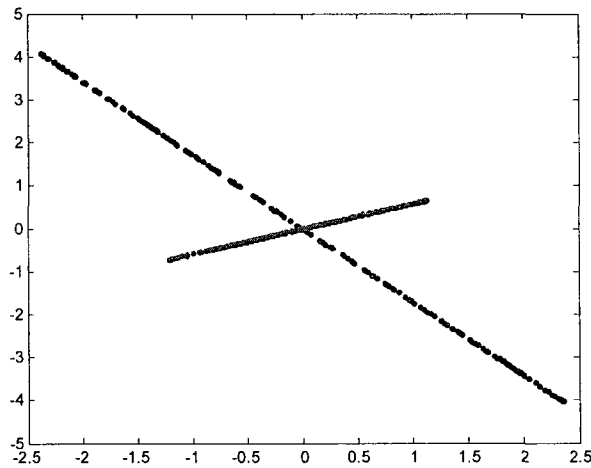
- Double Phase to Ground-Fault Phase  $bc$  to  $g$



(a)



(b)



(c)

Figure 4.19: Projection of the data of (positive and negative sequence for each phase) on each principal component (a) phase a, (b) phase b and (c) phase

- Phase to Phase-Fault Phase  $ab$

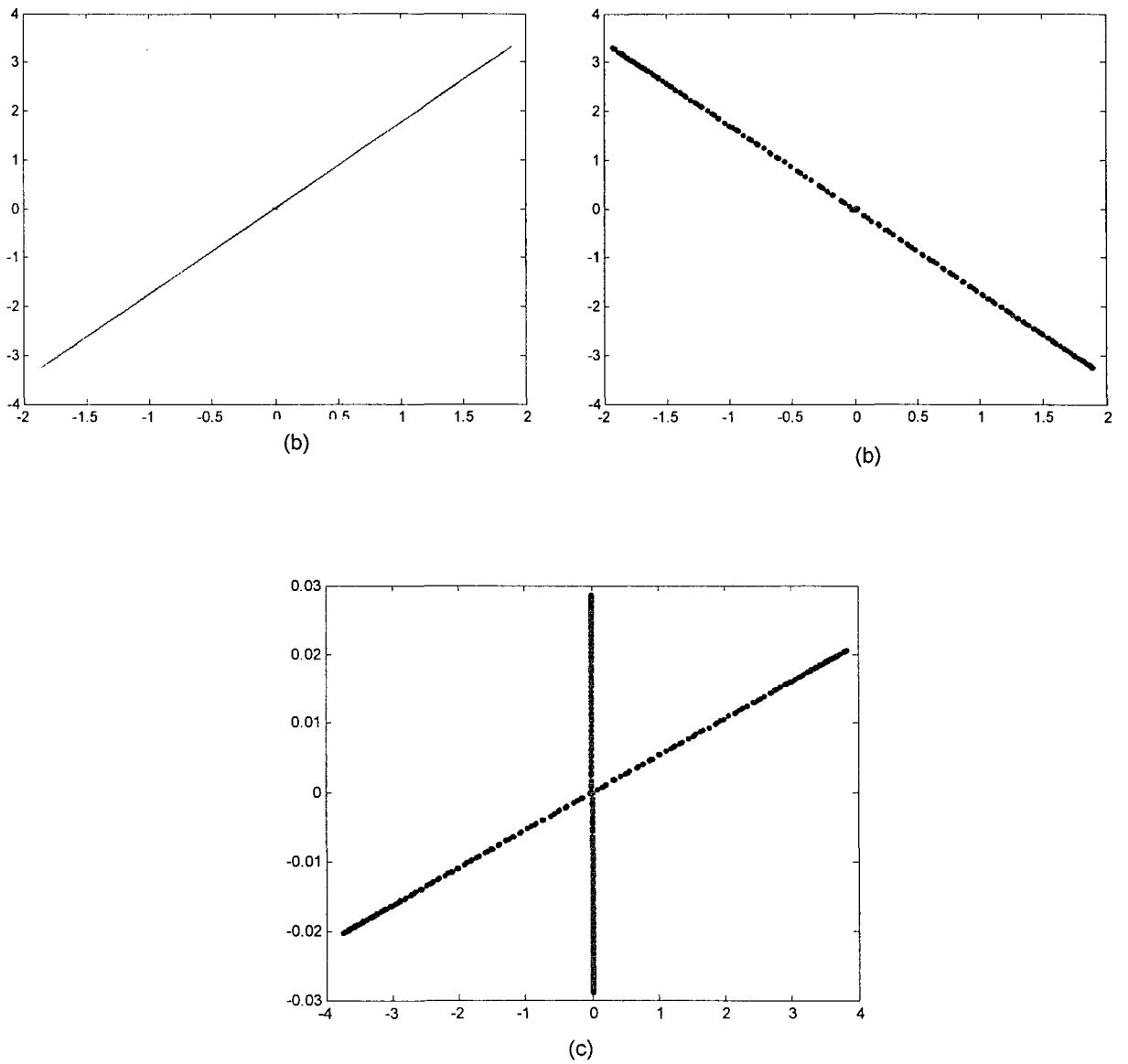


Figure 4.20: Projection of the data of (positive and negative sequence for each phase) on each principal component. In (a) phase a, (b) phase b, and in (c) phase c

• Phase to Phase-Fault Phase *ac*

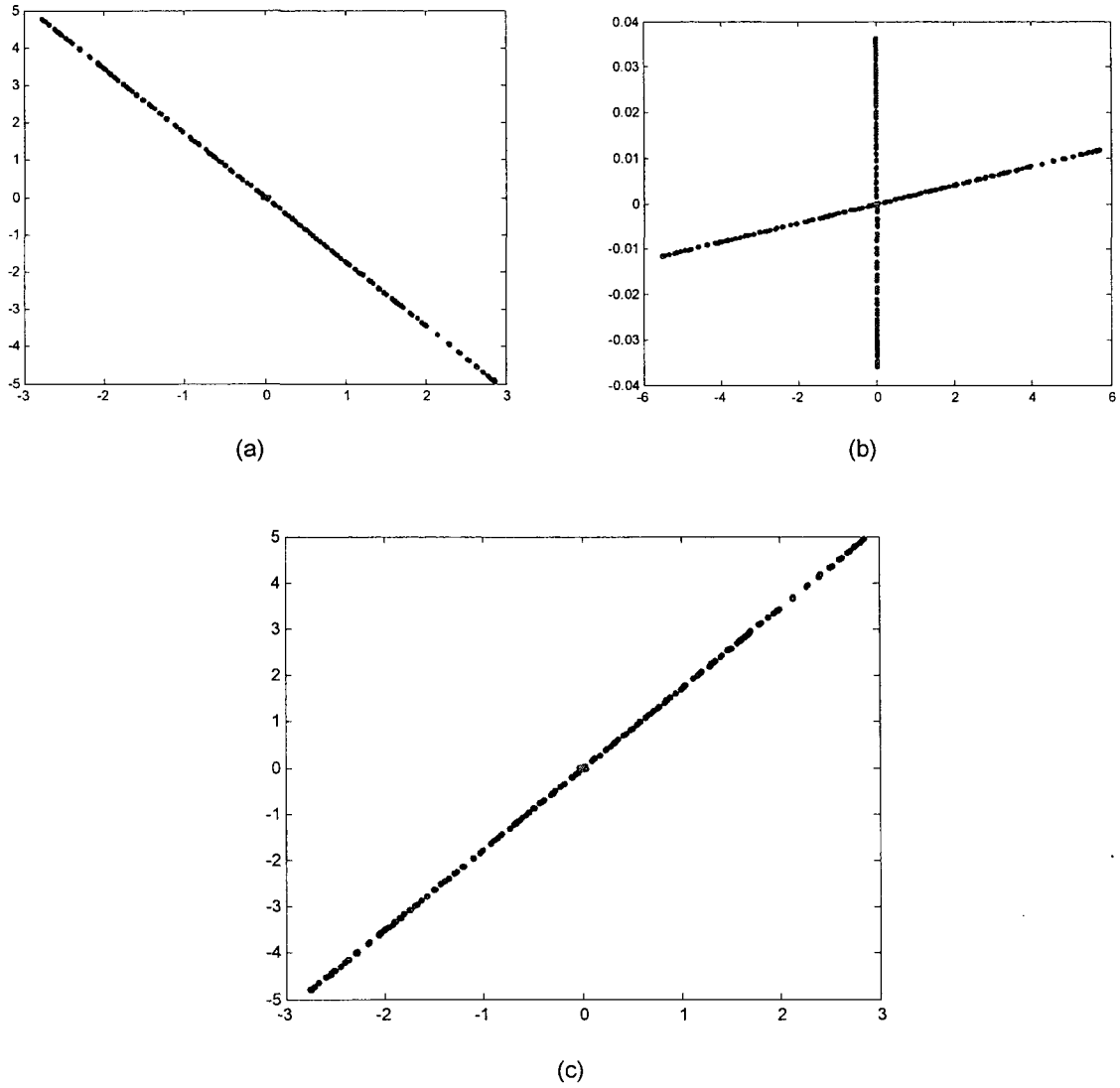


Figure 4.21: Projection of the data of (positive and negative sequences for each phase) on each principal component. In (a) phase a, (b) phase b, and (c) phase c

- Phase to Phase - Fault Phase  $bc$

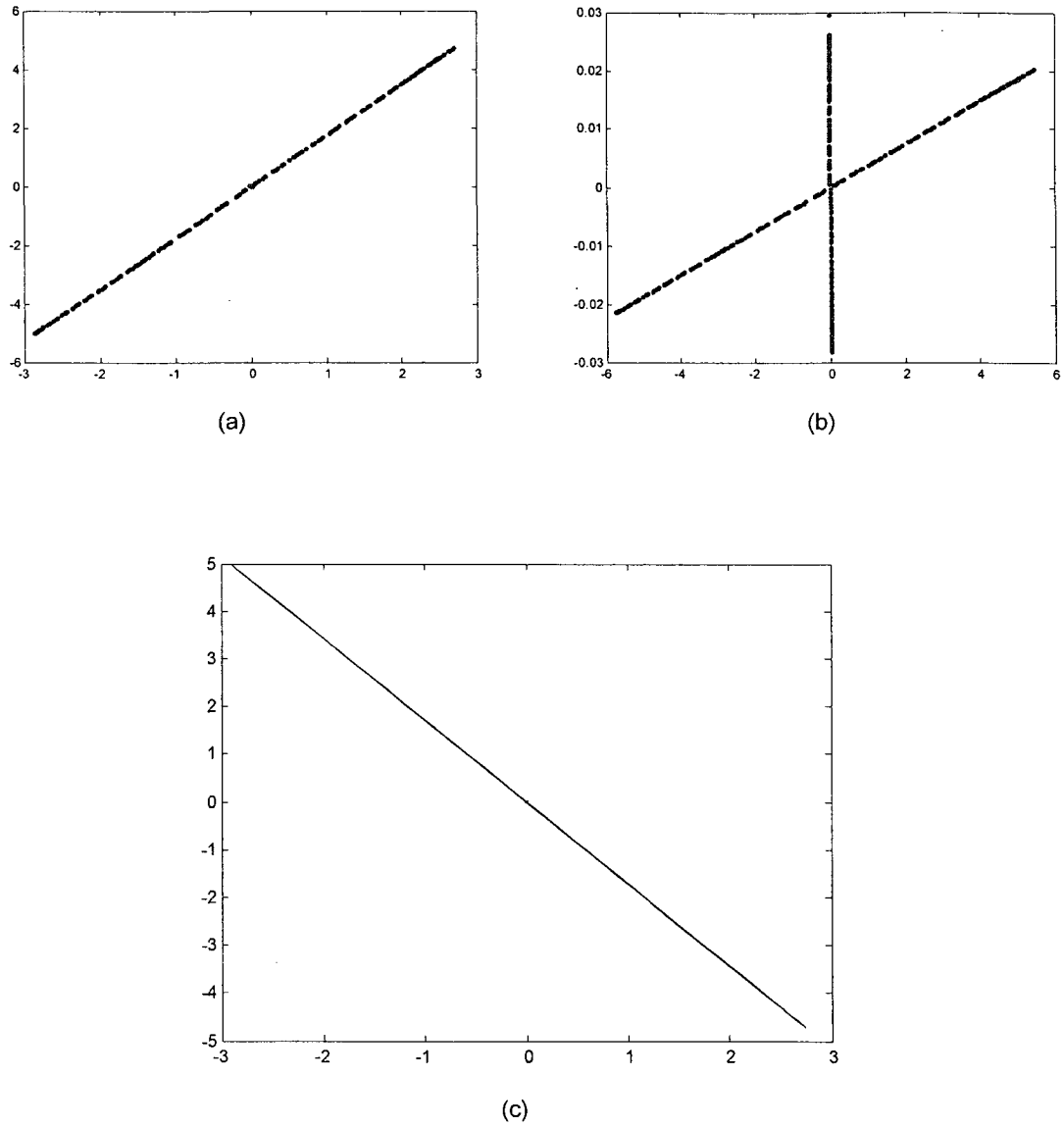


Figure 4.22: Projection of the data of (positive and negative sequence for each phase) on each principal component (a) phase a, (b) phase b and (c) phase c

- Fault Phase *abc*

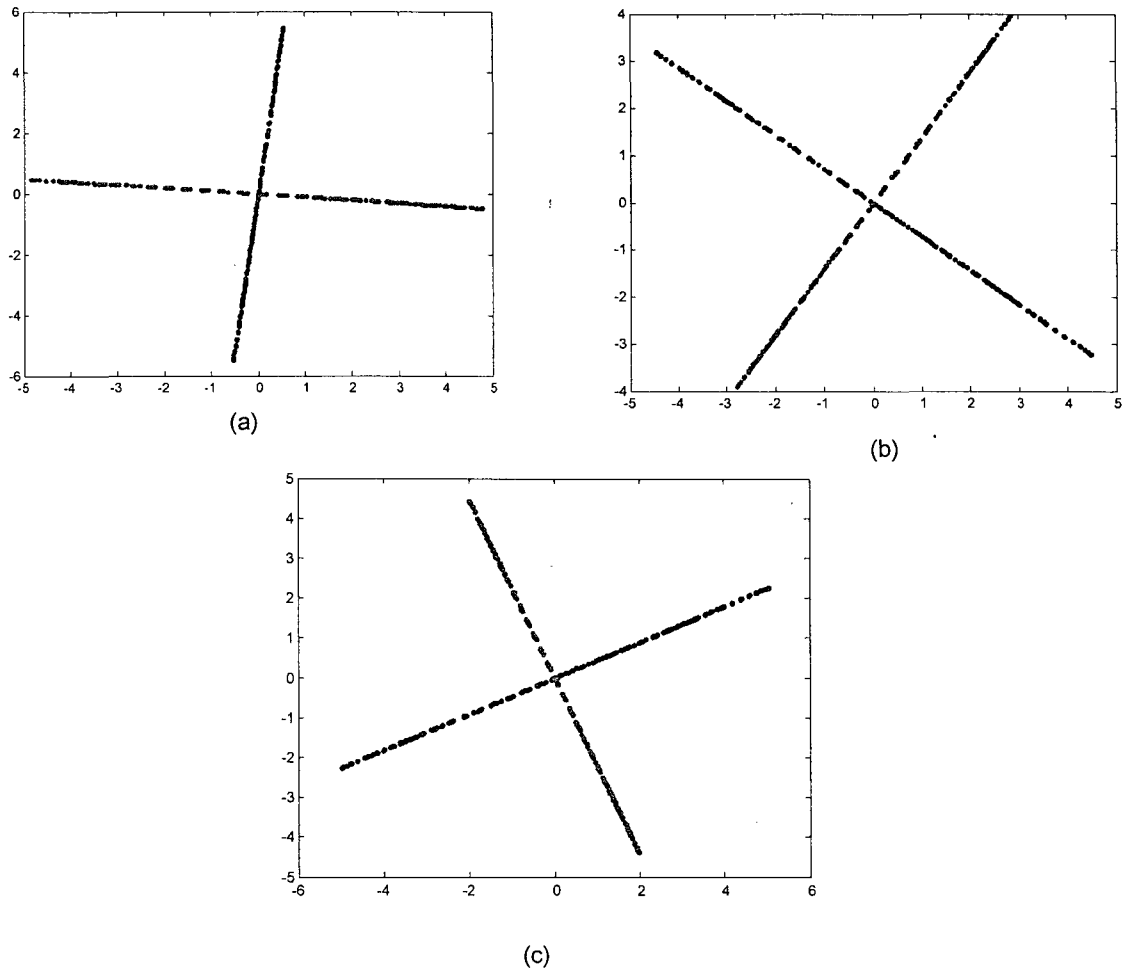


Figure 4.23: Projection of the data of (positive and negative sequence for each phase) on each principal component (a) phase a, (b) phase b and (c) phase c

### 4.3 Results on Fault Detection and Classification

After store these templates in training set, the classification process will start by measuring the Euclidean distance between the stored templates with unknown templates then compare all distances together to find the minimum distance. Since minimum distance means maximum similarity. In following table (1-10) we tested a total of 20 samples of each Fault on transmission line with total length 69 km , each sample was generated at different fault resistance and different location on transmission line .

The algorithm will be implemented using MATLAB while the simulations of power transmission are generated using PSCAD.

Step1: Generate Fault sample using PSCAD at different fault resistance value and at different location.

Step2: Loaded saved data to generate symmetrical Patterns.

Step3: Loaded the output in step 2 into the classifier to start the classification process. Calculating principal components and using the Euclidean Distance between the stored templates with tested events.

The simulations will use a set of synthetic data that will be generated for this purpose, the results will be divided to three group:

- 1- Fault classification for all fault types with low fault resistance.
- 2- Fault classification for all fault types with High Impedance Fault.
- 3- Examine the non-fault signal (Power Quality Disturbances)

### 4.3.1 Fault Classification for All Fault Types

- Fault *a-g*

Table 4.1: Classification Test for Fault *a-g*

Type of fault	Type of fault Detection/classification result	Distance (from Bus A)	$R_f \Omega$
<i>a-g</i>	<i>a-g</i>	59 km	10
<i>a-g</i>	<i>a-g</i>	59 km	20
<i>a-g</i>	<i>a-g</i>	59 km	40
<i>a-g</i>	<i>a-g</i>	39 km	50
<i>a-g</i>	<i>a-g</i>	19km	70
<i>a-g</i>	<i>a-g</i>	19km	30
<i>a-g</i>	<i>a-g</i>	20km	5
<i>a-g</i>	<i>a-g</i>	30km	15
<i>a-g</i>	<i>a-g</i>	40km	60
<i>a-g</i>	<i>a-g</i>	59 km	60
<i>a-g</i>	<i>a-g</i>	59	100
<i>a-g</i>	<i>a-g</i>	10	55
<i>a-g</i>	<i>a-g</i>	10	1
<i>a-g</i>	<i>a-g</i>	65	8
<i>a-g</i>	<i>a-g</i>	65	65
<i>a-g</i>	<i>a-g</i>	65	25
<i>a-g</i>	<i>a-g</i>	65	80
<i>a-g</i>	<i>a-g</i>	25	35
<i>a-g</i>	<i>a-g</i>	40	120
<i>a-g</i>	<i>No Fault</i>	40	140

Fault *a-g* test depends on one set of training data for this type of a fault. This training set was at  $R_f = 70 \Omega$  while all testing shown in table.4.1 spans faults with  $R_f=1$  to  $130 \Omega$ . Results are consistent classifying the fault as a (no fault) for all  $R_f$  above  $130\Omega$ . This problem can be resolved by using a larger training set.

- Fault *b-g*

Table 4.2: Classification Test for Fault *b-g*

Type of fault	Type of fault Detection/classification result	Distance (from Bus A)	$R_f \Omega$
<i>b-g</i>	<i>b-g</i>	59 km	10
<i>b-g</i>	<i>b-g</i>	19 km	20
<i>b-g</i>	<i>b-g</i>	19 km	40
<i>b-g</i>	<i>b-g</i>	39 km	50
<i>b-g</i>	<i>b-g</i>	19km	70
<i>b-g</i>	<i>b-g</i>	19km	30
<i>b-g</i>	<i>b-g</i>	20km	5
<i>b-g</i>	<i>b-g</i>	30km	15
<i>b-g</i>	<i>b-g</i>	40km	60
<i>b-g</i>	<i>b-g</i>	59 km	60
<i>b-g</i>	<i>No Fault</i>	59km	100
<i>b-g</i>	<i>b-g</i>	10 km	55
<i>b-g</i>	<i>b-g</i>	10 km	1
<i>b-g</i>	<i>b-g</i>	65 km	8
<i>b-g</i>	<i>b-g</i>	65 km	65
<i>b-g</i>	<i>b-g</i>	65 km	25
<i>b-g</i>	<i>b-g</i>	65 km	80
<i>b-g</i>	<i>b-g</i>	25 km	35
<i>b-g</i>	<i>b-g</i>	56 km	40
<i>b-g</i>	<i>b-g</i>	19 km	40

Fault *b-g* test depends on one set of training data for this type of a fault. This training set was at  $R_f = 30 \Omega$  while all testing shown in table.4.2 spans faults with  $R_f=1$  to  $80 \Omega$ . Results are consistent classifying the fault as a (no fault) for all  $R_f$  above  $80\Omega$ . This problem can be resolved by using a larger training set.

- Fault *c-g*

Table 4.3: Classification Test for Fault *c-g*

Type of fault	Type of fault Detection/classification result	Distance (from Bus A)	$R_f \Omega$
<i>c-g</i>	<i>c-g</i>	59 km	10
<i>c-g</i>	<i>c-g</i>	59 km	20
<i>c-g</i>	<i>c-g</i>	59 km	40
<i>c-g</i>	<i>c-g</i>	39 km	50
<i>c-g</i>	<i>c-g</i>	19km	70
<i>c-g</i>	<i>c-g</i>	19km	30
<i>c-g</i>	<i>c-g</i>	20km	5
<i>c-g</i>	<i>c-g</i>	30km	15
<i>c-g</i>	<i>c-g</i>	40km	60
<i>c-g</i>	<i>c-g</i>	59km	60
<i>c-g</i>	<i>c-g</i>	59 km	100
<i>c-g</i>	<i>c-g</i>	10 km	55
<i>c-g</i>	<i>c-g</i>	10 km	1
<i>c-g</i>	<i>c-g</i>	65 km	8
<i>c-g</i>	<i>c-g</i>	65 km	65
<i>c-g</i>	<i>c-g</i>	65 km	25
<i>c-g</i>	<i>c-g</i>	65 km	80
<i>c-g</i>	<i>c-g</i>	25 km	35
<i>c-g</i>	<i>c-g</i>	59 km	5
<i>c-g</i>	<i>c-g</i>	30 km	45

Fault *c-g* test depends on one set of training data for this type of a fault. This training set was at  $R_f = 30 \Omega$  while all testing shown in table.4.3 spans faults with  $R_f=1$  to  $100 \Omega$ . Results are consistent classifying the fault as a (no fault) for all  $R_f$  above  $100\Omega$ . This problem can be resolved by using a larger training set.

- Fault *ab-g*

Table 4.4: Classification Test for Fault *ab-g*

Type of fault	Type of fault Detection/classification result	Distance (from Bus A)	$R_f \Omega$
<i>ab-g</i>	<i>ab-g</i>	59 km	10
<i>ab-g</i>	<i>ab-g</i>	59 km	20
<i>ab-g</i>	<i>ab-g</i>	59 km	40
<i>ab-g</i>	<i>ab-g</i>	39 km	50
<i>ab-g</i>	<i>ab-g</i>	19km	70
<i>ab-g</i>	<i>ab-g</i>	19km	30
<i>ab-g</i>	<i>ab-g</i>	20km	5
<i>ab-g</i>	<i>ab-g</i>	30km	15
<i>ab-g</i>	<i>ab-g</i>	40km	60
<i>ab-g</i>	<i>ab-g</i>	59km	60
<i>ab-g</i>	<i>ab</i>	59 km	100
<i>ab-g</i>	<i>ab-g</i>	10 km	55
<i>ab-g</i>	<i>ab-g</i>	10 km	1
<i>ab-g</i>	<i>ab-g</i>	65 km	8
<i>ab-g</i>	<i>ab-g</i>	65 km	65
<i>ab-g</i>	<i>ab-g</i>	65 km	25
<i>ab-g</i>	<i>ab</i>	65 km	80
<i>ab-g</i>	<i>ab-g</i>	25 km	35
<i>ab-g</i>	<i>ab-g</i>	59 km	5
<i>ab-g</i>	<i>ab-g</i>	30 km	45

Fault *ab-g* test depends on one set of training data for this type of a fault. This training set was at  $R_f = 30 \Omega$  while all testing shown in table.4.4 spans faults with  $R_f=1$  to  $80 \Omega$ . Results are consistent classifying the fault as a (*ab* fault) for all  $R_f$  above  $80\Omega$ . This problem can be resolved by using a larger training set.

- Fault *ac-g*

**Table 4.5: Classification Test for Fault *ac-g***

Type of fault	Type of fault Detection/classification result	Distance (from Bus A)	$R_f \Omega$
<i>ac-g</i>	<i>ac-g</i>	59 km	10
<i>ac-g</i>	<i>ac-g</i>	59 km	20
<i>ac-g</i>	<i>ac-g</i>	59 km	40
<i>ac-g</i>	<i>ac-g</i>	39 km	50
<i>ac-g</i>	<i>ac-g</i>	19km	70
<i>ac-g</i>	<i>ac-g</i>	19km	30
<i>ac-g</i>	<i>ac-g</i>	20km	5
<i>ac-g</i>	<i>ac-g</i>	30km	15
<i>ac-g</i>	<i>ac-g</i>	40km	60
<i>ac-g</i>	<i>ac-g</i>	59km	60
<i>ac-g</i>	<i>ac-g</i>	59 km	100
<i>ac-g</i>	<i>ac-g</i>	10 km	55
<i>ac-g</i>	<i>ac-g</i>	10 km	1
<i>ac-g</i>	<i>ac-g</i>	65 km	8
<i>ac-g</i>	<i>ac-g</i>	65 km	65
<i>ac-g</i>	<i>ac-g</i>	65 km	25
<i>ac-g</i>	<i>ac-g</i>	65 km	80
<i>ac-g</i>	<i>ac-g</i>	25 km	35
<i>ac-g</i>	<i>ac-g</i>	59 km	5
<i>ac-g</i>	<i>ac-g</i>	30 km	45

Fault *ac-g* test depends on one set of training data for this type of a fault. This training set was at  $R_f = 30 \Omega$  while all testing shown in table.4.5 spans faults with  $R_f=1$  to  $100 \Omega$ . Results are consistent classifying the fault as a (no fault) for all  $R_f$  above  $100\Omega$ . This problem can be resolved by using a larger training set.

- Fault *bc-g*

Table 4.6: Classification Test for Fault *bc-g*

Type of fault	Type of fault detected/classified	Distance (from Bus A)	$R_f \Omega$
<i>bc-g</i>	<i>bc-g</i>	59 km	10
<i>bc-g</i>	<i>bc-g</i>	59 km	20
<i>bc-g</i>	<i>bc-g</i>	59 km	40
<i>bc-g</i>	<i>bc-g</i>	39 km	50
<i>bc-g</i>	<i>bc-g</i>	19km	70
<i>bc-g</i>	<i>bc-g</i>	19km	30
<i>bc-g</i>	<i>bc-g</i>	20km	5
<i>bc-g</i>	<i>bc-g</i>	30km	15
<i>bc-g</i>	<i>bc-g</i>	40km	60
<i>bc-g</i>	<i>bc-g</i>	59km	30
<i>bc-g</i>	<i>bc</i>	59 km	100
<i>bc-g</i>	<i>bc-g</i>	10 km	55
<i>bc-g</i>	<i>bc-g</i>	10 km	1
<i>bc-g</i>	<i>bc-g</i>	65 km	8
<i>bc-g</i>	<i>bc-g</i>	65 km	65
<i>bc-g</i>	<i>bc-g</i>	65 km	25
<i>bc-g</i>	<i>bc</i>	65 km	80
<i>bc-g</i>	<i>bc-g</i>	25 km	35
<i>bc-g</i>	<i>bc-g</i>	59 km	5
<i>bc-g</i>	<i>bc-g</i>	30 km	45

Fault *bc-g* test depends on one set of training data for this type of a fault. This training set was at  $R_f = 30 \Omega$  while all testing shown in table.4.6 spans faults with  $R_f=1$  to  $80 \Omega$ . Results are consistent classifying the fault as a (*bc* fault) for all  $R_f$  above  $80\Omega$ . This problem can be resolved by using a larger training set.

- Fault *ab*

Table 4.7: Classification Test for Fault *ab*

Type of fault	Type of fault detected/classified	Distance (from Bus A) Km	$R_f \Omega$
<i>ab</i>	<i>ab</i>	59	10
<i>ab</i>	<i>ab</i>	59	20
<i>ab</i>	<i>ab</i>	59	40
<i>ab</i>	<i>ab</i>	39	50
<i>ab</i>	<i>ag</i>	19	70
<i>ab</i>	<i>ab</i>	19	30
<i>ab</i>	<i>ab</i>	20	5
<i>ab</i>	<i>ab</i>	30	15
<i>ab</i>	<i>ab</i>	40	60
<i>ab</i>	<i>ab</i>	59	60
<i>ab</i>	<i>ag</i>	59	100
<i>ab</i>	<i>ab</i>	10	55
<i>ab</i>	<i>ab</i>	10	1
<i>ab</i>	<i>ab</i>	65	8
<i>ab</i>	<i>ab</i>	65	65
<i>ab</i>	<i>ab</i>	65	25
<i>ab</i>	<i>ag</i>	65	80
<i>ab</i>	<i>ab</i>	25	35
<i>ab</i>	<i>ab</i>	59	5
<i>ab</i>	<i>ab</i>	30	45

Fault *ab* test depends on one set of training data for this type of a fault. This training set was at  $R_f = 30 \Omega$  while all testing shown in table.4.7 spans faults with  $R_f=1$  to  $80 \Omega$ . Results are consistent classifying the fault as a (*a-g* fault) for all  $R_f$  above  $80 \Omega$ . This problem can be resolved by using a larger training set.

- Fault *ac*

**Table 4.8: Classification Test for Fault *ac***

Type of fault	Type of fault Detected/classified	Distance (from Bus A) in km	$R_f \Omega$
<i>ac</i>	<i>ac</i>	59	10
<i>ac</i>	<i>ac</i>	59	20
<i>ac</i>	<i>ac</i>	59	40
<i>ac</i>	<i>ac</i>	39	50
<i>ac</i>	<i>ac</i>	19	70
<i>ac</i>	<i>ac</i>	19	30
<i>ac</i>	<i>ac</i>	20	5
<i>ac</i>	<i>ac</i>	30	15
<i>ac</i>	<i>ac</i>	19	60
<i>ac</i>	<i>ac</i>	59	60
<i>ac</i>	<i>ac</i>	59	100
<i>ac</i>	<i>ac</i>	10	55
<i>ac</i>	<i>ac</i>	10	1
<i>ac</i>	<i>ac</i>	65	8
<i>ac</i>	<i>ac</i>	65	65
<i>ac</i>	<i>ac</i>	65	25
<i>ac</i>	<i>ac</i>	65	80
<i>ac</i>	<i>ac</i>	25	35
<i>ac</i>	<i>ac</i>	59	5
<i>ac</i>	<i>ac</i>	30	45

Fault *ac* test depends on one set of training data for this type of a fault. This training set was at  $R_f = 30 \Omega$  while all testing shown in table.4.8 spans faults with  $R_f=1$  to  $100 \Omega$ . Results are consistent classifying the fault as a (no fault) for all  $R_f$  above  $100\Omega$ . This problem can be resolved by using a larger training set.

- Fault *bc*

Table 4.9: Classification Test for Fault *bc*

Type of fault	Type of fault Detected/classified	Distance (from Bus A) in km	$R_f \Omega$
<i>bc</i>	<i>bc</i>	59	10
<i>bc</i>	<i>bc</i>	59	20
<i>bc</i>	<i>bc</i>	59	40
<i>bc</i>	<i>bc</i>	39	50
<i>bc</i>	No Fault	19	70
<i>bc</i>	<i>bc</i>	19	30
<i>bc</i>	<i>bc</i>	20	5
<i>bc</i>	<i>bc</i>	30	15
<i>bc</i>	<i>bc</i>	19	60
<i>bc</i>	<i>bc</i>	59	60
<i>bc</i>	No Fault	59	100
<i>bc</i>	<i>bc</i>	10	55
<i>bc</i>	<i>bc</i>	10	1
<i>bc</i>	<i>bc</i>	65	8
<i>bc</i>	<i>bc</i>	65	65
<i>bc</i>	<i>bc</i>	65	25
<i>bc</i>	No Fault	65	80
<i>bc</i>	<i>bc</i>	25	35
<i>bc</i>	<i>bc</i>	59	5
<i>bc</i>	<i>bc</i>	30	45

Fault *bc* test depends on one set of training data for this type of a fault. This training set was at  $R_f = 30 \Omega$  while all testing shown in table.4.9 spans faults with  $R_f=1$  to  $80 \Omega$ . Results are consistent classifying the fault as a (no fault) for all  $R_f$  above  $80\Omega$ . This problem can be resolved by using a larger training set.

- Fault *abc*

**Table 4.10: Classification Test for Fault *abc***

Type of fault	Type of fault detected/classified	Distance (from Bus A) km	$R_f \Omega$
<i>abc</i>	<i>abc</i>	59	10
<i>abc</i>	<i>abc</i>	59	20
<i>abc</i>	<i>abc</i>	59	40
<i>abc</i>	<i>abc</i>	39	50
<i>abc</i>	<i>abc</i>	19	70
<i>abc</i>	<i>abc</i>	19	30
<i>abc</i>	<i>abc</i>	20	5
<i>abc</i>	<i>abc</i>	30	15
<i>abc</i>	<i>abc</i>	40	60
<i>abc</i>	<i>abc</i>	59	60
<i>abc</i>	<i>abc</i>	59	100
<i>abc</i>	<i>abc</i>	10	55
<i>abc</i>	<i>abc</i>	10	1
<i>abc</i>	<i>abc</i>	65	8
<i>abc</i>	<i>abc</i>	65	65
<i>abc</i>	<i>abc</i>	65	25
<i>abc</i>	<i>abc</i>	65	80
<i>abc</i>	<i>abc</i>	25	35
<i>abc</i>	<i>abc</i>	59	5
<i>abc</i>	<i>abc</i>	35	40

Fault *bc* test depends on one set of training data for this type of a fault. This training set was at  $R_f = 30 \Omega$  while all testing shown in table.4.9 spans faults with  $R_f=1$  to  $80 \Omega$ . Results are consistent classifying the fault as a (no fault) for all  $R_f$  above  $80\Omega$ . This problem can be resolved by using a larger training set.

The Power system fault classifier was trained to classify the Faults into *a-g*, *b-g*, *c-g*, *ab-g*, *ac-g*, *bc-g*, *ab*, *ac*, *bc*, and *abc*. . In this way, we applied a total of 20 samples of each case and applied a total of 220 samples for testing. The classification accuracy

was calculated by taking the number of correctly classified samples by the network, and divided by the total number of samples into the test data set, is presented in the confusion matrix in Table 4.11. These results were obtained with one template/pattern in the training data set. Table 4.12 displays the results storing two templates in the training set. The error percentage in the later case is zero. Results are considered to be of significant improvement over the traditional approaches.

### **4.3.2 High Impedance Fault Test**

The detection of high impedance faults (HIFs) on electrical distribution systems is one of the most persistent and difficult problems facing the electrical utility industry. (HIFs) in distribution systems create unique challenges for the protection engineer since such faults do not produce enough fault current to be detected by the conventional over current relays or fuses. Recent advances in digital technology have enabled practical solutions for the detection of a high percentage of these previously undetectable faults [73] [74]. High impedance fault detection and classification tests with different values of fault resistance and fault location are displayed in Table 4.13. These results demonstrate that pattern based fault detection and classification algorithm can detect high impedance faults with 100% accuracy.

**Table 4.11 Classification Performance Using One Template for Each Fault Type in the Training Set Producing a 94.54% Average Accuracy**

Type of Fault	Samples	Confusion Matrix											Accuracy
		<i>a-g</i>	<i>b-g</i>	<i>c-g</i>	<i>ab-g</i>	<i>ac-g</i>	<i>bc-g</i>	<i>ab</i>	<i>ac</i>	<i>bc</i>	<i>abc</i>	No Fault	
<i>a-g</i>	20	19	0	0	0	0	0	0	0	0	0	1	95%
<i>b-g</i>	20	0	19	0	0	0	0	0	0	0	0	1	95%
<i>c-g</i>	20	0	0	20	0	0	0	0	0	0	0	0	100%
<i>ab-g</i>	20	0	0	0	18	0	0	2	0	0	0	0	90%
<i>ac-g</i>	20	0	0	0	0	20	0	0	0	0	0	0	100%
<i>bc-g</i>	20	0	0	0	0	0	18	0	0	2	0	0	90%
<i>ab</i>	20	3	0	0	0	0	0	17	0	0	0	0	85%
<i>ac</i>	20	0	0	0	0	0	0	0	20	0	0	0	100%
<i>bc</i>	20	0	0	0	0	0	0	0	0	17	0	3	85%
<i>abc</i>	20	0	0	0	0	0	0	0	0	0	20	0	100%
No Fault	20	0	0	0	0	0	0	0	0	0	0	20	100%

**Table 4.12 Classification Performance by Using Two Templates for Each Fault Type in the Training Set Producing 100% Accuracy**

Type of Fault	Samples	Confusion Matrix											Accuracy
		<i>a-g</i>	<i>b-g</i>	<i>c-g</i>	<i>ab-g</i>	<i>ac-g</i>	<i>bc-g</i>	<i>ab</i>	<i>ac</i>	<i>bc</i>	<i>abc</i>	No Fault	
<i>a-g</i>	20	20	0	0	0	0	0	0	0	0	0	0	100%
<i>b-g</i>	20	0	20	0	0	0	0	0	0	0	0	0	100%
<i>c-g</i>	20	0	0	20	0	0	0	0	0	0	0	0	100%
<i>ab-g</i>	20	0	0	0	20	0	0	0	0	0	0	0	100%
<i>ac-g</i>	20	0	0	0	0	20	0	0	0	0	0	0	100%
<i>bc-g</i>	20	0	0	0	0	0	20	0	0	0	0	0	100%
<i>ab</i>	20	0	0	0	0	0	0	20	0	0	0	0	100%
<i>ac</i>	20	0	0	0	0	0	0	0	20	0	0	0	100%
<i>bc</i>	20	0	0	0	0	0	0	0	0	20	0	0	100%
<i>abc</i>	20	0	0	0	0	0	0	0	0	0	20	0	100%
No Fault	20	0	0	0	0	0	0	0	0	0	0	20	100%

### 4.3.3 Power Quality Disturbance Test

Sudden or instantaneous increase of loads in a power system generates noise that may be detected as a fault if it does not cause a fault to occur. As a result, power quality monitoring has become a necessity in modern power systems [75]. Figure 4.24 shows examples of power quality disturbances.

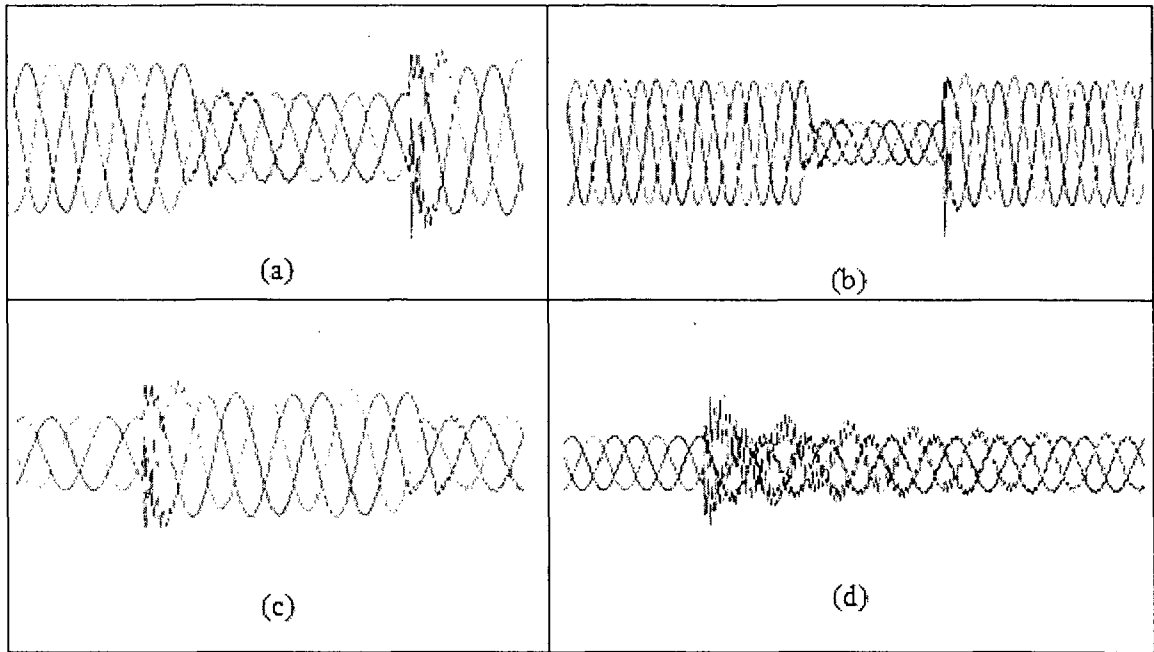


**Figure 4.24: Examples of power quality disturbances, (a) voltage Sag, (b) voltage sag with a different load from that in a, (c) voltage swells, and (d) capacitor switching**

The most important property for any fault detection and classification system is the ability to achieve a high degree of reliability and to achieve this; a system must demonstrate the ability to distinguish between real fault and other events such as load change or capacitor switching [76]. The Non-fault events such as voltage sag, voltage swell and capacitor switching detection and classification results are displayed in Table 1. Without any system training to such events, results indicate that sag and switching events are correctly classified as No-fault while it failed to identify the swell event and labeled it as a single phase-to-ground fault. However, after training the system to similar events, it was able to classify all events as no-fault events resulting in 100% accuracy.

**Table 4.13: Classification Test for High Impedance Fault**

Type of fault	Type of fault using algorithm	Distance from Bus A	$R_f \Omega$
<i>a-g</i>	<i>a-g</i>	59 km	200
<i>a-g</i>	<i>a-g</i>	19 km	250
<i>a-g</i>	<i>a-g</i>	30km	300
<i>a-g</i>	<i>a-g</i>	40km	500
<i>b-g</i>	<i>b-g</i>	59 km	200
<i>b-g</i>	<i>b-g</i>	19 km	250
<i>b-g</i>	<i>b-g</i>	30km	300
<i>c-g</i>	<i>c-g</i>	59 km	200
<i>c-g</i>	<i>c-g</i>	19 km	250
<i>c-g</i>	<i>c-g</i>	30km	400
<i>ab-g</i>	<i>ab-g</i>	59 km	200
<i>ab-g</i>	<i>ab-g</i>	19 km	250
<i>ab-g</i>	<i>ab-g</i>	30km	300
<i>ac-g</i>	<i>ac-g</i>	59 km	200
<i>ac-g</i>	<i>ac-g</i>	19 km	250
<i>ac-g</i>	<i>ac-g</i>	30km	300
<i>bc-g</i>	<i>bc-g</i>	59 km	200
<i>bc-g</i>	<i>bc-g</i>	19 km	250
<i>bc-g</i>	<i>bc-g</i>	30km	300
<i>ab</i>	<i>ab</i>	59 km	200
<i>ab</i>	<i>ab</i>	19 km	250
<i>ab</i>	<i>ab</i>	30kn	300
<i>ac</i>	<i>ac</i>	59 km	200
<i>ac</i>	<i>ac</i>	19 km	250
<i>ac</i>	<i>ac</i>	30km	30
<i>bc</i>	<i>bc</i>	59 km	200
<i>bc</i>	<i>bc</i>	19 km	250
<i>bc</i>	<i>bc</i>	30km	300
<i>abc</i>	<i>abc</i>	59 km	200
<i>abc</i>	<i>abc</i>	19 km	250
<i>abc</i>	<i>abc</i>	30km	300

**Table 4.14: Classification Test for Power Quality Disturbances**

<b>Type of Event</b>	<b>Type of fault using algorithm without training</b>	<b>Classify Event With Training</b>
Sag	No Fault	Sag
Sag	No Fault	Sag
Swell	<i>a-g</i>	Swell
Swell	<i>a-g</i>	Swell
Switching	No Fault	Switching
Switching	No Fault	Switching

## CHAPTER 5

### FAULT LOCALIZATION USING PATTERN RECOGNITION

#### 5.1 Introduction

Ultimately, elimination of reoccurring fault should be the goal of any respected electrical utilities provider. Meanwhile, immediate and accurate identification of faults can accelerate restoration of the faulted transmission line and limit the damage as it can allow for immediate equipment repair and restoration of service which also reduces revenue loss caused by outages. Moreover, accurate fault location reduces operating costs by avoiding lengthy and expensive patrols.

There are several different methods in today's market for fault localization such as,

- Digital Fault Recorders (DFR )and short circuit data match
- Traveling wave methods
- Impedance-based methods, which can be
  - One-ended methods without using source impedance data (simple reactance, Takagi)
  - One-ended methods using source impedance data
  - Two-ended methods

Currently, practiced methods for fault localization depend on many elements such as fault resistance and power angle, each introducing its own chances of error.

In this chapter, a fault localization method based on positive (+ve) and negative (-ve) patterns ratio obtained from the between voltage and current symmetrical patterns is presented.

## 5.2 Fault Localization Based on Impedance Method

Impedance-based fault locators calculate the fault location from the apparent Impedance seen by looking into the line from one end. In this method, fault location is based on voltage and current information from one termination or from both terminations of the monitored line. Because the line length is proportional to the line reactance [82], the calculated reactive component of the apparent impedance is used to calculate the fault location by using equation 5.1

$$L_f = L \frac{X_f}{X} \quad (5.1)$$

Where:

$L_f$ : Fault Distance (Distance Unit, Km or mile)

$L$ : Total length of transmission line (Distance Unit, Km or mile)

$X_f$ : the apparent impedance reactance from sending end to fault location ( $\Omega$ ).

$X$ : Total reactance of line ( $\Omega$ ).

## 5.3 Pattern Index Estimation

After estimating the positive and negative pattern in Chapter 3 Equation 3.10, we will use the same algorithm to estimate the pattern for voltage and current fault signal to estimate the pattern indices. The pattern indices for positive and negative sequences are defined as:

$$P_{k-Index(a)}^- = \frac{P_{k-va}^-}{P_{k-ia}^-} \quad (5.2)$$

$$P_{k-Index(a)}^+ = \frac{P_{k-va}^+}{P_{k-ia}^+} \quad (5.3)$$

Where:  $P_{k-Index(a)}^-$ ,  $P_{k-Index(a)}^+$  positive and negative pattern index,

$P_{k-ia}^+$ ,  $P_{k-ia}^-$  positive and negative pattern of current fault signal, and

$P_{k-va}^+$ ,  $P_{k-va}^-$  positive and negative pattern of voltage fault signal.

After extracting current and voltage fault signals and applying the pattern algorithm as shown in figure 3.5, the current pattern and voltage pattern will be:

$$P_{k-Index(a)}^+ = \frac{\left( |r_{k-va}| \angle \theta_k + a^2 |r_{k-va}| \angle \sigma_k + a |r_{k-va}| \angle \vartheta_k \right)}{\left( |r_{k-ia}| \angle \alpha_k + a^2 |r_{k-ia}| \angle \gamma_k + a |r_{k-ia}| \angle \beta_k \right)} \quad (5.4)$$

$$P_{k-Index(a)}^- = \frac{\left[ \left( |r_{k-va}| \angle \theta_k + a |r_{k-va}| \angle \sigma_k + a^2 |r_{k-va}| \angle \vartheta_k \right) \right]}{\left[ \left( |r_{k-ia}| \angle \alpha_k + a |r_{k-ia}| \angle \gamma_k + a^2 |r_{k-ia}| \angle \beta_k \right) \right]} \quad (5.5)$$

Where  $P_{k-Index(a)}^+$ ,  $P_{k-Index(a)}^-$  positive and negative pattern index for phase a.

$$\left. \begin{aligned} index^+ &= \sum_{i=1}^k P_{k-index(a)}^+ \\ index^- &= \sum_{i=1}^k P_{k-index(a)}^- \end{aligned} \right\} \quad (5.6)$$

where  $index_a^+$ ,  $index_a^-$  are the positive and negative Pattern indices for phase a.

## 5.4 Fault Localization

Using curve fitting, a training set is produced for the positive and negative pattern indices and their fault corresponding distances. The Positive and negative indices are calculated at different locations (5, 25, 35, 50, 75, 95) km from sending end of the transmission line with a variety of operating conditions such as power angles and source impedance but at a specific fault resistance. The polynomial of curve fitting for the data between positive pattern index and the fault location for phase a-g is shown in figure 5.1. To estimate the fault location, the positive and negative Pattern indices of the real incident/test signals are determined and projected onto the fitted curve polynomial, , figures 5.1 and 5.2, an average of the two readings is taken as the fault location shown in Eq.5.7.

$$D(index_a) = \frac{D(index_a^+) + D(index_a^-)}{2} \quad (5.7)$$

where  $D(index_a)$  is the average distance of the previous estimates taken to be an accurate estimate of the fault location

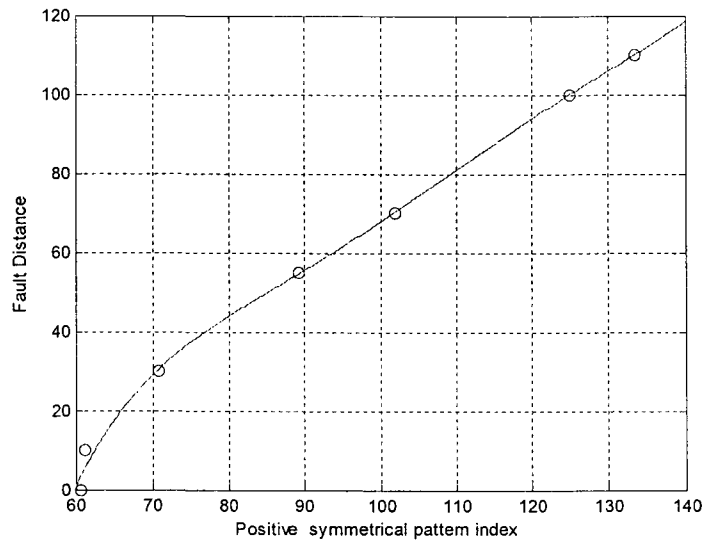


**Figure 5.1: The curve fitting between positive pattern index and the fault location for phase a to ground (ab-g).**

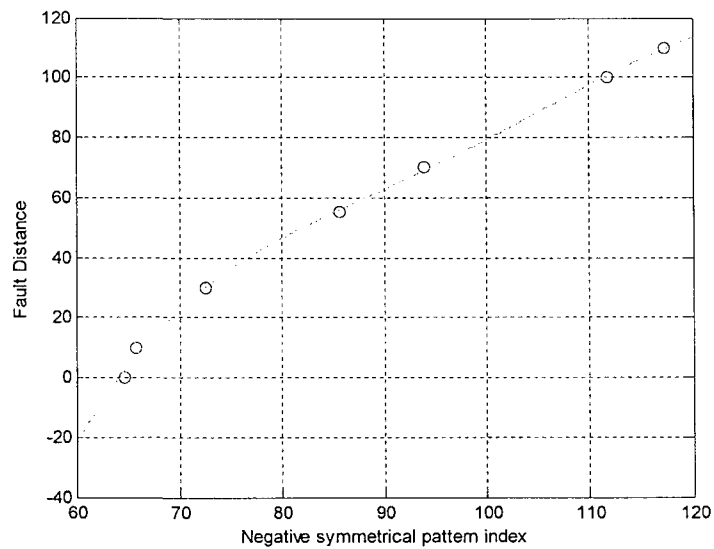


**Figure 5.2: The curve fitting between negative pattern index and the fault location for phase a to ground (a-g).**

The estimated distance in the first polynomial curve fitting is dependent on the specific value of the fault resistance and so if the fault to occur at a different values of fault resistance, that is, at a fault resistance not used in the first polynomial curve fitting,

then an error in the distance estimate will occur. However, the error can be compensated by accounting for the difference in the fault resistance. That is,  $\Delta R$ , the difference between the new fault resistance and the one used in the training, is used to generate a new polynomial curve to extract the corresponding  $\Delta D$ . Upon testing and if there is any change in fault resistance then  $\Delta D$ , the error in the distance, will be added to the calculated fault distance as shown in Eq.5.8.

$$D(index_a, \Delta D) = \frac{D(index_a^+) + D(index_a^-)}{2} + \Delta D \quad (5.8)$$

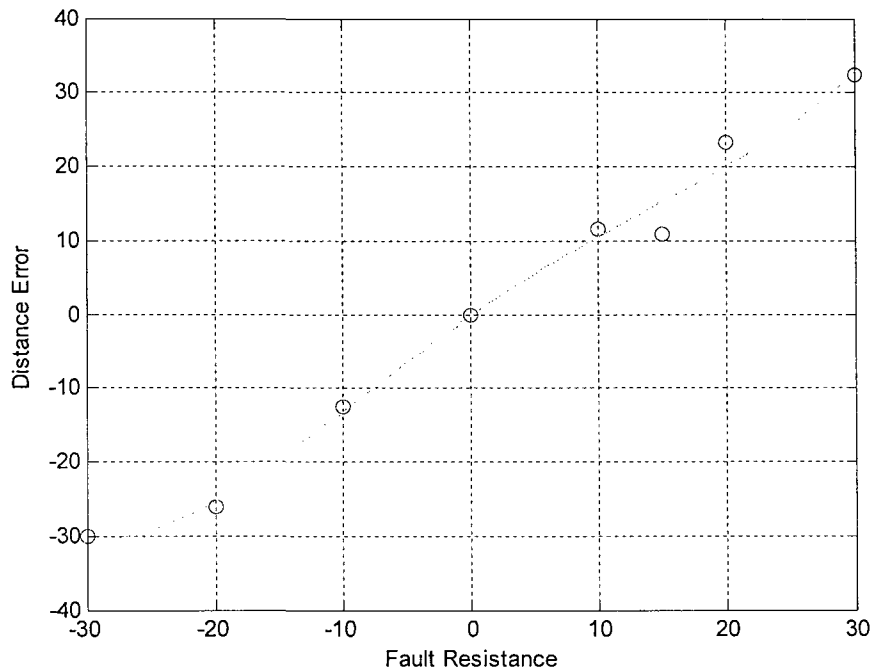


**Figure 5.3: The curve fitting between fault resistance and distance error**

### 5.5 Pattern-Based Fault Location Method-Procedure

Pattern -based methods require the following approach figure 5.4 shows the functional block diagram for this work.

1. Measure the voltage and current Fault signal.

2. Generate pattern for voltage and current signal.
3. Calculate the positive and negative indexes form symmetrical pattern.
4. Determine the fault type.
5. Estimation Fault Resistance
6. Select the suitable training set depend on fault type
7. Use pattern index training set to estimate fault distance
8. Calculate the Fault Resistance difference.
9. Calculate distance error from fault resistance difference.
10. Calculate the final fault distance.

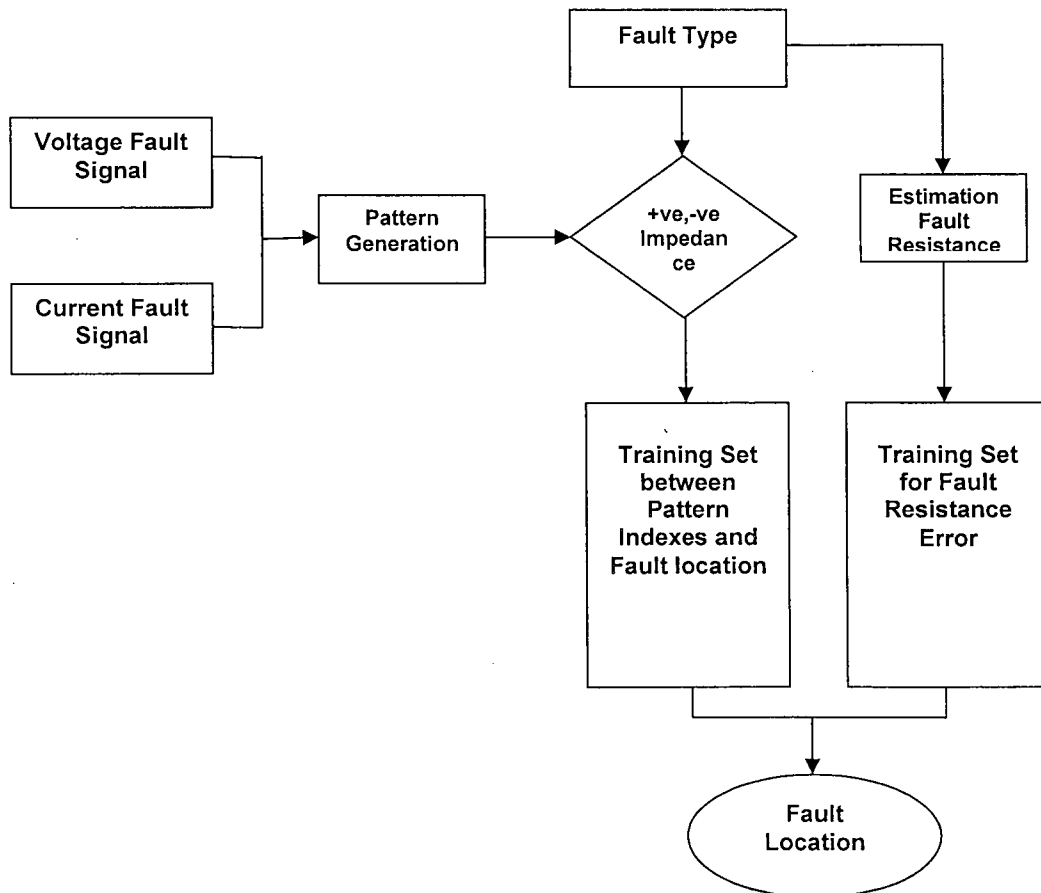


**Figure 5.4: Functional block diagram for fault location based on symmetrical patterns indexes**

## 5.6 Preliminary Experimental Results

The system studied is composed of 220KV single circuit transmission lines, 110 km in length, connected to a source at each end, as shown in figure 5.5. This system has been simulated with PSCAD/EMTDC to fault analysis to generate fault signals for various faults. Before starting simulation I need to introduce the Fault location error.

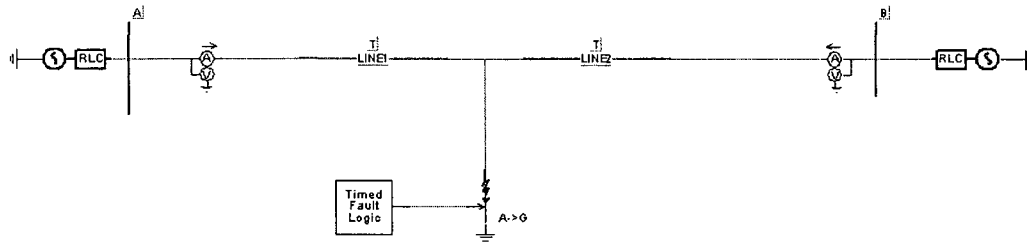


**Figure 5.5: 220KV single circuit transmission lines using PSCAD/EMTDC simulation**

### 5.6.1 Fault Location Error

IEEE PC37.114, “Draft Guide for Determining Fault Location on AC Transmission and Distribution Lines” [79] was recently balloted and is in the approval process. One of the important contributions of the guide is the definitions section.

Fault location error: Percentage error in fault location estimate based on the total line length: (error) = (instrument reading – exact distance to the fault) / total line length.

This definition can be written down as the following formula:

$$Error = \frac{(d - d_{Exact})}{l} \times 100\% \quad (5.9)$$

where  $d$  and  $d_{Exact}$  are the fault estimated and exact distances (Km) respectively,  $L$  is the total length of the transmission line. For example, suppose a line is 100 km long and

the actual fault is 90 km from the local terminal and if the fault location was estimated at 94 km, then the fault location error according to the IEEE Draft Guide for Determining Fault Location on AC Transmission and Distribution Lines [78], is

$$Error = \frac{(94 - 90)}{100} = 4\%$$

However, in this work we will take

$$Error = \frac{|d - d_{Exact}|}{l} \times 100\% \quad (5.10)$$

### 5.6.2 Pattern Training Set

The pattern indices are generated by generating positive and negative patterns for all phases using equations 5.5 and 5.6. The training set is developed using positive and negative pattern indices and distance of fault location for each type of fault using curve fitting technique.

- **Single line to Ground**

Per Table 5.1, symmetrical pattern indices at several fault distances and fault resistance value  $R_f = 40 \Omega$  were used with the curve fitting technique between the positive and negative pattern indices different values of fault distance to generate figure 5.6. In table 5.2, the validity of curve fitting is displayed and the fault distance error is around 0.004 km.

**Table 5.1: Pattern Indices with a Varying Fault Distance Value and  $R_f = 40 \Omega$  for Fault  $a-g$**

Average +ve Index	Average -ve Index	Distances from Bus A km	Distances (from Bus B) Km	$R_f \Omega$
128.6959	123.7983	0	110	40
131.7235	126.3450	10	100	40
154.4173	139.8513	30	80	40
190.3071	177.5850	55	55	40
188.8432	191.5677	70	40	40
198.8650	220.7560	100	10	40
140.2134	230.5150	110	0	40

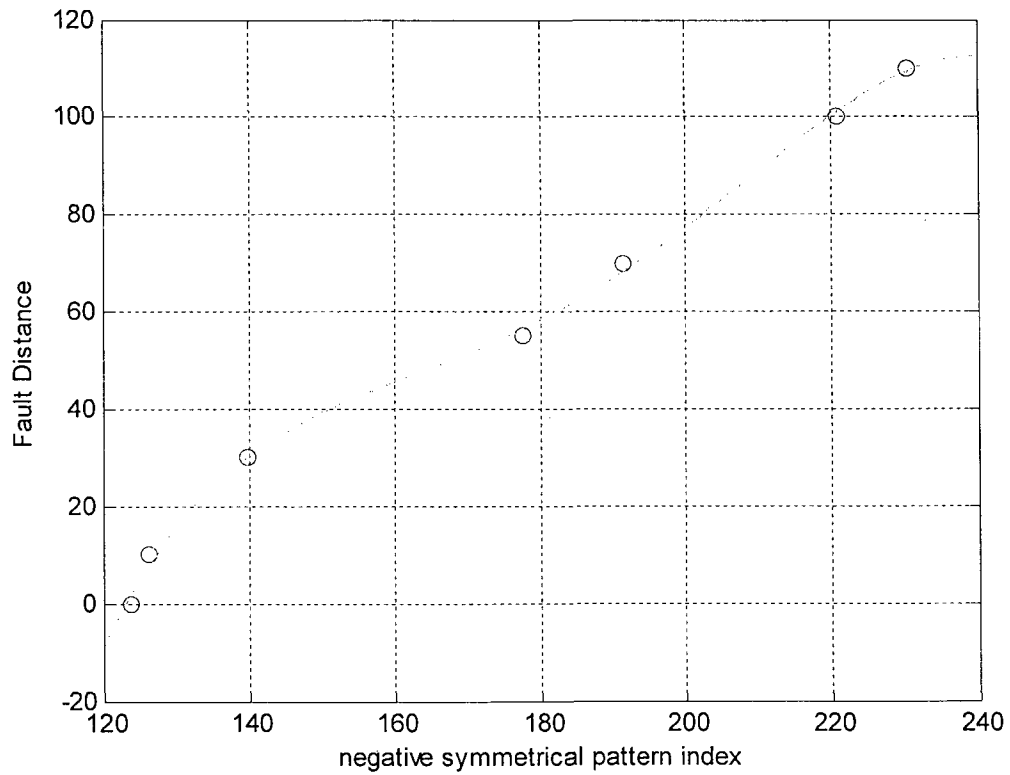


**Figure 5.6: The curve fitting between negative pattern index and the fault location for phase a to ground ( $a-g$ )**

**Table 5.2: The Validity of Curve Fitting in Figure 5.6 for *a-g* Fault**

Example Test						
Average +ve Index	Average -ve Index	Distances from Bus A Km	Distances from Bus B km	Estimated fault location Km	$R_f \Omega$	Error
202.3730	210.7622	90	20	89	40	0.009
189.3636	187.2261	65	45	65.5	40	0.004
199.0856	205.7129	85	25	84	40	0.009

The Training set shown in table 5.1 was generated for a fault resistance of  $R_f = 40 \Omega$  while table 5.3 is displaying a varying fault resistance which was used to generate the curve fitting between  $\Delta R_f$  and  $\Delta D$  shown in figure 5.7. The final fault distance will be present according Eq. 5.8, the training set for this type of fault *a-g* shown in figure 5.8.

**Table 5.3: Pattern Index at Different Fault Resistance Values**

Training Set for Error in Fault Resistance							
Average +ve index	Average -ve index	Distances from Bus A Km	Distances from Bus B km	Estimated fault location Km	$R_f \Omega$	Distance Error	$\Delta R_f$
201.4286	203.1918	85	25	81.4	30	3.6	10
217.2397	209.4602	85	25	87.7	50	-2.7	-10
109.9355	177.6713	85	25	55.1	20	29.9	20
90.1795	178.6265	85	25	56.1	10	28.9	30
228.3357	217.8455	85	25	96.7	60	-11.7	-20
235.0657	223.7489	85	25	103	70	-18	-30
77.2723	172.7976	85	25	49.8	15	35.2	25

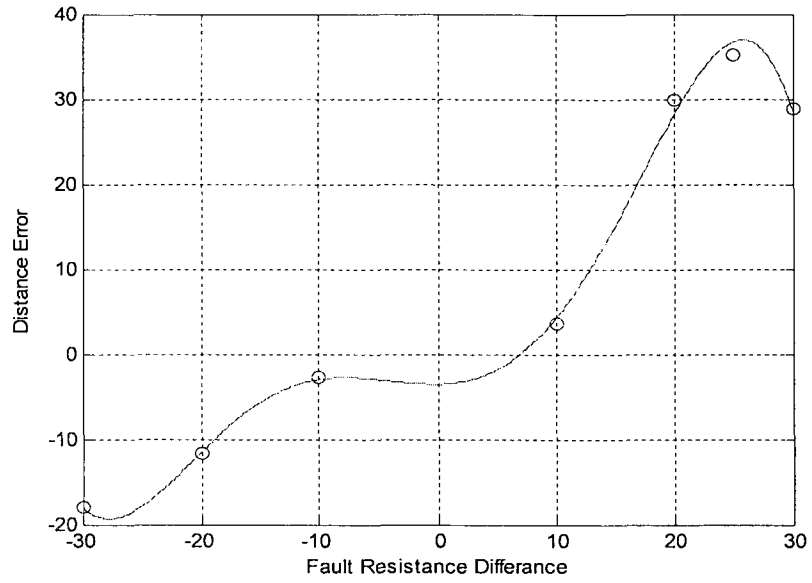


**Figure 5.7: The curve fitting between fault resistance and distance error**

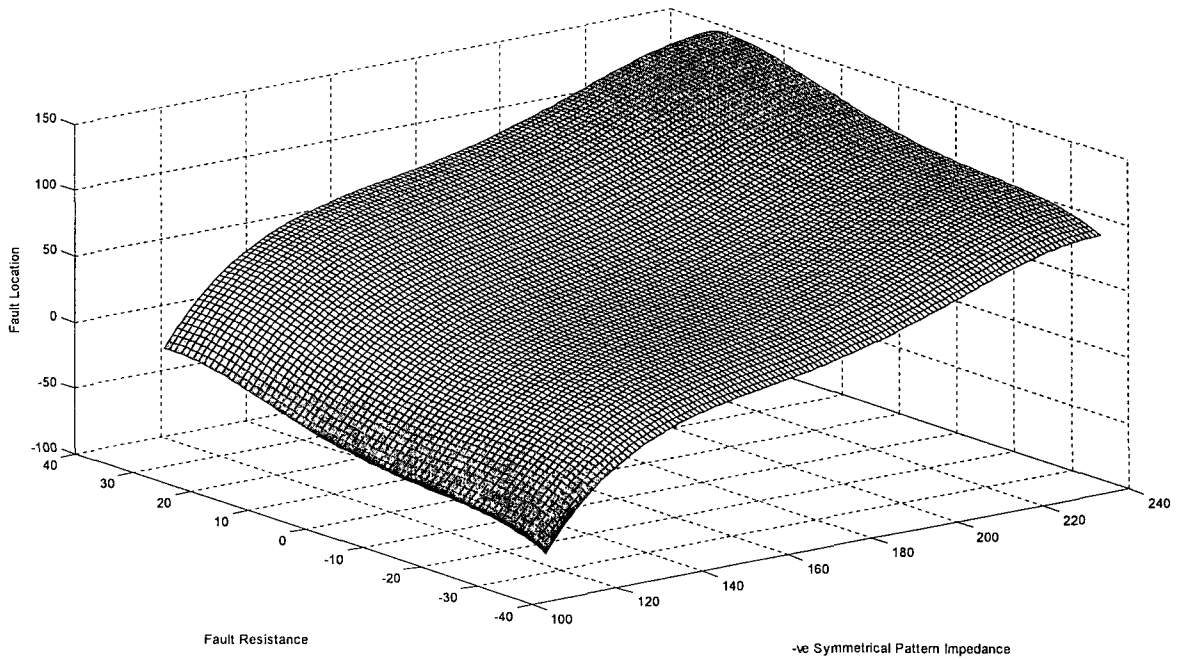


**Figure 5.8: Fault location training set for *a-g* fault**

- **Double phase to Ground**

Double phase to ground (ab to g) results are shown in Table 5.4 and figure 5.9 while Table 5.5 displays the validity of the algorithm with an error of less than 0.001 km.

**Table 5.4: Pattern Indices at Several Values of Fault Distance and  $R_f = 40 \Omega$  for Fault *ab-g***

Average +ve Index	Average -ve index	Distances from Bus A km	Distances from Bus B Km	$R_f \Omega$
63.6460	64.6688	0	110	40
64.6810	65.7264	10	100	40
72.3749	72.5658	30	80	40
86.6889	85.6971	55	55	40
95.7197	93.9210	70	40	40
114.9144	111.7198	100	10	40
121.0813	117.2873	110	0	40

**Table 5.5: The Validity of Curve Fitting in Figure 5.9 for *ab-g* Fault**

Example Test					
Average +ve Index	Average -ve index	Distances from Bus A km	Distances from Bus B km	Estimated fault location Km	$R_f \Omega$
108.3811	105.7108	90	20	90.35	40
92.5848	91.0004	65	45	64.5	40
105.1475	102.6548	85	25	85.2	40

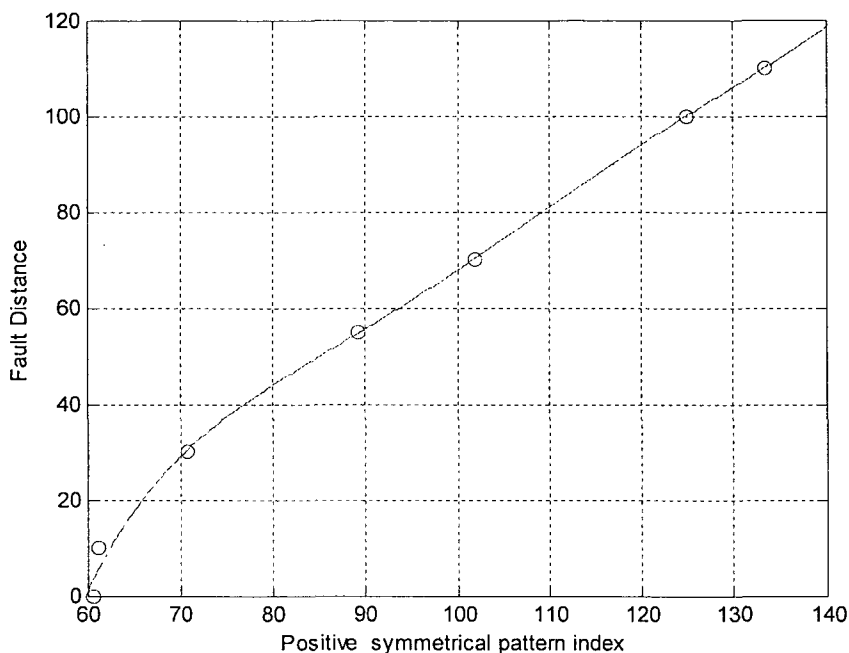


**Figure 5.9: Curve fitting between positive pattern index and distance of a fault**

Training set in table 5.4 was generated for a fault resistance of  $R_f = 40 \Omega$  while table 5.6 is displaying a varying fault resistance which was used to generate the curve fitting between  $\Delta R_f$  and  $\Delta D$  as shown in figure 5.10. By adding to curve fitting together according Eq. 5.9 the training set for this type of fault ab-g shown in figure 5.11.

**Table 5.6: Pattern Index at Different Fault Resistance Value**

Training Set for Error in Fault Resistance							
Average +ve Index	Average -ve index	Distances from Bus A km	Distances from Bus B km	Estimated fault location Km	$R_f \Omega$	Distance Error	$\Delta R_f$
98.0839	95.2576	85	25	73.85	30	11.15	10
112.6200	110.5756	85	25	97.55	50	-12.55	-10
91.8160	88.6809	85	25	61.65	20	23.35	20
6.8886	83.3486	85	25	52.45	10	32.55	30
120.2327	118.7457	85	25	111	60	-26	-20
135.5895	133.9542	85	25	115	70	-30.1	-30
98.3513	95.1958	85	25	74.05	25	10.95	15

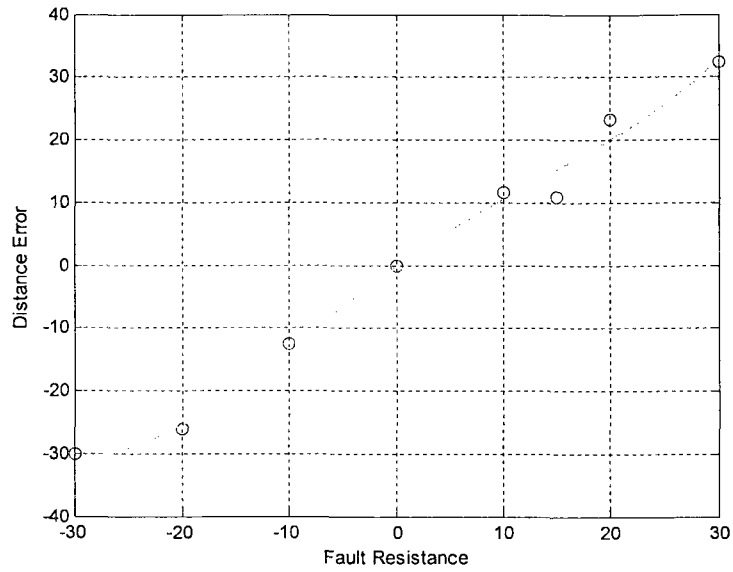


Figure 5.10: The curve fitting between fault resistance and distance error

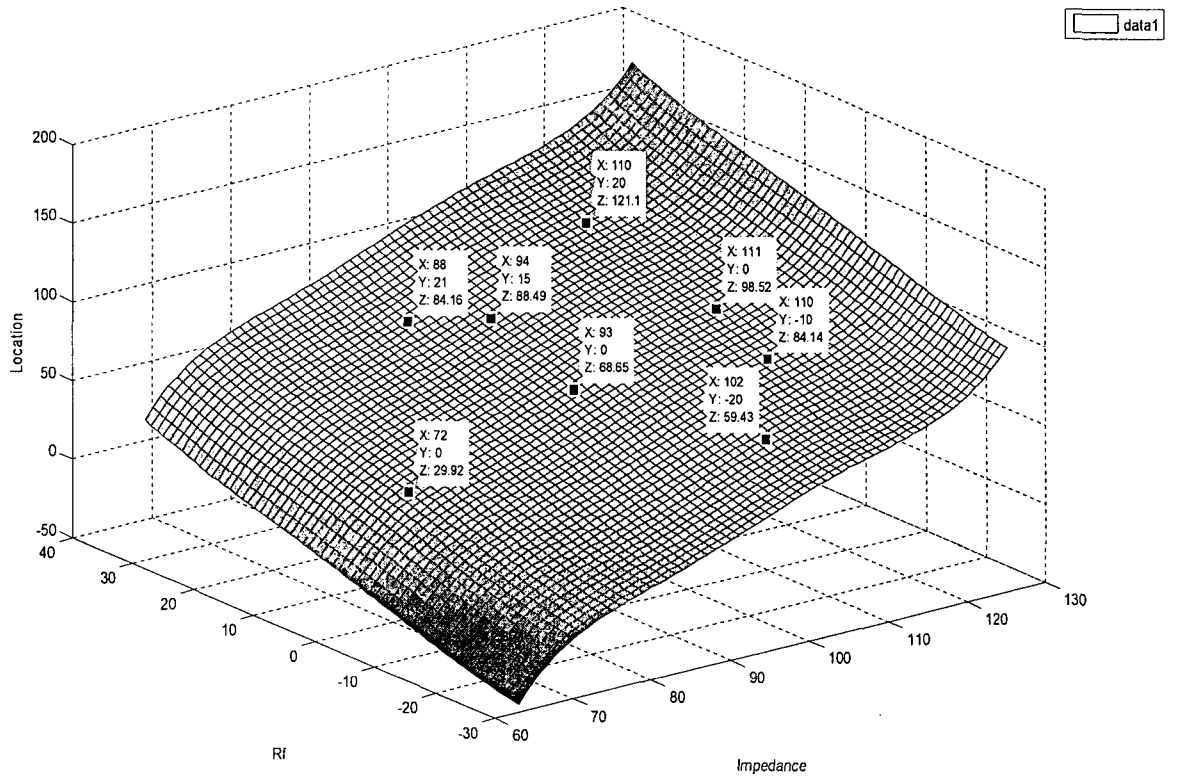


Figure 5.11: Fault localization- training set for *ab-g* fault

- **Line to Line**

In this case I will simulate line to line fault (ab), in Table 5.7 I generated symmetrical pattern index at many fault distance at fault resistance  $R_f = 40 \Omega$ , then I will generate curve fitting between positive and negative pattern index and distance of fault location in figure 5.12 shown the curve fitting . In table 5.8 I tested the validity of curve fitting I note the fault distance error less than 0.001 km.

**Table 5.7: Pattern Indices with a Varying Fault Distance Value and  $R_f = 40 \Omega$  for Fault *ab***

Average +ve Index	Average -ve index	Distances from Bus A Km	Distances from Bus B Km	$R_f \Omega$
60.7272	58.3914	0	110	40
61.2666	59.0104	10	100	40
70.8714	68.8974	30	80	40
89.1552	87.7113	55	55	40
101.9261	99.0332	70	40	40
124.9216	115.381	100	10	40
133.4281	124.000	110	0	40

**Table 5.8: The Validity of Curve Fitting in Figure 5.12 for *ab* Fault**

Example Test					
Average +ve index	Average -ve index	Distances from Bus A Km	Distances from Bus B km	Estimated fault location Km	$R_f \Omega$
64.6007	82.5309	90	20	89.9	40
57.3960	69.1787	65	45	64.7	40
61.5967	80.9140	85	25	86.6	40
68.9503	85.4069	105	5	105	40

Training set in table 5.6 was generated for a fault resistance of  $R_f = 40 \Omega$  while table 5.9 is displaying a varying fault resistance which was used to generate the curve fitting between  $\Delta R_f$  and  $\Delta D$  as shown in figure 5.13. By adding to curve fitting together according Eq. 5.9 the training set for this type of fault ab shown in figure 5.14.

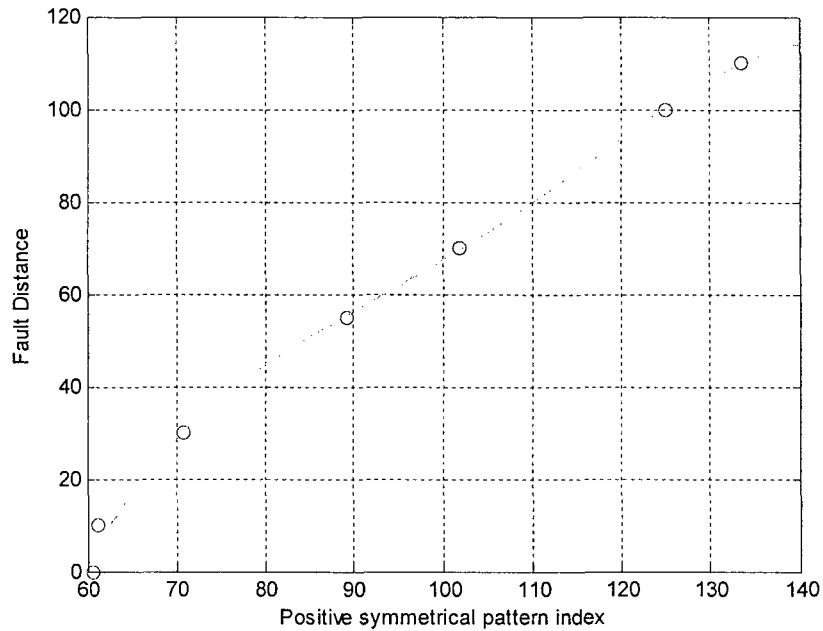


**Figure 5.12: The curve fitting between fault resistance and distance error**

**Table 5.9: Pattern Index at Different Fault Resistance Values**

Training Set for Error in Fault Resistance							
Average +ve Index	Average -ve index	Distances from Bus A Km	Distances from Bus B km	Estimated fault location Km	$R_f \Omega$	Distance Error	$\Delta R_f$
108.0676	101.647	85	25	77.4	30	7.6	10
116.4754	117.022	85	25	86.8	50	-1.8	-10
103.9742	110.493	85	25	73	20	12	20
93.1432	66.0367	85	25	59.3	10	25.7	30
120.9932	119.896	85	25	92.4	60	-7.4	-20
124.2245	123.0023	85	25	97.7	70	-12.6	-30

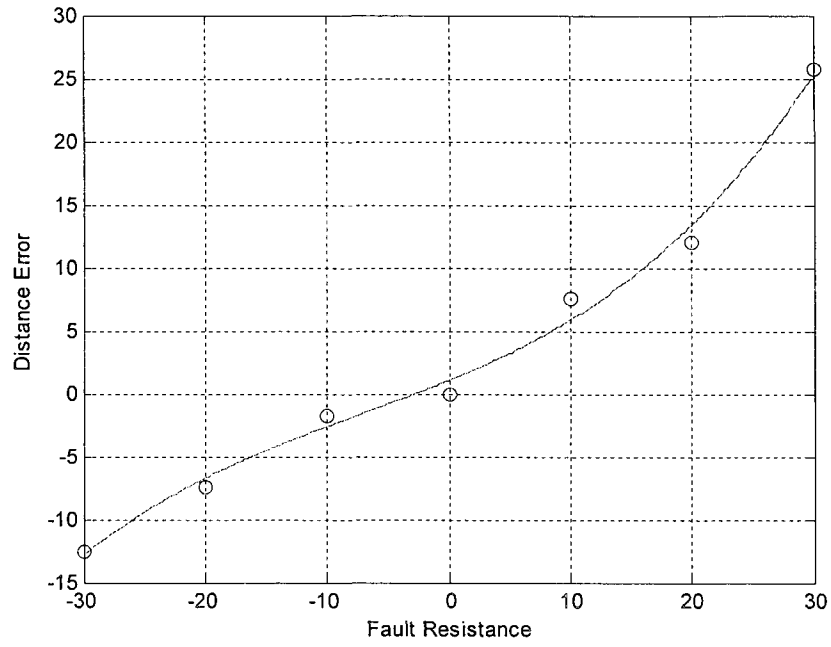


**Figure 5.13: The curve fitting between resistance and distance error**

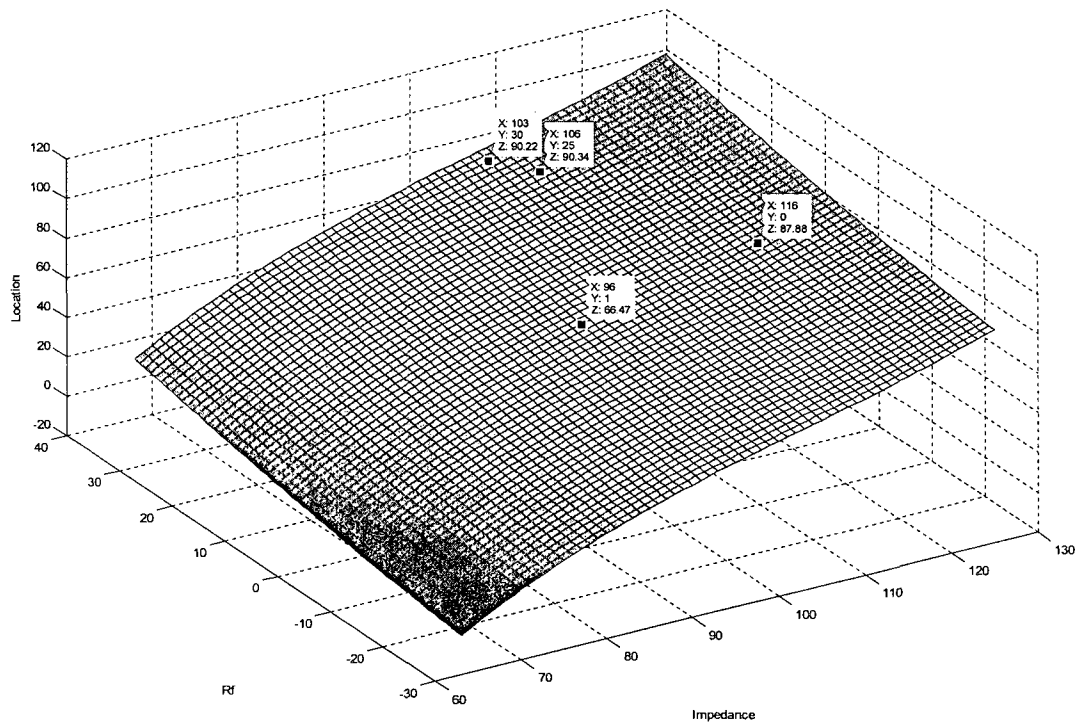


**Figure 5.14: Fault localization- training set for *ab* fault**

### 5.6.3 Results on Fault Localization

Table 5.10 provides the fault location estimates for *a-g*, *ab-g*, and *ab* faults at various network conditions. In the *ab-g* fault, it is noted that the maximum error is 2.7% at 15 km from relaying point with fault resistance of 77 $\Omega$  and maximum error of 0.3% at 45 km from relaying point with fault resistance of 40 $\Omega$ .

**Table 5.10: Results of Fault Location**

<b>Actual Fault Type</b>	<b>Fault Resistance <math>\Omega</math></b>	<b>Actual Fault Location (km)</b>	<b>Estimated Fault Location (km)</b>	<b>Error</b>
a-g	39	10	9.45	0.004
a-g	44	25	26.05	0.009
a-g	53	33	31	0.018
a-g	22	56	58.3	0.020
a-g	45	73	71.5	0.013
a-g	66	89	89.5	0.004
a-g	71	99	96	0.027
ab-g	35	70	69.08	0.009
ab-g	77	15	18	0.027
ab-g	40	45	44.6	0.003
ab-g	61	80	81.2	0.010
ab-g	57	65	67.4	0.021
ab-g	45	54	56.26	0.020
ab	10	90	90.8	0.007
ab	35	85	86.4	0.012
ab	25	90	92.8	0.025
ab	50	50	51.91	0.017
ab	60	15	17	0.018
ab	40	65	64.5	0.004

## CHAPTER 6

### ELECTRICAL PROTECTIVE RELAYING SYSTEM VIA PATTERN RECOGNITION

#### **6.1 Protective Relaying System**

The continuity of electricity supply is very important for consumers especially in the industrial sector. Protection relays are used in power systems to maximize the continuity of power supply and can be found in small and large systems, and in energy generation, transmission, or distribution systems [64]. Faults, if not detected quickly and corrected, will cause a sharp drop in the voltage signal, a loss of synchronization, and reductions in revenue in addition to the costly permanent damage to the equipment.

Protective relays, devices installed in various spots in a power system, detect defects and isolate the faulty part instantaneously. Depending on the application, relays uses values of voltages and/or currents as inputs from their power system via voltage and current transformers [81]. A protective relay is a very important component of a power system as it is in charge of making decisions to disconnect the generator from the transmission system or distribution system. Hence, a proper design for protective relaying system that will function properly is essential. However, a relay cannot open and isolate a faulted area in the power system. In figure 6.1 the Electrical protective relaying system is presented based on pattern recognition algorithm for fault detection, classification and localization. In this relay, we incorporate the fault detection, classification and fault localization in one relay. Once a relay detects and classifies a fault, the control circuit within it will isolate the faulty transmission line from the rest of the system by opening

the circuit breakers. To validate this system, the following models of complex power networks are used,

- 1- Mesh network with 3-Bus
- 2- 6-Bus Electrical Network
- 3- IEEE 14Bus

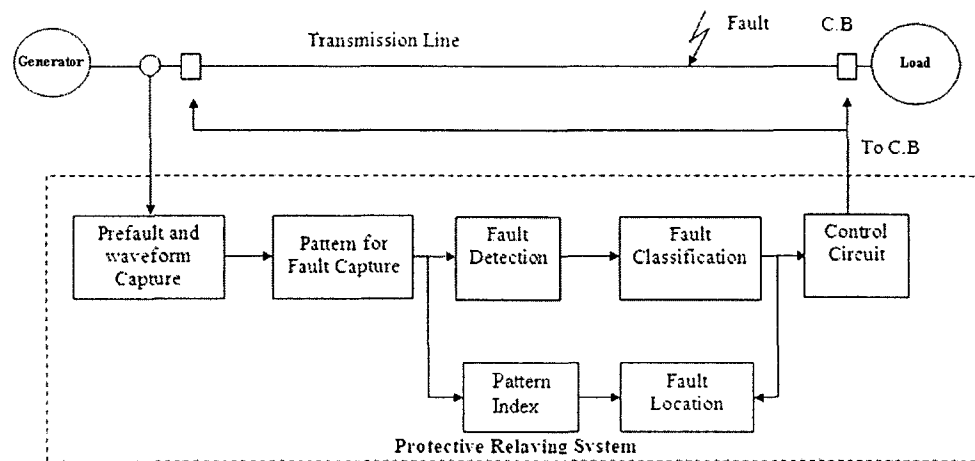


**Figure 6.1: Proposed electrical protective relaying system**

## 6.2 Case Study 1: Fault Detection, Classification, and Localization of a 3-Bus Mesh Network

The algorithm is tested on the mesh network as shown in figure 6.2 [82] with the following values: voltage sources are of 500 kV values, transmission line neutral/zero impedance sequence?  $Z(0)=96.45+j335.26 \Omega$ , positive sequence impedance  $Z(1)=9.78+j110.23 \Omega$ , length of transmission line between bus 1 and bus 2 is 400km, length of transmission line between bus 1 - bus 3, and length of transmission line between bus 2 –bus3 is 300km

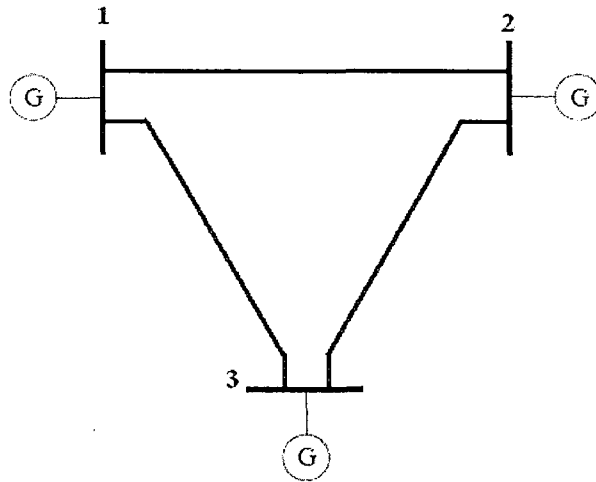


**Figure 6.2: Mesh network of 3-bus electrical power network**

The relaying point is located at bus 1, so the algorithm will be tested by simulating many faults in transmission line between bus 1 and 2 with a variety of operating conditions such as power angles, source impedance, and fault resistance values using PSCAD as shown in figure 6.3 with fault detection and classification results shown in Table 6.1 while in Table 6.2 we display the results for the fault location of this 3-bus network and compare them to the results were given in [82]. Our algorithm perform with a higher accuracy and less error values in most cases

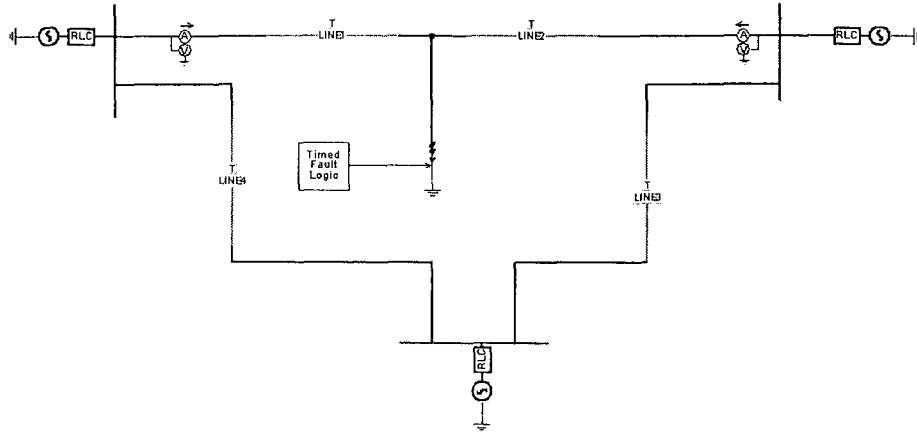


Figure 6.3: Mesh network 3-bus electrical power network using PSCAD

Table 6.1 Mesh 3-Bus Fault Detection and Classification Results

Actual Fault Type	Fault Resistance $\Omega$	Power Angle $\delta^\circ$	Type of Fault Detected
<i>a-g</i>	10	45°	<i>a-g</i>
<i>a-g</i>	200	60°	<i>a-g</i>
<i>b-g</i>	10	45°	<i>b-g</i>
<i>b-g</i>	200	60°	<i>b-g</i>
<i>c-g</i>	10	45°	<i>c-g</i>
<i>c-g</i>	200	60°	<i>c-g</i>
<i>ab-g</i>	10	45°	<i>ab-g</i>
<i>ab-g</i>	200	60°	<i>ab-g</i>
<i>ac-g</i>	10	45°	<i>ac-g</i>
<i>ac-g</i>	200	60°	<i>ac-g</i>
<i>bc-g</i>	10	45°	<i>bc-g</i>
<i>bc-g</i>	200	60°	<i>bc-g</i>
<i>ab</i>	10	45°	<i>ab</i>
<i>ab</i>	200	60°	<i>ab</i>
<i>ac</i>	10	45°	<i>ac</i>
<i>ac</i>	200	60°	<i>ac</i>
<i>bc</i>	10	45°	<i>bc</i>
<i>bc</i>	200	60°	<i>bc</i>
<i>abc</i>	10	45°	<i>abc</i>
<i>abc</i>	200	60°	<i>abc</i>

**Table 6.2 Mesh 3-Bus Fault Between Bus 1 and 2 Localization Results**

Fault distance	Fault resistance $\Omega$	Error(%) L-G faults	Error(%) LL-G faults	Error(%) LL faults	Error(%) LLL-G faults
60km from Bus 1	10	0.05	0.525	0.725	1.25
	200	1.35	2.3	1.3	0.5
140km from Bus 1	10	0.25	1	0	0.4
	200	0.35	0.5	0.08	1.7
220km from Bus 1	10	0.25	0.7	5.2	2.8
	200	1.5	2.8	0	3.2
300km from Bus 1	10	0.50	0.9	2.25	4
	200	2.3	3	4.2	5.3

### 6.3 Case Study 2: Fault Detection, Classification and Localization of 6-Bus Electrical Network

The system is simulated in this section is presented in figure 6.4 which has 6 buses (three generation buses and three loads buses) and 7 transmission lines. The voltage sources are of 132 Kv the transmission line parameters are:  $Z(0)= 82.5 + j308 \Omega$  and  $Z(1)= 8.25 + j94.5 \Omega$ , length of transmission line between bus 2 and 3, length of transmission line between bus 4 and 5 is 100km, and length of transmission line between bus 1 and 2 is 300km. In this system, 3 locations for protective relays are simulated at:

- 1- Relay at Bus 1 serving Transmission lines 1 and 2
- 2- Relay at Bus 5 serving Transmission lines 3, 5, 6.
- 3- Relay at Bus 3 serving Transmission lines 4 and 7

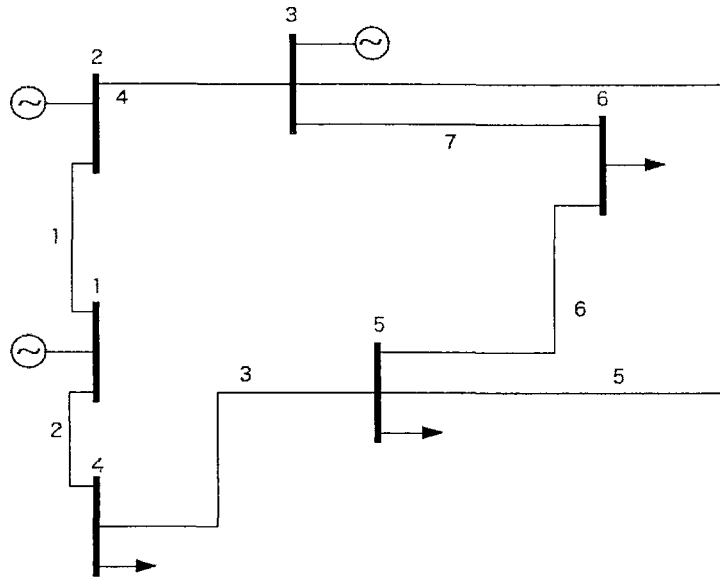


**Figure 6.4: 6-bus electrical power network**

Table 6.3 shows fault classification results and location estimates for a 6-bus network with maximum error of 3% for *bc-g* and *ab* faults with a 5Ω and a 100Ω fault resistance values respectively.

**Table 6.3 Fault Detection, Classification and Location Estimates for 6-Bus Network**

Actual Fault Type	Fault Between Bus	Actual Fault location Km	Fault Resistance Ω	Power Angle $\delta^\circ$	Fault Type	Estimated Fault Location Km	Error
<i>a-g</i>	2-3	30km from Bus 1	5	45°	<i>a-g</i>	31	0.010
<i>a-g</i>	2-3	30km from Bus 1	100	60°	<i>a-g</i>	31.8	0.018
<i>b-g</i>	1-2	45km from Bus 2	5	45°	<i>b-g</i>	45.5	0.005
<i>b-g</i>	1-2	45km from Bus 2	100	60°	<i>b-g</i>	43	0.020
<i>c-g</i>	4-5	80km from Bus 4	5	45°	<i>c-g</i>	77.9	0.021
<i>c-g</i>	4-5	80km from Bus 4	100	60°	<i>c-g</i>	78	0.020
<i>ab-g</i>	2-3	30km from Bus 1	5	45°	<i>ab-g</i>	30.2	0.002
<i>ab-g</i>	2-3	30km from Bus 1	100	60°	<i>ab-g</i>	32.4	0.024
<i>ac-g</i>	1-2	45km from Bus 2	5	45°	<i>ac-g</i>	45.7	0.007
<i>ac-g</i>	1-2	45km from Bus 2	100	60°	<i>ac-g</i>	45.8	0.008
<i>bc-g</i>	4-5	80km from Bus 4	5	45°	<i>bc-g</i>	77	0.030
<i>bc-g</i>	4-5	80km from Bus 4	100	60°	<i>bc-g</i>	83	0.030
<i>ab</i>	2-3	30km from Bus 1	5	45°	<i>ab</i>	33	0.030
<i>ab</i>	2-3	30km from Bus 1	100	60°	<i>ab</i>	31	0.010
<i>ac</i>	1-2	45km from Bus 2	5	45°	<i>ac</i>	44	0.010
<i>ac</i>	1-2	45km from Bus 2	100	60°	<i>ac</i>	46.1	0.011
<i>bc</i>	4-5	80km from Bus 4	5	45°	<i>bc</i>	80.5	0.005
<i>bc</i>	4-5	80km from Bus 4	100	60°	<i>bc</i>	81.3	0.013
<i>abc</i>	2-3	30km from Bus 1	5	45°	<i>abc</i>	30.2	0.002
<i>abc</i>	2-3	30km from Bus 1	100	60°	<i>abc</i>	30.1	0.001

### 6.4 Case Study 3: Fault Detection, Classification and Localization of the IEEE 14-Bus

A single line diagram of the IEEE 14-bus standard system, [82], is shown in figure 6.5. It consists of five synchronous machines with IEEE type-1 exciters, three of which are synchronous compensators used only for reactive power support. There are 11 loads in the system totaling 259 MW and 81.3 Mvar. Further details of this bus and its corresponding data are given in Appendix A.

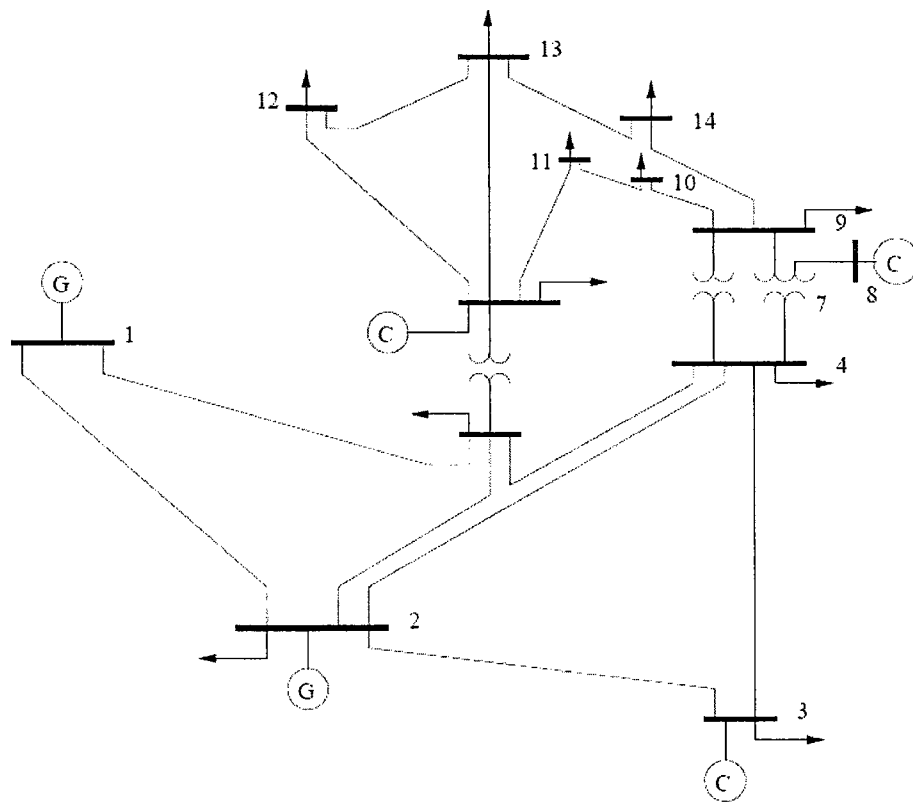


**Figure 6.5: The IEEE 14-bus electrical power network**

The relaying point is located at bus 2 and simulations will be conducted based on faults in transmission line between bus 2 and 4 with a variety of operating conditions such as varying values of power angles  $\delta$ , source impedance  $Z_s$ ,  $\Omega$  and fault resistance  $R_f$ . IEEE 14-bus network results for fault classification and location estimates are shown in

Tables 6.4 and 6.5 respectively. These results indicate that *ab* fault has the maximum error of 2.5%.

**Tale 6.4 Fault Detection, Classification for IEEE 14 Bus Network**

<b>Actual Fault Type</b>	<b>Fault Resistance <math>\Omega</math></b>	<b>Power Angle <math>\delta^\circ</math></b>	<b>Fault Type</b>
<i>a-g</i>	5	45°	<i>a-g</i>
<i>a-g</i>	100	60°	<i>a-g</i>
<i>b-g</i>	5	45°	<i>b-g</i>
<i>b-g</i>	100	60°	<i>b-g</i>
<i>c-g</i>	5	45°	<i>c-g</i>
<i>c-g</i>	100	60°	<i>c-g</i>
<i>ab-g</i>	5	45°	<i>ab-g</i>
<i>ab-g</i>	100	60°	<i>ab-g</i>
<i>ac-g</i>	5	45°	<i>ac-g</i>
<i>ac-g</i>	100	60°	<i>ac-g</i>
<i>bc-g</i>	5	45°	<i>bc-g</i>
<i>bc-g</i>	100	60°	<i>bc-g</i>
<i>ab</i>	5	45°	<i>ab</i>
<i>ab</i>	100	60°	<i>ab</i>
<i>ac</i>	5	45°	<i>ac</i>
<i>ac</i>	100	60°	<i>ac</i>
<i>bc</i>	5	45°	<i>bc</i>
<i>bc</i>	100	60°	<i>bc</i>
<i>abc</i>	5	45°	<i>abc</i>
<i>abc</i>	100	60°	<i>abc</i>

**Table 6.5 Fault Location Estimates for Different Faults on the IEEE 14-Bus Network**

<b>Fault Type</b>	<b>Fault Section Between Bus</b>	<b>Fault location Km</b>	<b>Estimation Fault Location Km</b>	<b>Error %</b>
<i>a-g</i>	2-4	20km from Bus 2	20.3	0.3
<i>a-g</i>	2-4	80km from Bus 2	79.6	0.4
<i>ab-g</i>	2-4	20km from Bus 2	21.3	1.3
<i>ab-g</i>	2-4	80km from Bus 2	80.8	0.8
<i>Ab</i>	2-4	20km from Bus 2	17.5	2.5
<i>Ab</i>	2-4	80km from Bus 2	80.9	0.9
<i>Abc</i>	2-4	20km from Bus 2	21.8	1.8
<i>Abc</i>	2-4	80km from Bus 2	80.4	0.4

## CHAPTER 7

### SUMMARY, CONTRIBUTIONS AND FUTURE WORK

#### 7.1 Summary

A vital attribute of an electrical power network is the continuity of service with a high level of reliability. This motivated many researchers to investigate power systems in an effort to improve power system reliability by focusing on fault detection, classification, and localization. I presented a new electrical protective relaying system framework to detect, classify, and localize any fault type in electrical power systems. This framework integrated fault detection, classification Unique patterns of events, signatures, were generated from the difference signal of pre- and post-fault current values during a  $(\frac{1}{4})^{\text{th}}$  of a cycle only. Experimental results show the validity of this proposed system.

Experimental results using a 3-bus, 6-bus, and IEEE 14-bus networks have shown a 100% in all cases for fault classification, and for fault location 3% maximum error in case of  $bc-g$  and  $ab$  faults with  $R_f$  of  $5\Omega$  and  $100\Omega$  in 6-bus case and a 2.5% maximum error in case of  $ab$  fault in IEEE 14-bus case.

#### 7.2 Contributions

This work presents an algorithm that monitors the electric current signal during  $(\frac{1}{4})^{\text{th}}$  of a cycle to instantaneously detect of a fault, and determine its type and location. The contributions of this dissertation are:

- 1- The protective relaying framework will be of a general applicability such that it can be deployed at any end of a transmission line without the need for communication devices between the two ends.
- 2- The algorithm presented in this dissertation has the ability to detect and classify any fault type and to distinguish a real fault from other events, rendering a high level of reliability.
- 3- The classification error resulted from using only two events' signatures is zero which is a significant improvement over the traditional approaches since the required training set size is smaller than those needed with existing approaches.
- 4- The protective relaying system can detect and classify high impedance fault, making it suitable for use in both transmission and distribution systems.

### **7.3 Future Work**

While this dissertation has a number of assumptions to secure the framework's successful implementation, there are several power network practices that can be possible future work to allow for improvements. These may include,

- 1- Inserting a series capacitor in the transmission lines to increase the power transfer capabilities is a common practice in power systems. This dissertation framework can be extended to include such a practice by adding a series capacitor or other FACTS (Flexible Alternating Current Transmission System).
- 2- This presented framework can be extended also to include other power system applications such as classification for power system quality disturbances.
- 3- Design a hardware implementation for the proposed relay system of this dissertation.

- 4- Replacing the PCA algorithm with other classifiers to enhance the results, specifically when the work scope is expanded to include other system's parameters such as the conditions mentioned in the above cases.

## BIBLIOGRAPHY

- 1- Math H. J. Bollen, Irene Yu-Hua Gu, "Signal processing of power quality disturbances," John Wiley & Sons Ltd, first Edition, 2006.
- 2- J. Lewis Blackburn, "Symmetrical components for power systems engineering", Marcel Dekker, Inc, First Edition, 1993.
- 3- M. Kezunovic, C. C. Liu, J. McDonald, and L. E. Smith, "Automated fault analysis," IEEE Tutorial, IEEE Power Engineering Society, 2000.
- 4- M. Kezunovic, I. Rikalo, "Detect and classify faults using neural nets," Computer Applications in Power, IEEE, Volume 9, Issue 4, Oct 1996.
- 5- K.Ferreira, "Fault Location for Power Transmission Systems Using Magnetic Field Sensing Coils," Master Thesis, April 2007.
- 6- M. Kezunovic, F. Fernandes, R. Sevcik, A. Hertz, J. Waight, S. Fukui and C. Liu, "Fault Analysis Using Intelligent Systems," Power Engineering Review, IEEE ,Volume 16, Issue 6, Jun 1996.
- 7- F. Crusca and M. Aldeen, "Fault Detection and Identification of Power Systems," in IASTED-Intelligent Systems & Control (ISC'03). 2003. Salzburg - Austria: IASTED.
- 8- Kasinathan, Karthikeyan, "Power System Fault Detection and Classification By Wavelet Transforms And Adaptive Resonance Theory Neural Networks," 2007, University of Kentucky.
- 9- A.K. Ghosh, D. L. Lubkeman, "The Classification Of Power System Disturbance Waveforms Using A Neural Network Approach," IEEE Transactions on Power Delivery, Vol. 10, No. 1, January 1995.
- 10- M. Sanaye-Pasand, H. Khorashadi-Zadeh, "Transmission Line Fault Detection & Phase Selection using ANN," International Conference on Power Systems Transients – IPST 2003 , New Orleans, USA.
- 11- A. Jain, A.Thoke, and R. N. Patel, "Fault Classification of Double Circuit Transmission. Line Using Artificial Neural Network," International Journal of Electrical and Electronics Engineering, Vol. 1, No. 4, 2008.

- 12- A. Jain, A. Thoke, "Classification of Single Line to Ground Faults on Double Circuit Transmission Line using ANN," International Journal of Computer and Electrical Engineering, Vol. 1, No. 2, June 2009.
- 13- S. Ramaswamy, B. Kiran, K. Kashyap, U. Shenoy, "Classification of power system transients using wavelet transforms and probabilistic neural networks," TENCON 2003. Conference on Convergent Technologies for Asia-Pacific Region, Volume: 4, Oct.2003.
- 14- K. H. Kashyap, U. J. Shenoyb, "Classification of power system faults using wavelet transforms and probabilistic neural networks," Circuits and Systems, 2003. ISCAS '03. Proceedings of the 2003 International Symposium on, vol.3.
- 15- K. Gayathri and N. Kumarappan, "Comparative Study of Fault Identification and Classification on EHV Lines Using Discrete Wavelet Transform and Fourier Transform Based ANN," International Journal of Electrical, Computer, and Systems Engineering, spring 2008.
- 16- J. Upendar, C. P. Gupta and G. K. Singh, "ART2 and wavelet based power system fault classification," International Conference on Energy and Environment (ENVIROENERGY 2009), 2009.
- 17- K.S. Swarup, N. Kamaraj and R. Rajeswari, "Fault Diagnosis of Parallel Transmission Lines Using Wavelet Based ANFIS," International Journal of Electrical and Power Engineering, Volume: 1, Issue: 4, 2007.
- 18- H. Zheng-you C. Xiaoqing F. Ling , " Wavelet Entropy Measure Definition and Its Application for Transmission Line Fault Detection and Identification (Part II: Fault Detection in Transmission line)," Power System Technology, 2006. Power Con 2006. International Conference on, Oct. 2006.
- 19- S. El Safty and A. El-Zonkoly, "Applying Wavelet Entropy Principle in Fault Classification," World Academy of Science, Engineering and Technology, 2008.
- 20- V. Malathi, N. Marimuthu, "Multi-class Support Vector Machine approach for fault classification in power transmission line," Energy Technologies, 2008. ICSET 2008. IEEE International Conference on, Nov. 2008.
- 21- J. Upendar, C. P. Gupta and G. K. Singh, "Discrete Wavelet Transform and Genetic Algorithm based Fault Classification of Transmission Systems," National Power Systems Conference (NPSC-2008), Indian Institute of Technology, Bombay, India, December 16-18, 2008.

- 22- D. Biswarup and V. REDDY, "Fuzzy-logic-based fault classification scheme for digital distance protection," IEEE transactions on power delivery , vol. 20, 2005.
- 23- K. Razi, M Hagh, G Ahrabian, " High accurate fault classification of power transmission lines using fuzzy logic," Power Engineering Conference, 2007. IPEC 2007. International, 2007.
- 24- P. K. Dash, S. Mishra, M. M. A. Salama, and A. C. Liew, "Classification of Power System Disturbances Using a Fuzzy Expert System and a Fourier Linear Combiner," IEEE transactions on power delivery, Vol. 15, No. 2, 2000.
- 25- S. Vasilic; M. kezunovic, "Fuzzy ART neural network algorithm for classifying the power system faults," IEEE transactions on power delivery, Vol. 20, No.1, 2005.
- 26- Nan Zhang, M. Kezonovic, "Coordinating fuzzy ART neural networks to improve transmission line fault detection and classification," IEEE PES General Meeting, San Francisco, June 2005.
- 27- A. K. Pradhan, A. Routray, S. Pati, and D. K. Pradhan, "Wavelet fuzzy combined approach for fault classification of a series-compensated transmission line," IEEE Trans. Power Delivery, vol. 19, no. 4, 2004.
- 28- S. R. Samantaray, P. K. Dash and G.Panda, "Transmission Line Fault Detection Using Time-Frequency Analysis," INDICON, 2005 Annual IEEE, Volume, Issue, 11-13 Dec. 2005.
- 29- T. Adu, "An Accurate Fault Classification Technique for Power System Monitoring Devices," IEEE transactions on power delivery, Vol. 17, No. 3, 2002.
- 30- E. Styvaktakis, M. H. J. Bollen, I. Y. H. Gu, "Automatic classification of power system events using rms voltage measurements," Power Engineering Society Summer Meeting, vol. 2, pp. 824–829, 2002
- 31- H. Hizam, P. Crossley, "Single-ended fault location technique on a radial distribution network using fault generated current signals," Seminar on Engineering and Technology (2006: Putrajaya).
- 32- F. Magnago, A. Abur, " Fault location using wavelets," IEEE transactions on power delivery, Volume 13, Issue 4, Oct 1998.

- 33- S. Bhunia and K. Roy, "A Novel Wavelet Transform Based Transient Current Analysis for Fault Detection and Localization", Design Automation Conference, pp. 361-366, 2002.
- 34- A. Borghetti, S. Corsi, C.A. Nucci, M. Paolone, L. Peretto, R. Tinarelli," On the use of continuous-wavelet transform for fault location in distribution power networks", Electrical Power and Energy Systems, 608–617, 2006.
- 35- A. Borghetti, M. Bosetti, M. Di Silvestro, C.A. Nucci and M. Paolone," Continuous-Wavelet Transform for Fault Location in Distribution Power Networks: Definition of Mother Wavelets Inferred from Fault Originated Transients", IEEE Transactions on Power Systems, Volume 23, Issue 2, May 2008.
- 36- S.Yerekar," Fault Location System for Transmission Lines in One-terminal By using Impedance-Traveling Wave Assembled Algorithm", Ninth International Conference on Environment and Electrical Engineering, 2010.
- 37- P. Chen, B. Xu, J. Li and Y. Ge, "Modern travelling wave based fault location techniques for HVDC transmission lines," Transactions of Tianjin University, Volume 14, Number 2, February, 2008.
- 38- M. Gilany, D. Ibrahim and T. Elsayed, " Traveling-wave-based fault-location scheme for multiend-aged underground cable system," IEEE transactions on power delivery, vol. 22, no1, 2007.
- 39- A.ABUR, " Locating Faults in Power Systems: An Approach based on the Wavelet Transform of Travelling Waves," IEEE Central & South Italy/North Italy Sections - Power Engineering Society Joint Chapter, November, 2004.
- 40- V. Malathi, N. S. Marimuthu, "Wavelet Transform and Support Vector Machine Approach for Fault Location in Power Transmission Line," International Journal of Electrical, Computer, and Systems Engineering 4:4 2010.
- 41- P. Raval, "ANN based Classification and Location of Faults in EHV Transmission Line," Proceedings of the International Multi-Conference of Engineers and Computer Scientists, Vol. I, 2008.
- 42- J. Gracia, A. Mazon, I. Zamora, "Best ANN structures for fault location in single- and double-circuit transmission lines," IEEE Transactions on Power Delivery, Volume 20, Issue 4, Oct. 2005.

- 43- M. Hagh, K. Razi, H.Taghizadeh, "Fault classification and location of power transmission lines using artificial neural network," International Power Engineering Conference, 2007. IPEC 2007.
- 44- T. BOUTHIBA, "Fault Location in EHV Transmission Lines using Artificial Neural Networks," Int. J. App. Math. Comput. Sci. 14 No. 1 (2004), 69–78.
- 45- S. Ekici, S. Yildirim, " Fault location estimation on transmission lines using wavelet transform and artificial neural network," Proceedings of the International Conference on Artificial Intelligence (ICAI'06), vol. 1, 2006, pp. 181–184.
- 46- A. Ngaopitakkul , C. Pothisarn, "Discrete Wavelet Transform and Back-propagation neural networks algorithm for fault location on Single circuit transmission line," IEEE International Conference on Robotics and Biomimetics, 2009. ROBIO 2009.
- 47- S. Ekici, "A transmission line fault locator based on Elman recurrent networks," Applied Soft Computing archive, Volume 9, Issue 1, January 2009.
- 48- M. Reddy and D. Mohanta, "A comparative Study of Artificial Neural Network (ANN) and Fuzzy Inference System (FIS) Approach for Digital Relaying of Transmission Line Faults," AIML Journal, Volume (6), Issue (4), December, 2006.
- 49- J. Sadeh, H. Afradi, " A new and accurate fault location algorithm for combined transmission lines using Adaptive Network-Based Fuzzy Inference System," Electrical Power Systems Research, Volume 79, Issue 11, November 2009.
- 50- F. Han, X. Yu, M. Al-Dabbagh1, Y. Wang, "Fault location in power distribution networks using sinusoidal steady state analysis," Proceedings of the 7th Asia Pacific Complex Systems Conference, 2004.
- 51- F. Carvalho, S. Carneiro, "Detection of Fault Induced Transients in E.H.V. Transmission Lines for the Development of a Fault Locator System," International Conference on Power Systems Transients – IPST 2003 in New Orleans, USA.
- 52- M. B. de Sousa, Allan K. Barros, "Fault location in medium and high voltage transmission line through efficient coding," Transmission and Distribution Conference and Exposition, 2007. IEEE/PES.

- 53- C.S .Chang, J.M. Chen, D. Srinivasan, F.S. Wen and Liew A. C, “ Fuzzy logic approach in power system fault section identification,” IEE proceedings. Generation, transmission and distribution, 1997, vol. 144, no5, pp. 406-414.
- 54- G. Sudha, T. Basavaraju, “A comparison between different approaches for fault classification in transmission lines”, IET Digest, Volume 2007, Issue 2.
- 55- U. Abhisek, Z. Rastko, “ Abrupt change detection in power system fault analysis using adaptive whitening filter and wavelet transform,” Electrical Power Systems Research, Volume 76, Issues 9-10, June 2006.
- 56- D. Chanda , N. K. Kishore , A. K. Sinha, “ Identification and Classification of Faults on Transmission Lines Using Wavelet Multiresolution Analysis ,” Electrical Power Components and Systems, Volume 32, Issue 4 April 2004.
- 57- R.N. Mahanty, P. B. Gupta, “A fuzzy logic based fault classification approach using current samples only,” Electrical Power Systems Research Volume 77, Issues 5-6, April 2007.
- 58- H. Saadat, “Power System analysis,” 2<sup>nd</sup> Edition, McGraw Hill, 2002.
- 59- J. Grainger, W. Stevenson, “Power System analysis,” 1<sup>st</sup> Edition, McGraw Hill, 1994.
- 60- PSCAD/EMTDC User’s Manual, Manitoba HVDC Research Center, Winnipeg, Manitoba, Canada.
- 61- I. T. Jolliffe, “Principal Component Analysis,” Springer - Verlag, NY, 1986.
- 62- J. Karhunen, J. Joutsensalo, “Generalizations of principal component analysis, optimization problems, and neural networks,” Neural Networks 8, pp. 549-562, 1995.
- 63- L. Smith, “A tutorial on principal component analysis,” 2002.  
[http://kybele.psych.cornell.edu/~edelman/Psych-465-Spring-2003/PCA\\_tutorial.pdf](http://kybele.psych.cornell.edu/~edelman/Psych-465-Spring-2003/PCA_tutorial.pdf)
- 64- R. D. Boyle, “Scaling additional contributions to principal component analysis,” Pattern Recognition Letters, Volume 31, pp. 2047- 2053, 1998.

- 65- S. K. Nayar, T. Poggio, "Early visual learning," Oxford University Press, NY, 1996.
- 66- C. Y. Chen, R.C.T. Lee, "A near pattern-matching scheme based upon principal components analysis," Pattern Recognition Letters, Volume 16, pp. 339-345, 1995.
- 67- B. Pinkowski, "Principal component analysis of speech spectrogram images," Pattern Recognition, Volume 30, pp. 777-787, 1997.
- 68- H. Murasae, S.K Nayar, "Learning and recognition of 3-D objects from brightness images," Proc. AAAI Fall symp. Machine Learning in Computer Vision, pp. 25-29, 1993.
- 69- S. Rodtook, Y. Rangsanseri, "Adaptive thresholding of document images based on Laplacian sign," International Conference of information technology 01, pp. 501-505, 2001.
- 70- A. Blake, M. Isard, "Active contours," Springer, NY, 1998.
- 71- M. A. Turk, A.P. Pentland, "Face recognition using eigenfaces," Proc. Conf. Computer Vision Pattern Recognition, pp. 586-591, 1991.
- 72- D. Widdows, "Geometry and meaning," University of Chicago Press, 2003.
- 73- H. Tengdin, "Impedance Fault Detection Technology," Report of PSRC Working Group D15 March 1, 1996.
- 74- C. Wester, "High Impedance Fault Detection on Distribution Systems", GE Power Management, 20 Technology Parkway, Suite 330, Norcross, GA 30092 USA.
- 75- C. Sharmeela, M.R. Mohan, G. Uma and J. Baskaran, "Novel Detection and Classification Algorithm for Power Quality Disturbances using Wavelets," American Journal of Applied Sciences, 3 (10), 2049-2053, 2006.
- 76- S. Nath, A. Dey and A. Chakrabarti, "Detection of Power Quality Disturbances using Wavelet Transform," World Academy of Science, Engineering and Technology, 49, 2009.

- 77- K. Zimmerman and D. Costello, "Impedance-Based Fault Location Experience," Schweitzer Engineering Laboratories, Inc. Pullman, WA USA
- 78- E.O. Schweitzer, "A review of Impedance Based Fault Locating Experience," Schweitzer engineering Laboratories, INC, Pullman, Washington
- 79- M. M. Saha , J. Izykowski and E. Rosolowski, "Fault Location on Power Networks," Springer, 2009.
- 80- J. Blackburn Lewis and Thomas J. Domin, "Protective Relaying-Principles and Applications," Taylor & Francis Group, LLC, New York, Third Edition, 2006.
- 81- MATLAB, The Language of Technical Computing, Ver. 7.4.0.287 (R2007a).
- 82- S. R. Samantaray and P.K. Dash, " Transmission line distance relaying using a variable window short-time Fourier transform," Electric Power Systems Research 78 (2008) 595–604.
- 83- S. Kamel Mena Kodsı, C. Canizares, "Modeling and Simulation Of IEEE 14 Bus System With Facts Controllers," Technical Report, 2003.

## APPENDIX

## IEEE 14-BUS DATA [83]

Table A.1: Bus Data

Bus No.	P Generated (p.u.)	Q Generated (p.u.)	P Load (p.u.)	Q Load (p.u.)	Q Generated max.(p.u.)	Q Generated min.(p.u.)
1	2.32	0.00	0.00	0.00	10.0	-10.0
2	0.4	-0.424	0.2170	0.1270	0.5	-0.4
3	0.00	0.00	0.9420	0.1900	0.4	0.00
4	0.00	0.00	0.4780	0.00	0.00	0.00
5	0.00	0.00	0.0760	0.0160	0.00	0.00
6	0.00	0.00	0.1120	0.0750	0.24	-0.06
7	0.00	0.00	0.00	0.00	0.00	0.00
8	0.00	0.00	0.00	0.00	0.24	-0.06
9	0.00	0.00	0.2950	0.1660	0.00	0.00
10	0.00	0.00	0.0900	0.0580	0.00	0.00
11	0.00	0.00	0.0350	0.0180	0.00	0.00
12	0.00	0.00	0.0610	0.0160	0.00	0.00
13	0.00	0.00	0.1350	0.0580	0.00	0.00
14	0.00	0.00	0.1490	0.0500	0.00	0.00

Table A.2: Line Data

From Bus	To Bus	Resistance (p.u.)	Reactance (p.u)	Line charging (p.u.)
1	2	0.01938	0.05917	0.0528
1	5	0.05403	0.22304	0.0492
2	3	0.04699	0.19797	0.0438
2	4	0.05811	0.17632	0.0374
2	5	0.05695	0.17388	0.034
3	4	0.06701	0.17103	0.0346
4	5	0.01335	0.04211	0.0128
4	7	0.00	0.20912	0.00
4	9	0.00	0.55618	0.00
5	6	0.00	0.25202	0.00
6	11	0.09498	0.1989	0.00
6	12	0.12291	0.25581	0.00
6	13	0.06615	0.13027	0.00
7	8	0.00	0.17615	0.00
7	9	0.00	0.11001	0.00
9	10	0.03181	0.08450	0.00
9	14	0.12711	0.27038	0.00
10	11	0.08205	0.19207	0.00
12	13	0.22092	0.19988	0.00
13	14	0.17093	0.34802	0.00